Instytut Genetyki i Biotechnologii Zwierząt

Polskiej Akademii Nauki

mgr Paweł Leszczyński

Rola białka PRDM3 w procesie różnicowania neuronalnego

Role of PRDM3 protein in neuronal differentiation

Autoreferat rozprawy doktorskiej

Promotor:

Prof. dr hab. Mariusz Pierzchała

Instytut Genetyki i Biotechnologii Zwierząt

Polskiej Akademii Nauki

Promotor pomocniczy:

Dr Hiroaki Taniguchi

Instytut Genetyki i Biotechnologii Zwierząt

Polskiej Akademii Nauki

Praca wykonana w ramach grantu Narodowego Centrum Nauki PRELUDIUM13 o numerze: 2017/25/N/NZ3/01886 oraz Konsorcjum Naukowego "Zdrowe Zwierzę - Bezpieczna Żywność" KNOW (Krajowy Naukowy Ośrodek Wiodący) o numerze: 05-1/KNOW2/2015.

Jastrzębiec 2021

Recenzenci:

dr hab. inż. Katarzyna Ropka-Molik, prof. IZ
Zakład Biologii Molekularnej Zwierząt, Instytut Zootechniki, Państwowy Instytut Badawczy, Kraków

dr hab. Katarzyna Socała
Katedra Fizjologii Zwierząt i Farmakologii, Instytut Nauk Biologicznych, Uniwersytet Marii Curie-Skłodowskiej, Lublin

Lista publikacji stanowiących rozprawę doktorską

1. LESZCZYŃSKI P, Śmiech M, Teeli AS, Zołocińska A, Słysz A, Pojda Z, Pierzchała M, Taniguchi H. Neurogenesis Using P19 Embryonal Carcinoma Cells. Journal of Visualized Experiments. 2019 Apr 27;(146). doi: 10.3791/58225.

Impact Factor= 1.108
Punkty Ministerstwa Nauki i Szkolnictwa Wyższego= 70

2. LESZCZYŃSKI P, Śmiech M, Salam Teeli A, Haque E, Viger R, Ogawa H, Pierzchała M, Taniguchi H. Deletion of the *Prdm3* Gene Causes a Neuronal Differentiation Deficiency in P19 Cells. International Journal of Molecular Sciences. 2020 Sep 29;21(19):7192. doi: 10.3390/ijms21197192.

Impact Factor= 4.556
Punkty Ministerstwa Nauki i Szkolnictwa Wyższego= 140

3. LESZCZYŃSKI P, Śmiech M, Parvanov E, Watanabe C, Mizutani KI, Taniguchi H. Emerging Roles of PRDM Factors in Stem Cells and Neuronal System: Cofactor Dependent Regulation of PRDM3/16 and FOG1/2 (Novel PRDM Factors). Cells. 2020 Dec 4;9(12):E2603. doi: 10.3390/cells9122603.

Impact Factor= 4.366
Punkty Ministerstwa Nauki i Szkolnictwa Wyższego= 140

1. Wprowadzenie

1.1 Neurogeneza embrionalna

Podczas rozwoju zarodka obserwuje się intensywną proliferacje i różnicowanie komórek, co w konsekwencji prowadzi do ukształtowania się trzech listków zarodkowych (endo-, mezo- i ektodermy). Zarodek myszy wykształca zróżnicowaną warstwę ektodermalną w obszarze płytki nerwowej około 7,5 dnia rozwoju embrionalnego (E7,5). W E8,5 płytka nerwowa przekształca się w cewę nerwową, z której później tworzy się centralny układ nerwowy [1]. Najintensywniej neurogeneza zachodzi podczas rozwoju zarodkowego, natomiast w dojrzałym organizmie, w niektórych obszarach mózgu, utrzymuje się przez całe życie, jednak na znacznie niższym poziomie [2, 3]. Zarodkowe komórki macierzyste dzielą się symetrycznie, ale pod wpływem programu genetycznego i sygnałów zewnętrznych przekształcają się w neuronalne komórki progenitorowe. Ostatecznie, komórki różnicują się do postmitotycznych neuronów o określonej funkcji [4].

Jak wspomniano powyżej, określenie kierunku różnicowania komórki w zarodku kształtowane jest przez wewnętrzne i zewnętrzne czynniki. Utrzymanie stanu pluripotencji komórek macierzystych jest koordynowane głównie przez wysoką ekspresję czynnika transkrypcyjnego OCT4 (ang. *Octamer-binding transcription factor 4*) i NANOG (ang. *Nanog homeobox*) [5]. Sekwencyjna inaktywacja i aktywacja ekspresji określonych czynników transkrypcyjnych jest wymagana do prawidłowej specjalizacji komórek neuronalnych i precyzyjnego ukierunkowania neurogenezy podczas rozwoju zarodkowego [6, 7]. PAX6 (ang. *Paired box 6*) jest kluczowym czynnikiem transkrypcyjnym, wpływającym na przejście od niezróżnicowanych komórek macierzystych do neuronalnych progenitorów. Podczas rozwoju zarodkowego PAX6 koordynuje specjalizację neuroektodermy i jej regionalizację [7]. Dojrzewanie układu nerwowego zarodka jest ściśle związane z istotnymi zmianami profilu ekspresji genów [8]. Neurogenina i czynnik transkrypcyjny BHLH z rodziny Achaete-Scute 1, koordynują sieci transkrypcyjne i wpływają na kształtowanie się morfologii i funkcji neuronalnych progenitorów. Następnie, mitotycznie aktywne neuronalne komórki macierzyste przechodzą do fazy postmitotycznej [9-11]. Dojrzałe i w pełni funkcjonalne neurony uzyskują określony fenotyp, co jest ścisłe związane z wysokim poziomem ekspresji NeuN (ang. *Hexaribonucleotide Binding Protein-3*), MAP2 (ang. *Microtubule-associated protein 2*) i β-III TUBILIN (ang. *Tubulin beta 3 class III*) [2, 12-16].

1.2 Modele neurogenezy

Badania mechanizmów neurogenezy w zarodkach są problematyczne ze względu na wykorzystanie zwierząt, wysoki koszt materiałów oraz aspekty etyczne. Stąd, modele *in vitro* stały się szeroko stosowane do badań nad początkowymi etapami rozwoju tego procesu.

1.2.1 Modele wykorzystujące pluripotencjalne komórki macierzyste

Modele *in vitro* naśladujące neurogenezę zarodkową oparte są na pluripotencjalnych zarodkowych komórkach macierzystych (ESC) [17-20] oraz indukowanych pluripotencjalnych komórkach macierzystych (iPSC) [21-23]. ESC i iPSC mogą się różnicować do trzech listków zarodkowych pod wpływem ukierunkowanej stymulacji. Kontrolowane różnicowanie zależne od czynników podawanych z zewnątrz sprawia, że ESC i iPCS są użytecznymi modelami komórkowymi do badania wczesnych stadiów rozwoju układu nerwowego, w tym różnicowania podtypów neuronalnych. Istnieją trzy główne metody aktywowania procesu

neurogenezy w ESC i iPSC. Do pierwszej metody należy formowanie ciał zarodkowych (ang. *Embryoid bodies*, EB), naśladujących środowisko *in vivo* [24, 25], druga to hodowla z komórkami zrębu [26, 27] i ostatecznie metoda wykorzystująca hodowle jednowarstwową [28, 29]. Metody te mają jednak wiele wad. Przedstawione modele komórkowe wymagają skoordynowanego i ściśle określonego użycia czynników stymulujących i hamujących, a także wzbogacania hodowli neuronalnej poprzez izolację komórek. Metoda wspólnej hodowli z komórkami zrębu jest silnie uzależniona od dodatkowej warstwy komórek, jednakże większość czynników oddziałujących na rozwój neuronów jest niezbadana [28, 29].

1.2.2 Modele neurogenezy oparte na liniach komórkowych

Modele neurogenezy wykorzystujące zarodkowe i indukowane pluripotencjalne komórki macierzyste wymagają dużej liczby odczynników i są czasochłonne [30-32]. Do otrzymania ESC wykorzystuje się warstwę odżywczą mysich zarodkowych fibroblastów i suplementację podstawowym czynnikiem wzrostu fibroblastów bFGF (ang. *Basic fibroblast growth factor*) [33]. Ponadto, aby utrzymać ESC w stanie niezróżnicowanym, pożywka do hodowli komórkowej musi zawierać czynnik LIF (ang. *Leukemia inhibitory factor*) lub MEK (ang. *MAP kinase-ERK kinase*) [34]. Modele neurogenezy *in vitro* oparte na liniach komórkowych nie potrzebują wielu odczynników ani dodatkowej warstwy komórek, co upraszcza cały proces.

Szczurza linia komórek raka nadnercza PC12 (barwiak) wywodzi się z komórek zarodkowego grzebienia nerwowego [35, 36]. Linia PC12 wymaga stymulacji czynnikiem wzrostu nerwów NGF (ang. *Nerve growth factor*), aby aktywować neurogenezę. Zastosowanie NGF skutkuje zahamowaniem proliferacji komórkowej i rozwojem neuronów z wysokim stopniem złożoności komórkowej (rozwój drzewka dendrytycznego i pobudliwość elektryczna) [37, 38]. SH-SY5Y to ludzka linia komórkowa wyprowadzona z komórek neuroblastomy. Niezróżnicowane komórki SH-SY5Y wykazują cechy neuroblastów i wymagają stymulacji kwasem retinowym (ang. *Retinoic acid*, RA) oraz mózgowym czynnikiem neurotroficznym BDNF (ang. *Brain derived neurotrophic factor*) w celu aktywacji różnicowania neuronalnego [39, 40].

Komórki macierzyste raka zarodkowego (ang. *Embryonic carcinoma cells*, ECS) wykazują zbliżone cechy z zarodkowymi komórkami macierzystymi pod względem morfologii, rozwoju i ekspresji specyficznych markerów [41, 42]. ECS wywodzą się z komórek potworniaka i przejawiają złośliwy fenotyp w niezróżnicowanym stadium, lecz zróżnicowane komórki ESC tracą cechy nowotworowe [43-46]. Linia komórkowa NTERA-2 wyprowadzona została z ludzkich komórek raka zarodkowego [47]. Ponadto, NTERA-2 może różnicować się w neurony pod wpływem zewnętrznej stymulacji. W stadium niezróżnicowanym, komórki mają wysoką ekspresję SSEA-3 (ang. *Stage-specific embryonic antigen 3*) - markera pluripotencji, ale pod wpływem RA jego ekspresja obniża się i komórki nabywają cech neuronalnych [48, 49]. Niemniej jednak linia NTERA-2 wykazuje wyższy poziom globalnej metylacji genomu niż inne linie komórkowe raka zarodkowego, co może sugerować ograniczenia w różnicowaniu komórkowym [50, 51]. Linia NTERA-2 wymaga również długiego okresu stymulacji RA (4 tygodnie) oraz suplementacji inhibitorami mitotycznymi przez kolejne 2-4 tygodnie w celu wzbogacenia populacji komórek neuronalnych [52].

Linia P19 (komórki mysiego raka zarodkowego) otrzymana została przez przeszczepienie komórek 7,5-dniowego zarodka do jądra myszy [53]. Linia P19 jest powszechnie wykorzystywana do naśladowania początkowego rozwoju zarodka, w tym badań nad rozwojem

wszystkich trzech listków zarodkowych [53, 54]. Aby imitować rozwój zarodka, komórki P19 są hodowane w zawiesinie w celu utworzenia agregatów komórkowych [46, 55, 56]. Proces różnicowania mezodermalnego i endodermalnego w komórkach P19 jest wyzwalany przez zastosowanie DMSO (ang. *Dimethyl sulfoxide*) w stężeniu 0,5–1% [57–59]. Kardiomiogennemu różnicowaniu komórek P19 towarzyszy zwiększona ekspresja MEF2c (ang. *Myocyte enhancer factor* 2C), Nkx2.5 (ang. *Homeodomain-containing NK2 homeobox 5*) i GATA4 (ang. *GATA-binding factor 4*)- markerów swoistych dla komórek sercowych [46, 60]. Ponadto zróżnicowane komórki P19 wykazują rytmiczne skurcze, co wskazuje na ich dużą przydatność w badaniu molekularnych mechanizmów rozwoju komórek mięśnia sercowego [61]. Stymulacja RA podczas agregacji komórek indukuje różnicowanie neuronalne w komórkach P19 [62]. Neurony wywodzące się z komórek P19 są postmitotyczne i mają cechy charakterystyczne dla komórek neuronalnych. Kilka dni po stymulacji RA morfologia komórek ulega radykalnej zmianie, wraz z arboryzacją drzew dendrytycznych i wytworzeniem funkcjonalnych synaps [62, 63]. Zróżnicowane neuronalnie komórki P19 posiadają receptory kwasu γ-aminomasłowego (GABA) [64], a także jonotropowe receptory glutaminianu, zarówno NMDA (ang. *N-methyl-D-aspartate*), jak i AMPA (ang. *Alpha-amino-3-hydroxy-5-methyl-4-isoxazole propionate*)/KA (ang. *Kainite*) [64, 65]. Ponadto, neuronalnie zróżnicowane komórki P19 przeszczepione do prążkowia dorosłego szczura mogą przetrwać stosunkowo długi okres czasu, przy tym nie zaobserwowano formowania się guza w miejscu przeszczepu. W pełni rozwinięte neurony wywodzące się z linii P19 wykazują właściwości morfologiczne i elektrofizjologiczne, zasadniczo przypominające dojrzałe neurony [63, 66]. Co ważne, badania z wykorzystaniem komórek P19 ujawniły szereg genów, które okazały się być kluczowe podczas rozwoju neuronów *in vivo* [67-69]. To potwierdza ich wysoką użyteczność w badaniach nad neurogenezą u ssaków.

1.3 Regulacja neurogenezy

Indukcja neurogenezy zależy od czynników wewnętrznych i zewnętrznych. Do kluczowych czynników wymaganych do rozwoju neuronów należą między innymi: FGF (ang. *Fibroblast growth factors*), kwas retinowy, SHH (ang. *Sonic hedgehog*) i NOTCH [70-74]. Szlak sygnałowy zależny od NOTCH to konserwatywny mechanizm molekularny, który koordynuje interakcję z sąsiadującymi komórkami i znacząco wpływa na różnicowanie komórkowe. Podczas neurogenezy sygnalizacja zależna od NOTCH hamuje proces dojrzewania neuronów. Niemniej jednak ścieżka interakcji jest plejotropowa i silnie zależna od tkanki i typu komórek [75]. Aktywacja szlaku NOTCH promuje ekspresję genów represorowych, co skutkuje obniżeniem ekspresji genów dojrzewania neuronalnego i utrzymaniem puli komórek macierzystych. Z drugiej strony, wyłączenie ekspresji genów zaangażowanych w ścieżkę NOTCH wyzwala przedwczesne różnicowanie neuronów [76]. RA jest metabolitem witaminy A, który indukuje wczesną neurogenezę *in vivo* [77, 78]. Podczas tworzenia EB stosunkowo wysokie stężenie RA stymuluje neuronalną ekspresję genów i tłumienie różnicowania mezodermalnego [79, 80]. Cząsteczki RA ulegają translokacji z cytoplazmy do jądra przez białko CRABP2 (ang. *Cellular RA-binding protein 2*), gdzie funkcjonuje jako aktywator heterodimerowego kompleksu RAR (ang. *Retinoic acid receptor*) i RXR (ang. *Retinoid X receptor*) [81]. W zarodkowych komórkach macierzystych aktywny kompleks receptora RAR-RXR działa jako czynnik transkrypcyjny [82, 83] i pozytywnie moduluje sieci transkrypcyjne w kierunku rozwoju neuronalnego [84]. Następną grupą białek o fundamentalnym znaczeniu jest rodzina białek GATA. Należą one do czynników charakteryzujących się domenami palców cynkowych, które rozpoznają motyw WGATAR w regionach regulatorowych genów

docelowych [85]. GATA są istotne dla rozwoju wszystkich trzech listków zarodkowych i pochodnych narządów (w tym mózgu, skóry, struktur krwiotwórczych, wątroby i układu sercowo-naczyniowego). Znaczenie GATA dla rozwoju organizmu jest krytyczne, a większość inaktywujących mutacji w sekwencji GATA jest śmiertelna dla zarodków [86, 87]. Niemniej jednak rola białek GATA w rozwoju mózgu jest słabo poznana. Stwierdzono, że GATA2 i GATA3 wpływają na tworzenie podtypów neuronów podczas końcowego różnicowania neuronów glutaminergicznych i serotoninergicznych [88]. Ponadto, zależny od RA szlak sygnałowy może synergistycznie oddziaływać z GATA2 w trakcie rozwoju organizmu [89]. Ta obserwacja sugeruje, że podobny mechanizm może być również zaangażowany w rozwój neuronów.

1.4 Czynniki PRDM

Czynniki transkrypcyjne PRDM (ang. *PRDI-BFI (positive regulatory domain I-binding factor 1) and RIZ1 (retinoblastoma protein-interacting zinc finger gene 1) homologous domain containing*) tworzą grupę 19 białek mających znaczący wpływ na procesy komórkowe [90-93] (strukturę i rolę czynników PRDM w komórkach macierzystych i neuronalnych opisano w **Publikacji 3**). Na końcu *N* białka znajduje się domena PR (ang. *PRDF1-RIZ*), która jest strukturalnie podobna do domen katalitycznych SET (ang. *Suppressor of variegation, Enhancer of Zeste, Trithorax*). Domeny SET wykazują aktywność histonowej metylotransferazy lizynowej (ang. *Histone methyltransferases*, HMT) [94]. Jak dotąd, wewnętrzna aktywność HMT została udowodniona tylko dla kilku białek PRDM (PRDM2, PRDM3, PRDM8, PRDM9 i PRDM16) [95-103]. Czynniki PRDM działają jako mediatory w tłumieniu lub aktywacji transkrypcji w tkankowo-zależnym kontekście. Ponadto zmiany ekspresji genów regulowane przez białka PRDM odbywają się częściowo za pośrednictwem interakcji z kofaktorami [96, 99, 104–109]. Czynniki PRDM mogą nadzorować ekspresję genów poprzez interakcję z PRC2 (ang. *Polycomb complex 2*), HAT (ang. *Histone acetyltransferases*), HMT, HDAC (ang. *Histone deacetylases*), PRMT5 (ang. *Protein arginine 5 N-methyltransferase*) i LSD1 (ang. *Lysine-specific 1 demethylase 1*) [96, 99, 104-109]. Interakcja między Suv39H1 HMT i PRDM3 [110] skutkuje metylacją H3K9 i w konsekwencji prowadzi do zmniejszenia ekspresji docelowych genów. Inne białka z rodziny PRDM, takie jak PRDM1, PRDM5, PRDM6 i PRDM12 oddziałują z G9a HMT i hamują ekspresję genów poprzez metylację H3K9 [95-97, 101, 111]. Oprócz domeny PR, białka PRDM zawierają również powtarzające się domeny palca cynkowego. Domeny palców cynkowych działają jako struktury odpowiedzialne za interakcje z określonymi sekwencjami DNA lub z innymi białkami [112-118]. Rola PRDM3 jest ściśle zależna od kontekstu odziaływania z innymi kofaktorami. PRDM3 przejawia aktywność metylotransferazy histonu 3 lizyny 9 (H3K9) co bezpośrednio jest związane z funkcją represyjną [118]. Z drugiej strony, pozytywna regulacja genów zależna od PRDM3 zachodzi poprzez odziaływanie na poziom metylacji histonu 3 w pozycji lizyny 4 (H3K4) [118-121]. Szczegółowy opis białek oddziałujących z PRDM3 znajduje się w **Publikacji 3**.

1.5 Funkcja PRDM3 w komórkach neuronowych

W *Caenorhabditis elegans,* białko Egl-43 (homolog PRDM3) kontroluje inwazję komórek i jest niezbędny do określenia kierunku różnicowania [122]. Niedobór Egl-43 podczas rozwoju zarodkowego zatrzymuje migrację dwóch komórek neuronowych specyficznych dla neuronów typu serotoninergicznego [123]. U *Drosophila melanogaster*, Hamlet (homolog PRDM3) koordynuje zależny od ścieżki Notch rozwój neuronów receptora węchowego (ang. *Olfactory*

receptor neurons, ORN) [124]. Hamlet usuwa stan wywołany przez Notch w rozwijających się komórkach i zmienia profil ekspresji genów poprzez status metylacji regionów promotorowych i gęstość upakowania histonów. Opisane zmiany powodują zależną od białka Hamlet zwiększoną dostępność chromatyny, umożliwiając czynnikowi Su (H) (ang. *Hairless protein suppressor*) związanie się ze wzmacniaczami specyficznymi dla Notch. U kręgowców rola PRDM3 jest słabo poznana. Myszy z wyłączoną ekspresją *Prdm3* giną podczas rozwoju zarodka z wyraźnie zaznaczonymi wadami w układzie sercowo-naczyniowym i neuronalnym [125]. Ponadto wykazano, że RA istotnie zwiększa ekspresję genu *Prdm3* w mysim raku zarodkowym, a ektopowa nadekspresja *Prdm3* wyzwala rozwój neuronów niezależnie od stymulacji RA [126]. Zwiększenie poziomu ekspresji *Prdm3* obserwuje się podczas neuronalnego różnicowania się komórek macierzystych *in vitro* [25]. Ekspresja genów, która kieruje rozwojem mózgu, jest częściowo regulowana przez mechanizmy epigenetyczne [127]. PRDM3 ulega ekspresji w jądrze neuronów hipokampu, gdzie pośrednio kontroluje aktywność neuronalną związaną z AMPAR (ang. *α-amino-3-hydroxy-5-methyl-4-isoxazolepropionic acid receptor*) [128]. PRDM3 oddziałuje na zależną od AMPAR aktywność neuronalną poprzez promotor miR-124 [128]. Co ciekawe, obniżenie ekspresji miR-124 w korowych i hipokampowych neuronach odbywa się poprzez utworzenie aktywnego kompleksu PRDM3 z HDAC1 (ang. *Histone deacetylase 1*) [128].

2 Hipotezy

- Metoda generowania neuronów zróżnicowanych z komórek P19 może być uproszczona bez utraty wydajności neurogenezy.
- Niedobór PRDM3 znacząco wpływa na różnicowanie neuronów wyprowadzonych z komórek P19.
- Ekspresja *Prdm3* podczas neurogenezy zależy od wpływu białek GATA i szlaku sygnałowego RA.

3 Celem badań

- Opracowanie skutecznej i uproszczonej metody neurogenezy *in vitro* przy użyciu komórek P19 do badań nad rolą PRDM3.
- Określenie profilu ekspresji *Prdm3* podczas neurogenezy *in vitro*.
- Ocenienie i charakterystyka roli PRDM3 podczas różnicowania neuronów.
- Zbadanie mechanizmów regulujących aktywność promotora *Prdm3*.

4 Materiały i metody

4.1 Hodowla komórkowa

Komórki P19 (uzyskane od Katsuhiko Mikoshiba, RIKEN Center for Brain Science, Wako, Japonia) hodowano w pożywce DMEM (ang. *Dulbecco's modified eagle medium*, DMEM) z dodatkiem 4,5 g/l glukozy (Lonza, Bazylea, Szwajcaria), 100 jednostek/ml penicyliny i 100 jednostek jednostek/ml streptomycyny (Lonza, Bazylea, Szwajcaria). Pożywka była

suplementowana w 10% płodową surowicą bydlęcą (FBS) (EURx, Gdańsk, Polska). Komórki były hodowane w inkubatorze w 37 °C i 5% CO_2. W celu aktywacji procesu neurogenezy, komórki P19 (liczba wysianych komórek: 1 x 10^6) hodowano na 100 mm szalce Petriego (Corning, Corning, NY, USA) w zawiesinie. Pożywka do indukcji neurogenezy składała się z DMEM z 5% FBS z dodatkiem 0,5 µM kwasu all-trans retinowego (Sigma, St. Louis, MO, USA) przez okres 4 dni. W tym okresie komórki P19 ulegały agregacji i przypominały początkowe stadia embrionalne. Agregaty komórek zebrano po 1,5 min swobodnego spadku w probówce o pojemności 15 ml, aby uniknąć zanieczyszczenia pojedynczymi komórkami. Następnie komórki P19 poddano działaniu trypsyny i wysiano na płytki hodowlane na następne 4 dni w pożywce podtrzymującej (DMEM z 100 jednostkami/ml penicyliny i 100 jednostkami/ml streptomycyny z dodatkiem 10% FBS) w celu utrzymania dalszego różnicowania neuronów.

4.2 RT-PCR i RT-qPCR

RNA całkowity wyizolowano z komórek P19 za pomocą fenozolu (A&A Biotechnology, Gdynia, Polska). Odwrotną transkrypcję przeprowadzono z użyciem 0,5 µg całkowitego RNA zgodnie z zaleceniem producenta (EURx, Gdańsk, Polska). cDNA otrzymane w reakcji odwrotnej transkrypcji zastosowano do przeprowadzenia PCR lub qPCR. Do wyżej wymienionych metod zastosowano zestaw Fast SG qPCR Master Mix zgodnie z zaleceniami producenta (EURx, Gdańsk, Polska). Profil ekspresji genów oceniano za pomocą termocyklera LightCycler 96 (Roche, Mannheim, Niemcy). Warunki amplifikacji cDNA były następujące: denaturacja w 95 °C przez 5 min, następnie 95 °C przez 10 s, 60 °C przez 10 s i 72 °C przez 10 s (40 cykli). Każdy badany gen został znormalizowany względem genu *Gapdh* (ang. *Glyceraldehyde-3- phosphate dehydrogenase*). Sekwencje starterów zastosowane w RT-PCR i RT-qPCR przedstawiono w **Publikacji 1, Tabela 1** i **Publikacji 2, Tabela 1**.

4.3 Generowanie komórek P19 z niedoborem PRDM3

Wyłączenie ekspresji genu PRDM3 w komórkach P19 wykonano metodą CRISPR/Cas9. Sekwencja crRNA (5′-TCTCTAACCTTTGCAGATCG-3′) komplementarna do mysiego genu *Prdm3* (ekson 4) została zaprojektowana przy użyciu programu CHOPCHOPv2 [129]. crRNA i tracrRNA znakowany ATTO-550 zakupiono z Integrated DNA Technologies (Coralville, IA, USA). Komórki P19 wysiano 24 godziny przed transfekcją na 24-dołkowe płytki w stężeniu 3,5 x 10^4 komórek na każdy dołek. W dniu transfekcji, otrzymano dupleks crRNA i tracrRNA-ATTO-550 (stężenie równo molowe: 1 µM) poprzez inkubację w 95 °C przez 5 min i schłodzenie do temperatury pokojowej (ang. *Room temperature*, RT). Następnie dupleks crRNA:tracrRNA-ATTO-550 dodano do 25 µl Opti-MEM (Thermo Fisher Scientific, Waltham, MA, USA) i zmieszano z 1 µM białkiem Cas9 (Integrated DNA Technologies, Coralville, IA, USA) w celu stworzenia kompleksu rybonukleoproteinowego (RNP). Po 10 minutach inkubacji w temperaturze pokojowej kompleks RNP połączono z mieszaniną 25 µl Opti-MEM i 1,5 µl lipofektaminy CRISPRMAX (Thermo Fisher Scientific, Waltham, MA, USA) Mieszanina była trzymana w RT przez kolejne 10-15 min. Następnie, roztwór RNP dodano do pożywki. W celu analizy wystąpienia potencjalnych, niespecyficznych mutacji wygenerowanych przez metodę CRISPR/Cas9, wytypowano za pomocą oprogramowania CHOPCHOPv2 [129] miejsca o wysokim prawdopodobieństwie wiązania crRNA w genomie. Następnie, sekwencje DNA amplifikowano metodą PCR (sekwencje starterów przedstawiono

w **Publikacji 2, Tabela S1)** i zbadano metodą sekwencjonowania Sangera (Genomed, Warszawa, Polska) (**Publikacja 2, Rysunek S1**).

4.4 Western blotting

Do analizy ekspresji wybranych białek użyto frakcji jądrowej wyizolowanej z komórek P19. Stężenie białek jądrowych oceniano przy użyciu zestawu Pierce BCA Protein Assay Kit (Thermo Fisher Scientific, Waltham, MA, USA). Ekstrakt białek jądrowych (20 µg) separowano w 4-15% żelu poliakrylamidowym (Bio-Rad, Hercules, CA, USA) i następnie przeniesiono na membranę PVDF (Merck Millipore, Burlington, MA, USA). Membranę inkubowano przez noc z przeciwciałem pierwszorzędowym przeciwko PRDM3 (1: 1000, Cell Signaling Technology, Danvers, MA, USA) w 5% odtłuszczonym mleku w TBS Sigma-Aldrich, Saint Louis, MO, USA) z dodatkiem 0,1% tween-20 (Sigma-Aldrich, Saint Louis, MO, USA). Następnie, membranę inkubowano 1 godzinę z rozcieńczonym 1: 5000 kozim przeciwciałem przeciwkróliczym skoniugowanym z HRP (Sigma-Aldrich, Saint Louis, MO, USA) w TBST z 5% dodatkiem odtłuszczonego mleka w temperaturze pokojowej. Po przepłukaniu, membranę wywoływano przy użyciu ECL Western Blotting Analysis System (Amersham, Illinois, CA, USA), a następnie obrazowano za pomocą ChemiDoc XRS+ (Bio-Rad, Hercules, CA, USA). Do normalizacji ekspresji białka zastosowano białko jądrowe-lamininę B1 w rozcieńczeniu 1: 1000 (Santa Cruz Biotechnology, Dallas, TX, USA). Masę cząsteczkową frakcjonowanego białka oszacowano stosując standardy wielkości Precision Plus Protein WesternC (Bio-Rad, Hercules, CA, USA).

4.5 Analiza FACS

Po 24 godzinach od wykonanej transfekcji, komórki P19 wyznakowane tracrRNA-ATTO-550 (Integrated DNA Technologies, Coralville, IA, USA) rozdzielono metodą sortowania komórek aktywowanych fluorescencją (FACS). Komórki traktowane tylko kompleksem RNP (bez odczynnika do transfekcji) zastosowano, jako kontrole w celu określenia bramki odczytu podczas procesu sortowania komórek. Analizę i sortowanie komórek przeprowadzono za pomocą urządzenia FACSAria (BD Biosciences, San Jose, CA, USA) przy użyciu oprogramowania Cell Quest (BD Biosciences, San Jose, CA, USA) na Wydziale Immunologii Uniwersytetu Warszawskiego.

4.6 Wyprowadzenie klonu komórek P19 z wyłączoną ekspresją *Prdm3*

Komórki P19 uzyskane z sortowania FACS rozcieńczono w stężeniu: 1 komórka na 100 µl pożywki DMEM/10% FBS. Następnie komórki zostały wysiane do indywidualnych dołków 96-dołkowej płytki (100 µl pożywki/dołek) i inkubowane przez następne 7 dni. Do dalszych procedur wybrano dołki z pojedynczą kolonią. W dniu trypsynizacji komórki przemyto 100 µl soli fizjologicznej buforowanej fosforanem (PBS) bez wapnia i magnezu (Lonza, Bazylea, Szwajcaria) i rozdzielono na pojedyncze komórki za pomocą 20 µl trypsyny-EDTA (0,25%) (Biosera, Nuaille, Francja). Na koniec komórki wysiano w tym samym układzie na dwie 96-dołkowe płytki. Komórki użyto do dalszych analiz, gdy poziom konfluencji osiągnął około 80%.

4.7 Izolacja genomowego DNA, HRM PCR i sekwencjonowanie Sangera

Genomowe DNA z komórek P19 zostało wyekstrahowane przy użyciu zestawu Genomic Mini (A&A Biotechnology, Gdynia) zgodnie z instrukcją producenta. W skład mieszaniny

reakcyjnej do HRM PCR wchodziło: 5 µl RT HS-PCR Mix EvaGreen (A&A Biotechnology, Gdynia, Polska), 1 µl DNA (10 ng), 0,25 µl każdego startera (10 µM), a następnie dopełniono wodą do objętości 10 µl. Sekwencję starterów użytych do PCR i HRM PCR przedstawiono w **Publikacji 2, Tabela 2**. Testy HRM PCR przeprowadzono z użyciem aparatu LightCycler 96 (Roche, Mannheim, Niemcy). Warunki reakcji HRM PCR obejmowały: 95 °C przez 5 min, następnie 40 cykli 95 °C przez 15 s, 60 °C przez 15 s, 72 °C przez 20 s. Analizę krzywej topnienia przeprowadzono w następujących warunkach: wstępne ogrzanie produktu PCR do 95 °C. Następnie mieszaninę schładzano do 40 °C przez 60 s i ogrzewano do 65 °C. Sygnał fluorescencji rejestrowano w sposób ciągły od 65 do 97 °C. Amplifikowane krzywe oceniano przy użyciu oprogramowania LightCyler 96 (Roche, Mannheim, Niemcy). Sekwencja produktów PCR została potwierdzona sekwencjonowaniem Sangera (Genomed, Warszawa, Polska).

4.8 Konstrukcja plazmidów

Region promotorowy dla *Prdm3* (zlokalizowany 5' powyżej niekodującego eksonu 1) amplifikowano z genomowego DNA wyizolowanego z komórek P19 przy użyciu zestawu Genomic Mini (A&A Biotechnology, Gdynia, Polska). Startery dla regionu promotorowego *Prdm3* zaprojektowano w oparciu o sekwencję zlokalizowaną na chromosomie 3 (chr3: 30.014.710-30.013.010). Sekwencje nukleotydowe dla enzymów restrykcyjnych *KpnI* i *HindIII* zostały dodane odpowiednio do starterów (w **Publikacji 2, Tabela 3**, przedstawiono sekwencję starterów użytych do klonowania promotora *Prdm3*). Stosując metodę PCR, amplifikowano region promotora dla *Prdm3* za pomocą polimerazy DNA PrimeSTAR Max (TaKaRa, Shiga, Japonia) zgodnie z instrukcjami producenta. Enzymy *KpnI* i *HindIII* (Thermo Fisher Scientific, Waltham, MA, USA) zastosowano do strawienia odpowiednich miejsc restrykcyjnych w plazmidzie pGL3 kodującym gen lucyferazy (Promega, Madison, WI, USA), a następnie poddano ligacji z produktem PCR przy użyciu metody Gibsona. W skrócie, do klonowania użyto zestawu OverLap™ (A&A Biotechnology, Gdynia, Polska). Fragmenty DNA (stosunek molowy wektora pGL3 do insertu 1:9) rozpuszczono w wodzie wolnej od nukleaz, dodano 4 µl buforu do OverLap, 2 µl mieszaniny enzymów wchodzących w skład OverLap™ wraz z fragmentami DNA. Mieszaninę umieszczono na lodzie i dopełniono wodą do 20 µl. Reakcję łączenia wykonano w 50 °C przez 15 min. Po udanej transformacji bakteryjnej, wybrano pojedynczą kolonię bakterii do amplifikacji, a następnie izolacji plazmidów. Oczyszczone plazmidy zweryfikowano metodą sekwencjonowania Sangera (Genomed, Warszawa). Sekwencje kodujące VP16-RARα i VP16-RARβ wstawiono do plazmidu pCMX. Plazmidy pcDNA3-Gata3, pcDNA3-Gata4, pcDNA3-Gata6 i GATA DN (dominujący-negatywny konkurent) zostały opisane wcześniej [130, 131]. Zestaw Site-Directed Mutagenesis (Agilent Technologies, Santa Clara, Kalifornia, USA) zastosowano zgodnie z wytycznymi producenta, aby zmutować miejsce RARE w promotorze *Prdm3*. Sekwencję starterów do mutagenezy wygenerowano za pomocą QuikChange Primer Design (Agilent Technologies, Santa Clara, CA, USA). Mutacje w miejscach wiązania receptorów RARα i RARβ zostały potwierdzone przez sekwencjonowanie Sangera. Sekwencja starterów użytych do mutagenezy miejscowej RARE przedstawiona w **Publikacji 2, Tabela S2**.

4.9 Transfekcja komórek i test lucyferazowy

W teście lucyferazowym, wysiano 3 x 10^4 komórek na 24-dołkową płytkę. Po 24 godzinach komórki P19 transfekowano plazmidami z Lipofektaminą 3000 zgodnie z protokołem

producenta (Thermo Fisher Scientific, Waltham, MA, USA). Testy lucyferazowe przeprowadzono 48 godzin po transfekcji komórek przy użyciu zestawu Luciferase Assay Kit (Promega, Madison, WI, USA) zgodnie z protokołem dostarczonym przez producenta. Poziomu luminescencji został zmierzony za pomocą luminometru Synergy LX (Biotek, Winooski, VT, USA).

4.10 Immunofluorescencja

Komórki utrwalano w 4% roztworze paraformaldehydu w PBS (Sigma-Aldrich, Saint Louis, MO, USA) przez 15 minut w temperaturze pokojowej. Następnie komórki przepłukano w PBS i permeabilizowano w 0,5% Triton x-100 (Sigma-Aldrich, Saint Louis, MO, USA) przez 10 minut i inkubowano przez 20 minut w 1% roztworze odtłuszczonego mleka. Komórki P19 inkubowano z króliczym przeciwciałem anty-MAP2 (Thermo Fisher Scientific, Waltham, MA, USA, rozcieńczonym 1:200) i króliczym przeciwciałem anty-β-III TUBULIN (Cell Signaling Technology, Danvers, MA, USA), rozcieńczonym 1:200 w 1% roztworze odtłuszczonego mleka przez noc w temperaturze 4 °C. Następnego dnia komórki przemyto w PBS z 0,1% Triton x-100 i inkubowano z kozim przeciwciałem drugorzędowym anty-króliczym IgG (Alexa Fluor Plus 488, Thermo Fisher Scientific, Waltham, MA, USA, rozcieńczenie 1:500) przez okres 1 godz. w RT. Jądra komórkowe barwiono z użyciem 1 mg/ml DAPI (4',6-diamidyno-2-fenyloindol dichlorowodorek) (Thermo Fisher Scientific, Waltham, MA, USA) przez 10 minut. Na koniec komórki poddano końcowemu płukaniu w PBS, a następnie osadzono na szkiełkach przy użyciu ProLong™ Gold Antifade Mountant (Thermo Fisher Scientific, Waltham, MA, USA). Preparaty analizowano za pomocą mikroskopu konfokalnego Nikon A1R (Nikon, Tokio, Japonia). Obrazy mikroskopowe zostały przetworzone przy użyciu oprogramowania ImageJ (wersja 1.52q, NIH, Bethesda, MD, USA) i oprogramowania do przeglądania obrazów firmy Nikon.

4.11 Analiza statystyczna

Analizę statystyczną danych przeprowadzono za pomocą oprogramowania GraphPad PRISM w wersji 6 (GraphPad Software, La Jolla, CA, USA). Dla indywidualnej grupy prób w eksperymencie dane ilościowe przedstawiono jako średnią i błąd standardowy średniej (S.E.M.). Istotność statystyczną danych oceniano za pomocą jednostronnej analizy wariancji (ANOVA) z testem post hoc Tukeya, a wartości $p \leq 0,05$ uznano za statystycznie istotne.

5 Wyniki

W literaturze przedstawiono różnorodne metody umożliwiające badanie procesu neurogenezy [132-135], jednakże są to techniki czasochłonne i skomplikowane. Większość z tych metod często wymaga użycia drogich odczynników, takich jak Neurobasal i suplement B27 [132-135]. Stąd, jednym z celów było opracowanie uproszczonego protokołu różnicowania neuronalnego opartego na pluripotencjalnych komórkach embrionalnych linii P19, który stanowiłby bazę do badań molekularnych mechanizmów neurogenezy. W **Publikacji 1** udowodniono, że płyn hodowlany złożony z jedynie z DMEM z dodatkiem płodowej surowicy bydlęcej (ang. *Fetal bovine serum,* FBS) można stosować do utrzymywania i namnażania niezróżnicowanych komórek P19. Ponadto podejście to wykazało, że w nieskomplikowany sposób można wywołać indukcję neurogenezy. Pożywkę zawierającą DMEM + 5% FBS suplementowaną RA (schemat pracy przedstawiony w **Publikacji 1**, **Rycina 1**) użyto podczas tworzenia się agregatów

komórkowych. Co ważne, aby uniknąć zanieczyszczenia pojedynczymi komórkami, czas zbierania agregatów ustawiono na 1,5 minuty w probówce o pojemności 15 ml. Aby ocenić efekt uproszczenia w tej metodzie, oceniono zmiany fenotypu w komórkach P19 podczas neurogenezy. Dobrze rozwinięte morfologicznie neurony obserwowano 4 dni po wysianiu komórek (**Publikacja 1, Rycina 3**). Następnie zbadano profil ekspresji genów w komórkach w stanie niezróżnicowanym oraz podczas neurogenezy. Niezróżnicowane komórki P19 wykazywały wysoką ekspresję genów pluripotencji *Oct4* i *Nanog*. Stymulacja RA komórek P19 podczas agregacji komórkowej spowodowała znaczny spadek ekspresji *Nanog* i *Oct4*, natomiast ekspresja *Map2* i *NeuN* wzrosła znacząco po indukcji neurogenezy (**Publikacja 1, Rycina 2**) [68, 133, 134, 136]. Wreszcie, skuteczność protokołu zweryfikowano, oceniając ekspresję białka MAP2 w 4 dniu po wysianiu komórek za pomocą immunofluorescencji. Zróżnicowane neuronalnie komórki P19 wykazały wysoką ekspresję białka MAP2. Ponadto barwienie DAPI użyte do zdefiniowania jąder wraz z detekcją MAP2 wykazało, że większość komórek posiada cechy dojrzałych neuronów (**Publikacja 1, Rycina 4**) [133].

Ten uproszczony model neurogenezy [137] został wykorzystany do zbadania roli PRDM3 podczas rozwoju neuronów. W pierwszym etapie oceniano profil ekspresji genu *Prdm3* metodą RT-qPCR. Zaobserwowano znaczący wzrost ekspresji *Prdm3* podczas różnicowania komórek P19 w neurony (**Publikacja 2, Rycina 1b**). Następnie, aby ocenić wpływ PRDM3 na neurogenezę zastosowano CRISPR/Cas9 (ang. *Clustered regularly interspaced short palindromic repeats*) do wygenerowania komórek P19 z wyłączoną ekspresją genu *Prdm3*. Ogólny przegląd przebiegu wykorzystanych technik do utworzenia linii komórek P19 z niedoborem PRDM3 przedstawiono w **Publikacji 2, Rycina 2a**. Metoda lipofekcji została zastosowana do wprowadzenia kompleksu rybonukleoproteinowego zawierającego białko Cas9 wraz z crRNA: tracrRNA-ATTO-550 do niezróżnicowanych komórek P19. Po udanej transfekcji komórki izolowano za pomocą metody sortowania komórek aktywowanych fluorescencją. Wysortowane komórki (ATTO-550-pozytywne) namnażano jako pojedyncze klony. Po 2 tygodniach z wybranych kolonii komórek wyizolowano DNA. Klony komórek typu dzikiego (kontrolne) odróżniono od *Prdm3* KO (ang. *Knockout*) na podstawie analizy krzywej topnienia o wysokiej rozdzielczości (HRM) (**Publikacja 2, Rycina 2b**). Zsekwencjonowano wybrane próbki DNA z poszczególnych klonów w celu potwierdzenia generacji linii komórkowej niosącej mutację w genie *Prdm3*. Otrzymano klon P19_C5 (*Prdm3 KO)* z delecją 59 par zasad (pz) i insercją 2 pz w sekwencji genu *Prdm3* (**Publikacja 2, Rycina 2c**). Delecja została zweryfikowana metodą PCR z wykorzystaniem elektroforezy w żelu agarozowym (**Publikacja 2, Rycina 2d**). Ostatecznie poziom białka PRDM3 oceniano metodą Western blotting. Komórki typu dzikiego wykazywały wysoki poziom ekspresji PRDM3, podczas gdy w komórkach *Prdm3* KO białka PRDM3 nie były wykrywane (**Publikacja 2, Rycina 2e**). crRNA wiąże się z komplementarną sekwencją w DNA. Jednak prawdopodobne jest, że RNP łączy się do podobnych sekwencji nukleotydowych. Stąd, system CRISPR/Cas9 może generować mutacje w niepożądanych miejscach w genomie, określanych jako *off-targets* [138]. Z tego powodu komórki z niedoborem PRDM3 analizowano pod kątem mutacji. Przy użyciu oprogramowania CHOPCHOPv2 zidentyfikowano dwie lokalizacje w genomie z najwyższym prawdopodobieństwem wystąpienia zjawiska *off-targets* [129]. Próbki DNA badano za pomocą sekwencjonowania Sangera i ostatecznie potwierdzono brak niepożądanych mutacji poza wyznaczonym regionem DNA (**Publikacja 2, Rycina S1**).

W kolejnym kroku podjęto próbę określenia wpływu niedoboru PRDM3 na proces neurogenezy. W tym celu określono poziom ekspresji genów związanych z pluripotencją

(*Oct3/4* i *Nanog*). Podczas różnicowania neuronalnego komórek typu dzikiego nie obserwowano ekspresji *Oct3/4* i *Nanog*. Komórki *Prdm3* KO wykazały znaczne podwyższenie ekspresji obu genów w 5, 7 i 9 dniu po indukcji (ang. *Day after induction*, DAI) (**Publikacja 2, Rycina 3a, b**). Następnie zbadano ekspresję markerów neuronalnych [139, 140]. Gen *Pax6* odgrywa kluczową rolę w proliferacji neuronalnych progenitorów oraz w migracji niedojrzałych neuronów [140]. Komórki *Prdm3* KO wykazywały zmniejszoną tendencję w ekspresji *Pax6* w 7 i 9 DAI w porównaniu z komórkami kontrolnymi, ale różnice były statystycznie nieistotne (**Publikacja 2, Rycina 3c**). Niemniej jednak, komórki *Prdm3* KO miały wysoką ekspresję *Oct3/4* i *Nanog* podczas neurogenezy, co sugerowało rozregulowanie procesu różnicowania. Aby potwierdzić tę obserwację, oceniono ekspresję genu tubuliny β-III. Tubulina β-III obecna jest prawie wyłącznie w dojrzałych neuronach [15]. Komórki *Prdm3* KO wykazywały wyższy poziom ekspresji tubuliny β-III w 5 DAI, po czym następował znaczny spadek ekspresji w 7 i 9 DAI w porównaniu z komórkami typu dzikiego (**Publikacja 2, Rycina 3d**). Ponadto, proces neurogenezy oceniano za pomocą barwienia immunofluorescencyjnego w celu określenia różnic w ekspresji białek MAP2 [141] i β-III TUBULIN [15] (**Publikacja 2, Rycina 4a, b**). Komórki z niedoborem PRDM3 miały wysoki poziom MAP2- i β-III TUBULIN w 5 DAI w porównaniu z komórkami typu dzikiego. Z drugiej strony komórki *Prdm3* KO miały bardzo niską ekspresję w 9 DAI. Natomiast, komórki typu dzikiego wykazywały zwiększoną ekspresję białek MAP2 i β-III TUBULIN z dobrze zdefiniowaną morfologią neuronów w 9 DAI (**Publikacja 2, Rycina 4a, b**). Barwienie DAPI uwidoczniło wysoki współczynnik proliferacji komórek *Prdm3* KO, w przeciwieństwie do komórek kontrolnych (**Publikacja 2, Rycina 4a, b**).

W kolejnej części badań celem było zbadanie mechanizmów kontrolujących ekspresję genu *Prdm3* podczas neurogenezy. Uwagę skupiono na regulacji aktywności promotora *Prdm3*. Sekwencja promotora *Prdm3* została wytyczona wykorzystując bazę Eukariotic Promoter Database (EPD) [142]. Program wskazał wiele konsensusowych sekwencji wiązania białek GATA w obrębie sekwencji promotora *Prdm3* (**Publikacja 2, Rycina S2**). W celu oceny potencjalnego wpływu czynników GATA na aktywność promotora *Prdm3*, zbadano ekspresję genów *Gata* (*Gata1, Gata3, Gata4* i *Gata6*) w komórkach P19 podczas neurogenezy. Ekspresja mRNA dla *Gata1* była niewykrywalna (dane nieopublikowane). Poziomy ekspresji mRNA dla *Gata3* był podwyższany w 5 DAI, a ekspresja *Gata4* i *Gata6* była znacząco podniesiona w 9 DAI (**Publikacja 2, Rycina 5a-c**). Następnie, zastosowano plazmid kodujący gen reporterowy lucyferazy pod kontrolą promotora *Prdm3* do oceny wpływu białek GATA. Nadekspresja białek GATA znacząco zwiększyła aktywność promotora *Prdm3* (ponad 3-krotnie), a największe odziaływanie obserwowano przy nadekspresji *Gata6* (około 4,5-krotnie) (**Publikacja 2, Rycina 6a**). Aby określić mechanizm interakcji białek GATA z promotorem *Prdm3*, zastosowano plazmid kodujący skróconą wersję GATA4 (dominujący-negatywny konkurent, DN) [130]. Konstrukcja DN nie zawiera domen transaktywacyjnych białek GATA. Pomimo zredukowanej struktury białka, DN może wiązać się z promotorami zależnymi od GATA przez domeny palca cynkowego, ale bez funkcji aktywacji transkrypcji [130]. Chociaż rdzeń konstrukcji DN jest oparty na sekwencji kodującej białko GATA4, rodzina GATA jest wysoce konserwatywna w domenach palców cynkowych. W związku z tym, DN może być używany jako ogólny konkurent wiązania GATA [143]. Konstrukt DN zastosowano do przetestowania bezpośredniego wpływu GATA6 na promotor *Prdm3*. DN znacznie obniżył aktywność promotora *Prdm3*, jednak wyciszenie ekspresji lucyferazy nie było absolutne (**Publikacja 2, Rycina S3**). Następnie uwaga została skupiona na potencjalnym związku

między ścieżką molekularną zależną od RA a białkami GATA w kontekście promotora *Prdm3*. Zastosowanie RA zwiększało około 40-krotnie aktywność promotora *Prdm3* (**Publikacja 2, Rycina 6b**). Ponadto zbadano synergistyczny wpływ wybranych czynników GATA wraz z RA na aktywność promotora *Prdm3*. Niezróżnicowane komórki P19 transfekowano plazmidem kodującym *Gata3*, *Gata4* lub *Gata6*. Po 24 godzinach komórki stymulowano RA przez następne 24 godziny. Jednoczesne zastosowanie RA i nadekspresji *Gata* spowodowało silną synergistyczną aktywację promotora *Prdm3*. Najbardziej znaczący efekt wystąpił w przypadku nadekspresji GATA6 wraz z stymulacją zależną od RA (około 140-krotny) (**Publikacja 2, Rycina 6b**).

Głównymi mediatorami sygnalizacji RA w jądrze komórkowym są receptory RA (RAR), które oddziałują bezpośrednio z elementami odpowiedzi RA (RARE) w regulatorowych regionach DNA [144]. Wcześniej wykazano, że RA aktywuje ekspresję genów RARα i RARβ w komórkach P19 [145, 146]. Plazmidy kodujące konstytutywnie aktywną postać receptorów RA (pCMX-VP16-RARα i pCMX-VP16-RARβ) zastosowano do oceny ich roli w kontekście promotora *Prdm3*. Domena aktywacyjna VP16 jest połączona z białkiem RAR i umożliwia stałą aktywację RAR przy jednoczesnym braku RA w pożywce [147]. Zastosowanie VP16-RARα i VP16-RARβ spowodowało znaczący wzrost aktywności promotora *Prdm3* (**Publikacja 2, Rycina 6c**). Następnie podjęto próbę wyjaśnienia obserwowanego wcześniej efektu synergistycznego. Niemniej jednak kotransfekcja RARα/ RARβ z plazmidami kodującymi GATA6 wykazywała znacząco wysoki, ale niesynergistyczny wpływ na aktywność promotora *Prdm3* (**Publikacja 2, Rycina 6c**).

Analiza regionu promotora *Prdm3* wykazała odwróconą sekwencję konsensusową dla RARE (CGACCT*ttttg*TGACCT). RARE składa się z dwóch domen oddzielonych pięcioma nukleotydami (zaznaczone kursywą) [148]. Aby ocenić wpływ RARE na aktywność promotora, zmutowano miejsca sekwencji docelowej dla RARα i RARβ. Obie mutacje w sekwencji RARE nie wyeliminowały całkowicie aktywności promotora *Prdm3* po transfekcji VP16-RARα czy VP16-RARβ (**Publikacja 2, Rycina S4**). Wynik ten sugeruje tylko częściowy związek między promotorem *Prdm3* a receptorami RA.

6 Dyskusja

W celu zbadania roli PRDM3 podczas neurogenezy zastosowano uproszczony protokół wykorzystujący linię komórkową P19 (pochodząca z zarodkowego potworniaka u myszy). Komórki P19 przejawiają pluripotencjalne cechy i zdolność do różnicowania się we wszystkie trzy listki zarodkowe w obecności czynników stymulujących dojrzewanie komórkowe. Ekspozycja komórek P19 na RA indukuje różnicowanie się do komórek neuronalnych [57]. Model neurogenezy komórek P19 znacznie naśladuje wczesny rozwój neuronalny *in vivo* [68, 149], dlatego komórki te są szeroko stosowane w badaniach podstawowych molekularnych mechanizmów różnicowania neuronów [150, 151] oraz chorób neurodegeneracyjnych, takich jak choroba Alzheimera [152, 153]. Metody indukcji neurogenezy opartej na komórkach P19 zostały opisane w wielu badaniach, ale złożoność metodologii utrudnia jej użyteczność. W **Publikacji 1** opracowano uproszczony protokół neurogenezy z wykorzystaniem komórek P19. Metoda ta jest przyjazna dla użytkownika i wydajna w generowaniu komórek neuronów [137]. Jak wykazano w **Publikacji 1 (Rycina 2)**, niezróżnicowane komórki P19 hodowane w DMEM z 10% FBS miały wysoką ekspresję pluripotentnych genów (*Oct4* i *Nanog*) bez obserwowanego

samoróżnicowania się komórek (brak ekspresji *Map2* i *NeuN*, **Publikacja 1, Rycina 2**). Ponadto wykazano, że zastosowanie pożywki składającej się wyłącznie z DMEM i 5% FBS z dodatkiem RA skutecznie indukuje proces neurogenezy w komórkach P19. Markery różnicowania neuronalnego: *Map2* i *NeuN* miały znacząco wysoką ekspresję w kolejnych dniach różnicowania komórek (**Publikacja 1, Rycina 2, 4**). Ta uproszczona metoda w pełni spełnia wymagania modeli neurogenezy *in vitro* i dlatego została wykorzystana do badania roli PRDM3.

Wydaje się, że PRDM3 może pełnić funkcję represyjną podczas różnicowania neuronów, co wykazano u *Drosophila melanogaster* [154]. U kręgowców, funkcja PRDM3 jest słabo poznana. Wyłączenie ekspresji *Prdm3* jest letalne dla zarodków, które ponadto wykazują wady rozwojowe mózgu i kręgosłupa [125]. Ekspresję *Prdm3* obserwuje się również u innych kręgowców. I tak na przykład, *Prdm3* zidentyfikowano podczas rozwoju struktur mózgowych u danio pręgowanego [155]. Zwiększony poziom ekspresji *Prdm3* został zaobserwowany podczas neurogenezy ludzkich komórek embrionalnych oraz w mysich neuronach postmitotycznych [25,128]. W **Publikacji 2** wykazano zwiększoną ekspresję genu *Prdm3* podczas neurogenezy komórek P19 traktowanych RA (**Rycina 1b**). Aby określić jaką rolę może odgrywać PRDM3 w różnicowaniu neuronów, zastosowano metodę CRISPR/Cas9 w celu wygenerowania komórek P19 z wyłączoną ekspresją *Prdm3*. Komórki z niedoborem PRDM3 wykazywały podwyższoną ekspresję genów związanych z pluripotencją podczas neurogenezy (**Publikacja 2, Rycina 3a, b**). Oznacza to, że brak PRDM3 spowodował niepełne wyjście ze stadium niezróżnicowanych komórek, a tym samym spowodowało to rozregulowanie różnicowania neuronalnego. PAX6 jest jednym z najważniejszych czynników kontrolujących wczesną fazę neurogenezy [139]. Poziom ekspresji PAX6 dostraja program molekularny w celu utrzymania równowagi między samoodnową neuronalnych komórek macierzystych a różnicowaniem neuronów [139]. W **Publikacji 2** obserwowano podwyższenie poziomu *Pax6* podczas neurogenezy. Jednak komórki P19 z niedoborem PRDM3 wykazywały zmniejszoną ekspresję *Pax6* w porównaniu z komórkami typu dzikiego (**Publikacja 2, Rycina 3c**). W kolejnych dniach neurogenezy komórki z niedoborem PRDM3 wykazywały znaczący spadek ekspresji tubuliny β-III (**Publikacja 2, Rycina 3d**). Częściowo można to wytłumaczyć znacznym wzrostem ekspresji *Oct4* i *Nanog* (**Publikacja 2, Rycina 3a, b, d**). Wynik ten sugerował wysoką proliferację komórek nieneuronalnych w komórkach z wyłączoną ekspresją *Prdm3,* podczas gdy komórki typu dzikiego wykazywały stopniowy wzrost ekspresji markerów dojrzałych neuronów (**Publikacja 2, Rycina 3d i Rycina 4a, b**). Na podstawie powyższych obserwacji wydaje się, że PRDM3 może odgrywać istotną rolę w regulacji neurogenezy, zwłaszcza w fazie indukcji. Należy zauważyć, że komórki *Prdm3* KO weszły w fazę dojrzewania neuronalnego wcześniej niż komórki typu dzikiego, ale nie były w stanie utrzymać tego procesu.

Czynniki GATA są dobrze rozpoznane w rozwoju narządów pochodzenia endodermalnego [86]. Jednak wiedza na temat ich udziału w rozwoju układu nerwowego jest skromna. Wiadomo, że GATA2 i GATA3 są odpowiedzialne za ustalanie tożsamości neuronów glutaminergicznych i serotoninergicznych podczas wczesnego różnicowania [88]. W **Publikacji 2** wykazano, że ekspresja genów *Gata* była podwyższona w przebiegu neurogenezy (**Rycina 5a-c**). Ponadto, wcześniej opisywano, że GATA1 może oddziaływać z promotorem *Prdm3* [156]. W **Publikacji 2** wykazano, że aktywność promotora *Prdm3* zależy od czynników GATA, przy czym największy efekt obserwuje się przy nadekspresji *Gata6* (**Rycina 6a**).

Ekspresja *Prdm3* jest stymulowana przez RA w ludzkich komórkach NTERA-2 i ostrej białaczki szpikowej [157, 158]. Podobne zjawisko zostało przedstawione w **Publikacji 2**, gdzie odnotowano 40-krotny wzrost aktywności promotora *Prdm3* w obecności RA (**Rycina 6b**). Co ciekawe, zaobserwowano również odziaływanie między ścieżką sygnalizacyjną zależną od RA i GATA6 (**Publikacja 2, Rycina 6b**). Wcześniej podobną interakcję między sygnalizacją zależną od RA a GATA2 opisano w różnicowaniu układu krwiotwórczego [89]. Dane te są zgodne z wynikami przedstawionymi w **Publikacji 2** i sugerują wspólny udział szlaku sygnałowego zależnego od RA z białkami GATA podczas różnicowania komórek. Analiza sekwencji promotora *Prdm3* ujawniła liczne motywy konsensusowe wiążące GATA, co utrudnia zbadanie poszczególnych miejsc wiązania. Do rozszyfrowania wpływu czynników GATA na regulację ekspresji *Prdm3* wykorzystano plazmid kodujący konstrukt białka GATA4 (DN) [130]. GATA DN nie obniżył całkowicie aktywności promotora *Prdm3*. Tym samym, wynik ten sugeruje, że wpływ czynników GATA na promotor *Prdm3* może zależeć również od innych sygnałów transkrypcyjnych.

Aby wyjaśnić mechanizm działania RA na promotor *Prdm3*, skupiono się na efekcie synergistycznym między stymulacją zależną od RA a nadekspresją GATA. W sygnalizacji RA pośredniczą głównie receptory kwasu retinowego (RAR). RAR działają jako czynniki transkrypcyjne podczas różnicowania komórkowego i są aktywowane przez wiązanie agonisty-kwas retinowy [159-161]. W sekwencji promotora *Prdm3* zidentyfikowano element odpowiedzi kwasu retinowego (RARE) (**Publikacja 2, Rycina S2**). Badanie to ujawniło, że aktywność promotora *Prdm3* jest częściowo zależna od interakcji między RARα i RARβ z elementem RARE (**Publikacja 2, Rycina S4**). We wcześniejszych badaniach Tsuzuki i wsp. (2004) przedstawili synergistyczny efekt wywoływany przez GATA2 i RARα w ludzkich komórkach szpikowych KG1 [89]. W **Publikacji 2** (**Rycina 6c**) addytywny efekt stymulujący obserwowano po wywołaniu nadekspresji *RARα*, *RARβ* i *Gata6* w komórkach P19. Dlatego synergizm między czynnikami RA i GATA można częściowo wyjaśnić zaangażowaniem RAR. RA jest jednym z najważniejszych czynników kształtujących układ nerwowy zarodków [162]. Niemniej jednak wiele jego celów i ścieżek sygnalizacyjnych pozostaje niezbadanych. Dlatego dokładny mechanizm synergii między czynnikami RA i GATA nie został w pełni wyjaśniony w tym badaniu. Rola czynników GATA w rozwoju układu nerwowego pozostaje zagadkowa i wciąż słabo poznana [163]. Ostatecznie nie można wykluczyć wpływu innych czynników na aktywność promotora *Prdm3*, zwłaszcza tych, które mogą być istotnie zależne od szlaku sygnałowego GATA i RA.

7 Wnioski:

1. Metodologię różnicowania neuronów w komórkach P19 można uprościć bez negatywnego wpływu na proces neurogenezy.

2. Ekspresja *Prdm3* wzrasta podczas neurogenezy w komórkach P19.

3. Niedobór PRDM3 w komórkach P19 wywołuje przedwczesne różnicowanie neuronów i nasila proliferację komórek nieneuronalnych.

4. GATA3, GATA4, GATA6 zwiększają aktywność promotora *Prdm3*.

5. Kwas retinowy i czynniki GATA wykazują synergistyczny wpływ na aktywność promotora *Prdm3*.

6. RARα i RARβ zwiększają aktywność promotora *Prdm3*.

7. RARα i RARβ częściowo stymulują aktywność promotora *Prdm3* poprzez ich wiązanie z domeną RARE.

8. Literatura

1. 1.Alvarez-Buylla, A., J. M. García-Verdugo, and A. D. Tramontin. "A Unified Hypothesis on the Lineage of Neural Stem Cells." Nat Rev Neurosci 2, no. 4 (2001): 287-93.
2. Kempermann, G., H. Song, and F. H. Gage. "Neurogenesis in the Adult Hippocampus." Cold Spring Harb Perspect Biol 7, no. 9 (2015): a018812.
3. Mira, H., and J. Morante. "Corrigendum: Neurogenesis from Embryo to Adult - Lessons from Flies and Mice." Front Cell Dev Biol 8 (2020): 686.
4. Lupo, G., M. Bertacchi, N. Carucci, G. Augusti-Tocco, S. Biagioni, and F. Cremisi. "From Pluripotency to Forebrain Patterning: An in Vitro Journey Astride Embryonic Stem Cells." Cell Mol Life Sci 71, no. 15 (2014): 2917-30.
5. Olariu, V., C. Lövkvist, and K. Sneppen. "Nanog, Oct4 and Tet1 Interplay in Establishing Pluripotency." Sci Rep 6 (2016): 25438.
6. Yamanaka, Y., A. Ralston, R. O. Stephenson, and J. Rossant. "Cell and Molecular Regulation of the Mouse Blastocyst." Dev Dyn 235, no. 9 (2006): 2301-14.
7. Blake, J. A., and M. R. Ziman. "Pax Genes: Regulators of Lineage Specification and Progenitor Cell Maintenance." Development 141, no. 4 (2014): 737-51.
8. He, P., and B. A. Williams. "The Changing Mouse Embryo Transcriptome at Whole Tissue and Single-Cell Resolution." 583, no. 7818 (2020): 760-67.
9. Ghysen, A., and C. Dambly-Chaudiere. "Genesis of the Drosophila Peripheral Nervous System." Trends Genet 5, no. 8 (1989): 251-5.
10. Kiefer, J. C., A. Jarman, and J. Johnson. "Pro-Neural Factors and Neurogenesis." Dev Dyn 234, no. 3 (2005): 808-13.
11. Wilkinson, G., D. Dennis, and C. Schuurmans. "Proneural Genes in Neocortical Development." Neuroscience 253 (2013): 256-73.
12. Yu, P., E. C. McKinney, M. M. Kandasamy, A. L. Albert, and R. B. Meagher. "Characterization of Brain Cell Nuclei with Decondensed Chromatin." Dev Neurobiol 75, no. 7 (2015): 738-56.
13. Huber, G., and A. Matus. "Differences in the Cellular Distributions of Two Microtubule-Associated Proteins, Map1 and Map2, in Rat Brain." J Neurosci 4, no. 1 (1984): 151-60.
14. Caceres, A., G. Banker, O. Steward, L. Binder, and M. Payne. "Map2 Is Localized to the Dendrites of Hippocampal Neurons Which Develop in Culture." Brain Res 315, no. 2 (1984): 314-8.
15. Lyu, J., F. Costantini, E. H. Jho, and C. K. Joo. "Ectopic Expression of Axin Blocks Neuronal Differentiation of Embryonic Carcinoma P19 Cells." J Biol Chem 278, no. 15 (2003): 13487-95.
16. Behm, M., H. Wahlstedt, A. Widmark, M. Eriksson, and M. Öhman. "Accumulation of Nuclear Adar2 Regulates Adenosine-to-Inosine Rna Editing During Neuronal Development." 130, no. 4 (2017): 745-53.

17. Zhang, S. C., M. Wernig, I. D. Duncan, O. Brüstle, and J. A. Thomson. "In Vitro Differentiation of Transplantable Neural Precursors from Human Embryonic Stem Cells." Nat Biotechnol 19, no. 12 (2001): 1129-33.
18. Schulz, T. C., S. A. Noggle, G. M. Palmarini, D. A. Weiler, I. G. Lyons, K. A. Pensa, A. C. Meedeniya, B. P. Davidson, N. A. Lambert, and B. G. Condie. "Differentiation of Human Embryonic Stem Cells to Dopaminergic Neurons in Serum-Free Suspension Culture." Stem Cells 22, no. 7 (2004): 1218-38.
19. Zeng, X., J. Cai, J. Chen, Y. Luo, Z. B. You, E. Fotter, Y. Wang, B. Harvey, T. Miura, C. Backman, G. J. Chen, M. S. Rao, and W. J. Freed. "Dopaminergic Differentiation of Human Embryonic Stem Cells." Stem Cells 22, no. 6 (2004): 925-40.
20. Fathi, A., H. Rasouli, M. Yeganeh, G. H. Salekdeh, and H. Baharvand. "Efficient Differentiation of Human Embryonic Stem Cells toward Dopaminergic Neurons Using Recombinant Lmx1a Factor." Mol Biotechnol 57, no. 2 (2015): 184-94.
21. Lu, H. E., Y. C. Yang, S. M. Chen, H. L. Su, P. C. Huang, M. S. Tsai, T. H. Wang, C. P. Tseng, and S. M. Hwang. "Modeling Neurogenesis Impairment in Down Syndrome with Induced Pluripotent Stem Cells from Trisomy 21 Amniotic Fluid Cells." Exp Cell Res 319, no. 4 (2013): 498-505.
22. Compagnucci, C., M. Nizzardo, S. Corti, G. Zanni, and E. Bertini. "In Vitro Neurogenesis: Development and Functional Implications of Ipsc Technology." Cell Mol Life Sci 71, no. 9 (2014): 1623-39.
23. Velasco, I., P. Salazar, A. Giorgetti, V. Ramos-Mejía, J. Castaño, D. Romero-Moya, and P. Menendez. "Concise Review: Generation of Neurons from Somatic Cells of Healthy Individuals and Neurological Patients through Induced Pluripotency or Direct Conversion." Stem Cells 32, no. 11 (2014): 2811-7.
24. Schulz, T. C., G. M. Palmarini, S. A. Noggle, D. A. Weiler, M. M. Mitalipova, and B. G. Condie. "Directed Neuronal Differentiation of Human Embryonic Stem Cells." BMC Neurosci 4 (2003): 27.
25. Elkabetz, Y., G. Panagiotakos, G. Al Shamy, N. D. Socci, V. Tabar, and L. Studer. "Human Es Cell-Derived Neural Rosettes Reveal a Functionally Distinct Early Neural Stem Cell Stage." Genes Dev 22, no. 2 (2008): 152-65.
26. Kawasaki, H., K. Mizuseki, S. Nishikawa, S. Kaneko, Y. Kuwana, S. Nakanishi, S. I. Nishikawa, and Y. Sasai. "Induction of Midbrain Dopaminergic Neurons from Es Cells by Stromal Cell-Derived Inducing Activity." Neuron 28, no. 1 (2000): 31-40.
27. Vazin, T., J. Chen, C. T. Lee, R. Amable, and W. J. Freed. "Assessment of Stromal-Derived Inducing Activity in the Generation of Dopaminergic Neurons from Human Embryonic Stem Cells." Stem Cells 26, no. 6 (2008): 1517-25.
28. Ying, Q. L., M. Stavridis, D. Griffiths, M. Li, and A. Smith. "Conversion of Embryonic Stem Cells into Neuroectodermal Precursors in Adherent Monoculture." Nat Biotechnol 21, no. 2 (2003): 183-6.
29. Gerrard, L., L. Rodgers, and W. Cui. "Differentiation of Human Embryonic Stem Cells to Neural Lineages in Adherent Culture by Blocking Bone Morphogenetic Protein Signaling." Stem Cells 23, no. 9 (2005): 1234-41.
30. Wongpaiboonwattana, W., and M. P. Stavridis. "Neural Differentiation of Mouse Embryonic Stem Cells in Serum-Free Monolayer Culture." J Vis Exp, no. 99 (2015): e52823.
31. Zhang, M., J. Ngo, F. Pirozzi, Y. P. Sun, and A. Wynshaw-Boris. "Highly Efficient Methods to Obtain Homogeneous Dorsal Neural Progenitor Cells from Human and Mouse Embryonic Stem Cells and Induced Pluripotent Stem Cells." Stem Cell Res Ther 9, no. 1 (2018): 67.

32. Tukker, A. M., F. M. J. Wijnolts, A. de Groot, and R. H. S. Westerink. "Human Ipsc-Derived Neuronal Models for in Vitro Neurotoxicity Assessment." Neurotoxicology 67 (2018): 215-25.
33. Xu, C., M. S. Inokuma, J. Denham, K. Golds, P. Kundu, J. D. Gold, and M. K. Carpenter. "Feeder-Free Growth of Undifferentiated Human Embryonic Stem Cells." Nat Biotechnol 19, no. 10 (2001): 971-4.
34. Martello, G., and A. Smith. "The Nature of Embryonic Stem Cells." Annu Rev Cell Dev Biol 30 (2014): 647-75.
35. Greene, L. A., and A. S. Tischler. "Establishment of a Noradrenergic Clonal Line of Rat Adrenal Pheochromocytoma Cells Which Respond to Nerve Growth Factor." Proc Natl Acad Sci U S A 73, no. 7 (1976): 2424-8.
36. Westerink, R. H., and A. G. Ewing. "The Pc12 Cell as Model for Neurosecretion." Acta Physiol (Oxf) 192, no. 2 (2008): 273-85.
37. Das, K. P., T. M. Freudenrich, and W. R. Mundy. "Assessment of Pc12 Cell Differentiation and Neurite Growth: A Comparison of Morphological and Neurochemical Measures." Neurotoxicol Teratol 26, no. 3 (2004): 397-406.
38. Yang, X., X. Liu, X. Zhang, H. Lu, J. Zhang, and Y. Zhang. "Investigation of Morphological and Functional Changes During Neuronal Differentiation of Pc12 Cells by Combined Hopping Probe Ion Conductance Microscopy and Patch-Clamp Technique." Ultramicroscopy 111, no. 8 (2011): 1417-22.
39. Shipley, M. M., C. A. Mangold, and M. L. Szpara. "Differentiation of the Sh-Sy5y Human Neuroblastoma Cell Line." J Vis Exp, no. 108 (2016): 53193.
40. Forster, J. I., S. Köglsberger, C. Trefois, O. Boyd, A. S. Baumuratov, L. Buck, R. Balling, and P. M. Antony. "Characterization of Differentiated Sh-Sy5y as Neuronal Screening Model Reveals Increased Oxidative Vulnerability." J Biomol Screen 21, no. 5 (2016): 496-509.
41. Andrews, P. W., M. M. Matin, A. R. Bahrami, I. Damjanov, P. Gokhale, and J. S. Draper. "Embryonic Stem (Es) Cells and Embryonal Carcinoma (Ec) Cells: Opposite Sides of the Same Coin." Biochem Soc Trans 33, no. Pt 6 (2005): 1526-30.
42. Przyborski, S. A., V. B. Christie, M. W. Hayman, R. Stewart, and G. M. Horrocks. "Human Embryonal Carcinoma Stem Cells: Models of Embryonic Development in Humans." Stem Cells Dev 13, no. 4 (2004): 400-8.
43. Martin, G. R. "Isolation of a Pluripotent Cell Line from Early Mouse Embryos Cultured in Medium Conditioned by Teratocarcinoma Stem Cells." Proc Natl Acad Sci U S A 78, no. 12 (1981): 7634-8.
44. McBurney, M. W., E. M. Jones-Villeneuve, M. K. Edwards, and P. J. Anderson. "Control of Muscle and Neuronal Differentiation in a Cultured Embryonal Carcinoma Cell Line." Nature 299, no. 5879 (1982): 165-7.
45. Soprano, D. R., B. W. Teets, and K. J. Soprano. "Role of Retinoic Acid in the Differentiation of Embryonal Carcinoma and Embryonic Stem Cells." Vitam Horm 75 (2007): 69-95.
46. van der Heyden, M. A., and L. H. Defize. "Twenty One Years of P19 Cells: What an Embryonal Carcinoma Cell Line Taught Us About Cardiomyocyte Differentiation." Cardiovasc Res 58, no. 2 (2003): 292-302.
47. Lee, V. M., and P. W. Andrews. "Differentiation of Ntera-2 Clonal Human Embryonal Carcinoma Cells into Neurons Involves the Induction of All Three Neurofilament Proteins." J Neurosci 6, no. 2 (1986): 514-21.
48. Andrews, P. W. "Retinoic Acid Induces Neuronal Differentiation of a Cloned Human Embryonal Carcinoma Cell Line in Vitro." Dev Biol 103, no. 2 (1984): 285-93.

49. Coyle, D. E., J. Li, and M. Baccei. "Regional Differentiation of Retinoic Acid-Induced Human Pluripotent Embryonic Carcinoma Stem Cell Neurons." PLoS One 6, no. 1 (2011): e16174.
50. Tamai, Y., Y. Takemoto, M. Matsumoto, T. Morita, A. Matsushiro, and M. Nozaki. "Sequence of Endoa Gene Encoding Mouse Cytokeratin and Its Methylation State in the Cpg-Rich Region." Gene 104, no. 2 (1991): 169-76.
51. Marikawa, Y., T. C. Fujita, and V. B. Alarcón. "Heterogeneous DNA Methylation Status of the Regulatory Element of the Mouse Oct4 Gene in Adult Somatic Cell Population." Cloning Stem Cells 7, no. 1 (2005): 8-16.
52. Darbinian, N. "Cultured Cell Line Models of Neuronal Differentiation: Nt2, Pc12." Methods Mol Biol 1078 (2013): 23-33.
53. Solnica-Krezel, L., and D. S. Sepich. "Gastrulation: Making and Shaping Germ Layers." Annu Rev Cell Dev Biol 28 (2012): 687-717.
54. Ramkumar, N., and K. V. Anderson. "Snapshot: Mouse Primitive Streak." Cell 146, no. 3 (2011): 488-88.e2.
55. Sajini, A. A., L. V. Greder, J. R. Dutton, and J. M. Slack. "Loss of Oct4 Expression During the Development of Murine Embryoid Bodies." Dev Biol 371, no. 2 (2012): 170-9.
56. ten Berge, D., W. Koole, C. Fuerer, M. Fish, E. Eroglu, and R. Nusse. "Wnt Signaling Mediates Self-Organization and Axis Formation in Embryoid Bodies." Cell Stem Cell 3, no. 5 (2008): 508-18.
57. McBurney, M. W., and B. J. Rogers. "Isolation of Male Embryonal Carcinoma Cells and Their Chromosome Replication Patterns." Dev Biol 89, no. 2 (1982): 503-8.
58. McLoughlin, G. A., J. E. Hede, J. G. Temple, J. Bradley, D. M. Chapman, and J. McFarland. "The Role of Iga in the Prevention of Bacterial Colonization of the Jejunum in the Vagotomized Subject." Br J Surg 65, no. 6 (1978): 435-7.
59. Monzen, K., I. Shiojima, Y. Hiroi, S. Kudoh, T. Oka, E. Takimoto, D. Hayashi, T. Hosoda, A. Habara-Ohkubo, T. Nakaoka, T. Fujita, Y. Yazaki, and I. Komuro. "Bone Morphogenetic Proteins Induce Cardiomyocyte Differentiation through the Mitogen-Activated Protein Kinase Kinase Kinase Tak1 and Cardiac Transcription Factors Csx/Nkx-2.5 and Gata-4." Mol Cell Biol 19, no. 10 (1999): 7096-105.
60. Yang, J., S. J. Ko, B. S. Kim, H. S. Kim, S. Park, D. Hong, S. W. Hong, J. H. Choi, C. Y. Park, S. C. Choi, S. J. Hong, and D. S. Lim. "Enhanced Cardiomyogenic Differentiation of P19 Embryonal Carcinoma Stem Cells." Korean Circ J 39, no. 5 (2009): 198-204.
61. Jasmin, D. C. Spray, A. C. Campos de Carvalho, and R. Mendez-Otero. "Chemical Induction of Cardiac Differentiation in P19 Embryonal Carcinoma Stem Cells." Stem Cells Dev 19, no. 3 (2010): 403-12.
62. McBurney, M. W., K. R. Reuhl, A. I. Ally, S. Nasipuri, J. C. Bell, and J. Craig. "Differentiation and Maturation of Embryonal Carcinoma-Derived Neurons in Cell Culture." J Neurosci 8, no. 3 (1988): 1063-73.
63. Morassutti, D. J., W. A. Staines, D. S. Magnuson, K. C. Marshall, and M. W. McBurney. "Murine Embryonal Carcinoma-Derived Neurons Survive and Mature Following Transplantation into Adult Rat Striatum." Neuroscience 58, no. 4 (1994): 753-63.
64. MacPherson, P. A., S. Jones, P. A. Pawson, K. C. Marshall, and M. W. McBurney. "P19 Cells Differentiate into Glutamatergic and Glutamate-Responsive Neurons in Vitro." Neuroscience 80, no. 2 (1997): 487-99.

65. Magnuson, D. S., D. J. Morassutti, M. W. McBurney, and K. C. Marshall. "Neurons Derived from P19 Embryonal Carcinoma Cells Develop Responses to Excitatory and Inhibitory Neurotransmitters." Brain Res Dev Brain Res 90, no. 1-2 (1995): 141-50.
66. Magnuson, D. S., D. J. Morassutti, W. A. Staines, M. W. McBurney, and K. C. Marshall. "In Vivo Electrophysiological Maturation of Neurons Derived from a Multipotent Precursor (Embryonal Carcinoma) Cell Line." Brain Res Dev Brain Res 84, no. 1 (1995): 130-41.
67. McBurney, M. W. "P19 Embryonal Carcinoma Cells." Int J Dev Biol 37, no. 1 (1993): 135-40.
68. Bain, G., W. J. Ray, M. Yao, and D. I. Gottlieb. "From Embryonal Carcinoma Cells to Neurons: The P19 Pathway." Bioessays 16, no. 5 (1994): 343-8.
69. Wei, Y., T. Harris, and G. Childs. "Global Gene Expression Patterns During Neural Differentiation of P19 Embryonic Carcinoma Cells." Differentiation 70, no. 4-5 (2002): 204-19.
70. Haushalter, C., L. Asselin, V. Fraulob, P. Dollé, and M. Rhinn. "Retinoic Acid Controls Early Neurogenesis in the Developing Mouse Cerebral Cortex." Dev Biol 430, no. 1 (2017): 129-41.
71. Hatakeyama, J., Y. Bessho, K. Katoh, S. Ookawara, M. Fujioka, F. Guillemot, and R. Kageyama. "Hes Genes Regulate Size, Shape and Histogenesis of the Nervous System by Control of the Timing of Neural Stem Cell Differentiation." Development 131, no. 22 (2004): 5539-50.
72. Sahara, S., and D. D. O'Leary. "Fgf10 Regulates Transition Period of Cortical Stem Cell Differentiation to Radial Glia Controlling Generation of Neurons and Basal Progenitors." Neuron 63, no. 1 (2009): 48-62.
73. Kageyama, R., T. Ohtsuka, H. Shimojo, and I. Imayoshi. "Dynamic Notch Signaling in Neural Progenitor Cells and a Revised View of Lateral Inhibition." Nat Neurosci 11, no. 11 (2008): 1247-51.
74. Antonelli, F., A. Casciati, and S. Pazzaglia. "Sonic Hedgehog Signaling Controls Dentate Gyrus Patterning and Adult Neurogenesis in the Hippocampus." Neural Regen Res 14, no. 1 (2019): 59-61.
75. Grandbarbe, L., J. Bouissac, M. Rand, M. Hrabé de Angelis, S. Artavanis-Tsakonas, and E. Mohier. "Delta-Notch Signaling Controls the Generation of Neurons/Glia from Neural Stem Cells in a Stepwise Process." Development 130, no. 7 (2003): 1391-402.
76. Bolós, V., J. Grego-Bessa, and J. L. de la Pompa. "Notch Signaling in Development and Cancer." Endocr Rev 28, no. 3 (2007): 339-63.
77. Blumberg, B. "An Essential Role for Retinoid Signaling in Anteroposterior Neural Specification and Neuronal Differentiation." Semin Cell Dev Biol 8, no. 4 (1997): 417-28.
78. Ross, S. A., P. J. McCaffery, U. C. Drager, and L. M. De Luca. "Retinoids in Embryonal Development." Physiol Rev 80, no. 3 (2000): 1021-54.
79. Bain, G., W. J. Ray, M. Yao, and D. I. Gottlieb. "Retinoic Acid Promotes Neural and Represses Mesodermal Gene Expression in Mouse Embryonic Stem Cells in Culture." Biochem Biophys Res Commun 223, no. 3 (1996): 691-4.
80. Okada, Y., T. Shimazaki, G. Sobue, and H. Okano. "Retinoic-Acid-Concentration-Dependent Acquisition of Neural Cell Identity During in Vitro Differentiation of Mouse Embryonic Stem Cells." Dev Biol 275, no. 1 (2004): 124-42.
81. Niederreither, K., and P. Dollé. "Retinoic Acid in Development: Towards an Integrated View." Nat Rev Genet 9, no. 7 (2008): 541-53.
82. Duester, G. "Retinoic Acid Synthesis and Signaling During Early Organogenesis." Cell 134, no. 6 (2008): 921-31.

83. Maden, M. "Retinoic Acid in the Development, Regeneration and Maintenance of the Nervous System." Nat Rev Neurosci 8, no. 10 (2007): 755-65.
84. Simandi, Z., A. Horvath, I. Cuaranta-Monroy, S. Sauer, J. F. Deleuze, and L. Nagy. "Rxr Heterodimers Orchestrate Transcriptional Control of Neurogenesis and Cell Fate Specification." Mol Cell Endocrinol 471 (2018): 51-62.
85. Engels, M., P. N. Span, R. T. Mitchell, Jjtm Heuvel, M. A. Marijnissen-van Zanten, A. E. van Herwaarden, C. A. Hulsbergen-van de Kaa, E. Oosterwijk, N. M. Stikkelbroeck, L. B. Smith, Fcgj Sweep, and H. L. Claahsen-van der Grinten. "Gata Transcription Factors in Testicular Adrenal Rest Tumours." Endocr Connect 6, no. 8 (2017): 866-75.
86. Lentjes, M. H., H. E. Niessen, Y. Akiyama, A. P. de Bruïne, V. Melotte, and M. van Engeland. "The Emerging Role of Gata Transcription Factors in Development and Disease." Expert Rev Mol Med 18 (2016): e3.
87. Tremblay, M., O. Sanchez-Ferras, and M. Bouchard. "Gata Transcription Factors in Development and Disease." 145, no. 20 (2018).
88. Haugas, M., L. Tikker, K. Achim, M. Salminen, and J. Partanen. "Gata2 and Gata3 Regulate the Differentiation of Serotonergic and Glutamatergic Neuron Subtypes of the Dorsal Raphe." 143, no. 23 (2016): 4495-508.
89. Tsuzuki, S., K. Kitajima, T. Nakano, A. Glasow, A. Zelent, and T. Enver. "Cross Talk between Retinoic Acid Signaling and Transcription Factor Gata-2." Mol Cell Biol 24, no. 15 (2004): 6824-36.
90. Buyse, I. M., G. Shao, and S. Huang. "The Retinoblastoma Protein Binds to Riz, a Zinc-Finger Protein That Shares an Epitope with the Adenovirus E1a Protein." Proc Natl Acad Sci U S A 92, no. 10 (1995): 4467-71.
91. Huang, S. "Blimp-1 Is the Murine Homolog of the Human Transcriptional Repressor Prdi-Bf1." Cell 78, no. 1 (1994): 9.
92. Keller, A. D., and T. Maniatis. "Identification and Characterization of a Novel Repressor of Beta-Interferon Gene Expression." Genes Dev 5, no. 5 (1991): 868-79.
93. Turner, C. A., Jr., D. H. Mack, and M. M. Davis. "Blimp-1, a Novel Zinc Finger-Containing Protein That Can Drive the Maturation of B Lymphocytes into Immunoglobulin-Secreting Cells." Cell 77, no. 2 (1994): 297-306.
94. Xiao, B., J. R. Wilson, and S. J. Gamblin. "Set Domains and Histone Methylation." Curr Opin Struct Biol 13, no. 6 (2003): 699-705.
95. Duan, Z., R. E. Person, H. H. Lee, S. Huang, J. Donadieu, R. Badolato, H. L. Grimes, T. Papayannopoulou, and M. S. Horwitz. "Epigenetic Regulation of Protein-Coding and Microrna Genes by the Gfi1-Interacting Tumor Suppressor Prdm5." Mol Cell Biol 27, no. 19 (2007): 6889-902.
96. Davis, C. A., M. Haberland, M. A. Arnold, L. B. Sutherland, O. G. McDonald, J. A. Richardson, G. Childs, S. Harris, G. K. Owens, and E. N. Olson. "Prism/Prdm6, a Transcriptional Repressor That Promotes the Proliferative Gene Program in Smooth Muscle Cells." Mol Cell Biol 26, no. 7 (2006): 2626-36.
97. Gyory, I., J. Wu, G. Fejér, E. Seto, and K. L. Wright. "Prdi-Bf1 Recruits the Histone H3 Methyltransferase G9a in Transcriptional Silencing." Nat Immunol 5, no. 3 (2004): 299-308.
98. Pinheiro, I., R. Margueron, N. Shukeir, M. Eisold, C. Fritzsch, F. M. Richter, G. Mittler, C. Genoud, S. Goyama, M. Kurokawa, J. Son, D. Reinberg, M. Lachner, and T. Jenuwein. "Prdm3 and Prdm16 Are H3k9me1 Methyltransferases Required for Mammalian Heterochromatin Integrity." Cell 150, no. 5 (2012): 948-60.
99. Kim, K. C., L. Geng, and S. Huang. "Inactivation of a Histone Methyltransferase by Mutations in Human Cancers." Cancer Res 63, no. 22 (2003): 7619-23.

100. Hayashi, K., K. Yoshida, and Y. Matsui. "A Histone H3 Methyltransferase Controls Epigenetic Events Required for Meiotic Prophase." Nature 438, no. 7066 (2005): 374-8.
101. Fog, C. K., G. G. Galli, and A. H. Lund. "Prdm Proteins: Important Players in Differentiation and Disease." Bioessays 34, no. 1 (2012): 50-60.
102. Eom, G. H., K. Kim, S. M. Kim, H. J. Kee, J. Y. Kim, H. M. Jin, J. R. Kim, J. H. Kim, N. Choe, K. B. Kim, J. Lee, H. Kook, N. Kim, and S. B. Seo. "Histone Methyltransferase Prdm8 Regulates Mouse Testis Steroidogenesis." Biochem Biophys Res Commun 388, no. 1 (2009): 131-6.
103. Derunes, C., K. Briknarová, L. Geng, S. Li, C. R. Gessner, K. Hewitt, S. Wu, S. Huang, V. I. Woods, Jr., and K. R. Ely. "Characterization of the Pr Domain of Riz1 Histone Methyltransferase." Biochem Biophys Res Commun 333, no. 3 (2005): 925-34.
104. Yoshimi, A., S. Goyama, N. Watanabe-Okochi, Y. Yoshiki, Y. Nannya, E. Nitta, S. Arai, T. Sato, M. Shimabe, M. Nakagawa, Y. Imai, T. Kitamura, and M. Kurokawa. "Evi1 Represses Pten Expression and Activates Pi3k/Akt/Mtor Via Interactions with Polycomb Proteins." Blood 117, no. 13 (2011): 3617-28.
105. Su, S. T., H. Y. Ying, Y. K. Chiu, F. R. Lin, M. Y. Chen, and K. I. Lin. "Involvement of Histone Demethylase Lsd1 in Blimp-1-Mediated Gene Repression During Plasma Cell Differentiation." Mol Cell Biol 29, no. 6 (2009): 1421-31.
106. Ancelin, K., U. C. Lange, P. Hajkova, R. Schneider, A. J. Bannister, T. Kouzarides, and M. A. Surani. "Blimp1 Associates with Prmt5 and Directs Histone Arginine Methylation in Mouse Germ Cells." Nat Cell Biol 8, no. 6 (2006): 623-30.
107. Alliston, T., T. C. Ko, Y. Cao, Y. Y. Liang, X. H. Feng, C. Chang, and R. Derynck. "Repression of Bone Morphogenetic Protein and Activin-Inducible Transcription by Evi-1." J Biol Chem 280, no. 25 (2005): 24227-37.
108. Chittka, A., J. C. Arevalo, M. Rodriguez-Guzman, P. Pérez, M. V. Chao, and M. Sendtner. "The P75ntr-Interacting Protein Sc1 Inhibits Cell Cycle Progression by Transcriptional Repression of Cyclin E." J Cell Biol 164, no. 7 (2004): 985-96.
109. Yu, J., C. Angelin-Duclos, J. Greenwood, J. Liao, and K. Calame. "Transcriptional Repression by Blimp-1 (Prdi-Bf1) Involves Recruitment of Histone Deacetylase." Mol Cell Biol 20, no. 7 (2000): 2592-603.
110. Cattaneo, F., and G. Nucifora. "Evi1 Recruits the Histone Methyltransferase Suv39h1 for Transcription Repression." J Cell Biochem 105, no. 2 (2008): 344-52.
111. Yang, C. M., and Y. Shinkai. "Prdm12 Is Induced by Retinoic Acid and Exhibits Anti-Proliferative Properties through the Cell Cycle Modulation of P19 Embryonic Carcinoma Cells." Cell Struct Funct 38, no. 2 (2013): 197-206.
112. Hohenauer, T., and A. W. Moore. "The Prdm Family: Expanding Roles in Stem Cells and Development." Development 139, no. 13 (2012): 2267-82.
113. Mzoughi, S., Y. X. Tan, D. Low, and E. Guccione. "The Role of Prdms in Cancer: One Family, Two Sides." Curr Opin Genet Dev 36 (2016): 83-91.
114. Sorrentino, A., M. Rienzo, A. Ciccodicola, A. Casamassimi, and C. Abbondanza. "Human Prdm2: Structure, Function and Pathophysiology." Biochim Biophys Acta Gene Regul Mech (2018).
115. Ren, B., K. J. Chee, T. H. Kim, and T. Maniatis. "Prdi-Bf1/Blimp-1 Repression Is Mediated by Corepressors of the Groucho Family of Proteins." Genes Dev 13, no. 1 (1999): 125-37.
116. Di Zazzo, E., C. De Rosa, C. Abbondanza, and B. Moncharmont. "Prdm Proteins: Molecular Mechanisms in Signal Transduction and Transcriptional Regulation." Biology (Basel) 2, no. 1 (2013): 107-41.

117. Huang, S., G. Shao, and L. Liu. "The Pr Domain of the Rb-Binding Zinc Finger Protein Riz1 Is a Protein Binding Interface and Is Related to the Set Domain Functioning in Chromatin-Mediated Gene Expression." J Biol Chem 273, no. 26 (1998): 15933-9.
118. Bartholomew, C., A. Kilbey, A. M. Clark, and M. Walker. "The Evi-1 Proto-Oncogene Encodes a Transcriptional Repressor Activity Associated with Transformation." Oncogene 14, no. 5 (1997): 569-77.
119. Baizabal, J. M., M. Mistry, M. T. García, N. Gómez, O. Olukoya, D. Tran, M. B. Johnson, C. A. Walsh, and C. C. Harwell. "The Epigenetic State of Prdm16-Regulated Enhancers in Radial Glia Controls Cortical Neuron Position." Neuron 98, no. 5 (2018): 945-62.e8.
120. Hanotel, J., N. Bessodes, A. Thélie, M. Hedderich, K. Parain, B. Van Driessche, O. Brandão Kde, S. Kricha, M. C. Jorgensen, A. Grapin-Botton, P. Serup, C. Van Lint, M. Perron, T. Pieler, K. A. Henningfeld, and E. J. Bellefroid. "The Prdm13 Histone Methyltransferase Encoding Gene Is a Ptf1a-Rbpj Downstream Target That Suppresses Glutamatergic and Promotes Gabaergic Neuronal Fate in the Dorsal Neural Tube." Dev Biol 386, no. 2 (2014): 340-57.
121. Zhou, B., J. Wang, S. Y. Lee, J. Xiong, N. Bhanu, Q. Guo, P. Ma, Y. Sun, R. C. Rao, B. A. Garcia, J. L. Hess, and Y. Dou. "Prdm16 Suppresses Mll1r Leukemia Via Intrinsic Histone Methyltransferase Activity." Mol Cell 62, no. 2 (2016): 222-36.
122. Hwang, B. J., A. D. Meruelo, and P. W. Sternberg. "C. Elegans Evi1 Proto-Oncogene, Egl-43, Is Necessary for Notch-Mediated Cell Fate Specification and Regulates Cell Invasion." Development 134, no. 4 (2007): 669-79.
123. Garriga, G., C. Guenther, and H. R. Horvitz. "Migrations of the Caenorhabditis Elegans Hsns Are Regulated by Egl-43, a Gene Encoding Two Zinc Finger Proteins." Genes Dev 7, no. 11 (1993): 2097-109.
124. Endo, K., M. R. Karim, H. Taniguchi, A. Krejci, E. Kinameri, M. Siebert, K. Ito, S. J. Bray, and A. W. Moore. "Chromatin Modification of Notch Targets in Olfactory Receptor Neuron Diversification." Nat Neurosci 15, no. 2 (2011): 224-33.
125. Hoyt, P. R., C. Bartholomew, A. J. Davis, K. Yutzey, L. W. Gamer, S. S. Potter, J. N. Ihle, and M. L. Mucenski. "The Evi1 Proto-Oncogene Is Required at Midgestation for Neural, Heart, and Paraxial Mesenchyme Development." Mech Dev 65, no. 1-2 (1997): 55-70.
126. Kazama, H., T. Kodera, S. Shimizu, H. Mizoguchi, and K. Morishita. "Ecotropic Viral Integration Site-1 Is Activated During, and Is Sufficient for, Neuroectodermal P19 Cell Differentiation." Cell Growth Differ 10, no. 8 (1999): 565-73.
127. Hirabayashi, Y., and Y. Gotoh. "Epigenetic Control of Neural Precursor Cell Fate During Development." Nat Rev Neurosci 11, no. 6 (2010): 377-88.
128. Hou, Q., H. Ruan, J. Gilbert, G. Wang, Q. Ma, W. D. Yao, and H. Y. Man. "Microrna Mir124 Is Required for the Expression of Homeostatic Synaptic Plasticity." Nat Commun 6 (2015): 10045.
129. CHOPCHOPv2. "Chopchopv2." accessed on 2018 October 22.
130. Tremblay, J. J., N. M. Robert, and R. S. Viger. "Modulation of Endogenous Gata-4 Activity Reveals Its Dual Contribution to Müllerian Inhibiting Substance Gene Transcription in Sertoli Cells." Mol Endocrinol 15, no. 9 (2001): 1636-50.
131. Tremblay, J. J., and R. S. Viger. "Gata Factors Differentially Activate Multiple Gonadal Promoters through Conserved Gata Regulatory Elements." Endocrinology 142, no. 3 (2001): 977-86.

132. Solari, M., J. Paquin, P. Ducharme, and M. Boily. "P19 Neuronal Differentiation and Retinoic Acid Metabolism as Criteria to Investigate Atrazine, Nitrite, and Nitrate Developmental Toxicity." Toxicol Sci 113, no. 1 (2010): 116-26.
133. Babuška, V., V. Kulda, Z. Houdek, M. Pešta, J. Cendelín, N. Zech, J. Pacherník, F. Vožeh, P. Uher, and M. Králíčková. "Characterization of P19 Cells During Retinoic Acid Induced Differentiation." Prague Med Rep 111, no. 4 (2010): 289-99.
134. Monzo, H. J., T. I. H. Park, J. M. Montgomery, R. L. M. Faull, M. Dragunow, and M. A. Curtis. "A Method for Generating High-Yield Enriched Neuronal Cultures from P19 Embryonal Carcinoma Cells." J Neurosci Methods 204, no. 1 (2012): 87-103.
135. Popova, D., J. Karlsson, and S. O. P. Jacobsson. "Comparison of Neurons Derived from Mouse P19, Rat Pc12 and Human Sh-Sy5y Cells in the Assessment of Chemical- and Toxin-Induced Neurotoxicity." 18, no. 1 (2017): 42.
136. Hamada-Kanazawa, M., K. Ishikawa, K. Nomoto, T. Uozumi, Y. Kawai, M. Narahara, and M. Miyake. "Sox6 Overexpression Causes Cellular Aggregation and the Neuronal Differentiation of P19 Embryonic Carcinoma Cells in the Absence of Retinoic Acid." FEBS Lett 560, no. 1-3 (2004): 192-8.
137. Leszczyński, P., M. Śmiech, A. S. Teeli, A. Zołocińska, A. Słysz, Z. Pojda, M. Pierzchała, and H. Taniguchi. "Neurogenesis Using P19 Embryonal Carcinoma Cells." J Vis Exp, no. 146 (2019).
138. Zhang, X. H., L. Y. Tee, X. G. Wang, Q. S. Huang, and S. H. Yang. "Off-Target Effects in Crispr/Cas9-Mediated Genome Engineering." Mol Ther Nucleic Acids 4, no. 11 (2015): e264.
139. Sansom, S. N., D. S. Griffiths, A. Faedo, D. J. Kleinjan, Y. Ruan, J. Smith, V. van Heyningen, J. L. Rubenstein, and F. J. Livesey. "The Level of the Transcription Factor Pax6 Is Essential for Controlling the Balance between Neural Stem Cell Self-Renewal and Neurogenesis." PLoS Genet 5, no. 6 (2009): e1000511.
140. Osumi, N., H. Shinohara, K. Numayama-Tsuruta, and M. Maekawa. "Concise Review: Pax6 Transcription Factor Contributes to Both Embryonic and Adult Neurogenesis as a Multifunctional Regulator." Stem Cells 26, no. 7 (2008): 1663-72.
141. Matus, A., R. Bernhardt, and T. Hugh-Jones. "High Molecular Weight Microtubule-Associated Proteins Are Preferentially Associated with Dendritic Microtubules in Brain." Proc Natl Acad Sci U S A 78, no. 5 (1981): 3010-4.
142. EPD. "Eukaryotic Promoter Database Accessed on 10 October 2018."
143. Viger, R. S., S. M. Guittot, M. Anttonen, D. B. Wilson, and M. Heikinheimo. "Role of the Gata Family of Transcription Factors in Endocrine Development, Function, and Disease." Mol Endocrinol 22, no. 4 (2008): 781-98.
144. Pozzi, S., S. Rossetti, G. Bistulfi, and N. Sacchi. "Rar-Mediated Epigenetic Control of the Cytochrome P450 Cyp26a1 in Embryocarcinoma Cells." Oncogene 25, no. 9 (2006): 1400-7.
145. Jonk, L. J., M. E. de Jonge, F. A. Kruyt, C. L. Mummery, P. T. van der Saag, and W. Kruijer. "Aggregation and Cell Cycle Dependent Retinoic Acid Receptor Mrna Expression in P19 Embryonal Carcinoma Cells." Mech Dev 36, no. 3 (1992): 165-72.
146. Pratt, M. A., C. A. Crippen, and M. Ménard. "Spontaneous Retinoic Acid Receptor Beta 2 Expression During Mesoderm Differentiation of P19 Murine Embryonal Carcinoma Cells." Differentiation 65, no. 5 (2000): 271-9.
147. Lipkin, S. M., T. L. Grider, R. A. Heyman, C. K. Glass, and F. H. Gage. "Constitutive Retinoid Receptors Expressed from Adenovirus Vectors That Specifically Activate Chromosomal Target Genes Required for Differentiation of Promyelocytic Leukemia and Teratocarcinoma Cells." J Virol 70, no. 10 (1996): 7182-9.

148. Bastien, J., and C. Rochette-Egly. "Nuclear Retinoid Receptors and the Transcription of Retinoid-Target Genes." Gene 328 (2004): 1-16.
149. Ulrich, H., and P. Majumder. "Neurotransmitter Receptor Expression and Activity During Neuronal Differentiation of Embryonal Carcinoma and Stem Cells: From Basic Research Towards Clinical Applications." Cell Prolif 39, no. 4 (2006): 281-300.
150. Hong, S., J. Heo, S. Lee, S. Heo, S. S. Kim, Y. D. Lee, M. Kwon, and S. Hong. "Methyltransferase-Inhibition Interferes with Neuronal Differentiation of P19 Embryonal Carcinoma Cells." Biochem Biophys Res Commun 377, no. 3 (2008): 935-40.
151. Harada, Y., F. Takayama, K. Tanabe, J. Ni, Y. Hayashi, K. Yamamoto, Z. Wu, and H. Nakanishi. "Overexpression of Cathepsin E Interferes with Neuronal Differentiation of P19 Embryonal Teratocarcinoma Cells by Degradation of N-Cadherin." Cell Mol Neurobiol 37, no. 3 (2017): 437-43.
152. Woodgate, A., G. MacGibbon, M. Walton, and M. Dragunow. "The Toxicity of 6-Hydroxydopamine on Pc12 and P19 Cells." Brain Res Mol Brain Res 69, no. 1 (1999): 84-92.
153. Tsukane, M., and T. Yamauchi. "Ca2+/Calmodulin-Dependent Protein Kinase Ii Mediates Apoptosis of P19 Cells Expressing Human Tau During Neural Differentiation with Retinoic Acid Treatment." J Enzyme Inhib Med Chem 24, no. 2 (2009): 365-71.
154. Kinameri, E., T. Inoue, J. Aruga, I. Imayoshi, R. Kageyama, T. Shimogori, and A. W. Moore. "Prdm Proto-Oncogene Transcription Factor Family Expression and Interaction with the Notch-Hes Pathway in Mouse Neurogenesis." PLoS One 3, no. 12 (2008): e3859.
155. Sun, X. J., P. F. Xu, T. Zhou, M. Hu, C. T. Fu, Y. Zhang, Y. Jin, Y. Chen, S. J. Chen, Q. H. Huang, T. X. Liu, and Z. Chen. "Genome-Wide Survey and Developmental Expression Mapping of Zebrafish Set Domain-Containing Genes." PLoS One 3, no. 1 (2008): e1499.
156. Maicas, M., I. Vázquez, C. Vicente, M. A. García-Sánchez, N. Marcotegui, L. Urquiza, M. J. Calasanz, and M. D. Odero. "Functional Characterization of the Promoter Region of the Human Evi1 Gene in Acute Myeloid Leukemia: Runx1 and Elk1 Directly Regulate Its Transcription." Oncogene 32, no. 16 (2013): 2069-78.
157. Verhagen, H. J., M. A. Smit, A. Rutten, F. Denkers, P. J. Poddighe, P. A. Merle, G. J. Ossenkoppele, and L. Smit. "Primary Acute Myeloid Leukemia Cells with Overexpression of Evi-1 Are Sensitive to All-Trans Retinoic Acid." Blood 127, no. 4 (2016): 458-63.
158. Bingemann, S. C., T. A. Konrad, and R. Wieser. "Zinc Finger Transcription Factor Ecotropic Viral Integration Site 1 Is Induced by All-Trans Retinoic Acid (Atra) and Acts as a Dual Modulator of the Atra Response." Febs j 276, no. 22 (2009): 6810-22.
159. Lee, K., and I. Skromne. "Retinoic Acid Regulates Size, Pattern and Alignment of Tissues at the Head-Trunk Transition." Development 141, no. 22 (2014): 4375-84.
160. Purton, L. E., I. D. Bernstein, and S. J. Collins. "All-Trans Retinoic Acid Enhances the Long-Term Repopulating Activity of Cultured Hematopoietic Stem Cells." Blood 95, no. 2 (2000): 470-7.
161. Purton, L. E., S. Dworkin, G. H. Olsen, C. R. Walkley, S. A. Fabb, S. J. Collins, and P. Chambon. "Rargamma Is Critical for Maintaining a Balance between Hematopoietic Stem Cell Self-Renewal and Differentiation." J Exp Med 203, no. 5 (2006): 1283-93.
162. Janesick, A., S. C. Wu, and B. Blumberg. "Retinoic Acid Signaling and Neuronal Differentiation." Cell Mol Life Sci 72, no. 8 (2015): 1559-76.

163. Kamnasaran, D., and A. Guha. "Expression of Gata6 in the Human and Mouse Central Nervous System." Brain Res Dev Brain Res 160, no. 1 (2005): 90-5.

9 Publikacje stanowiące rozprawę doktorską

Video Article

Neurogenesis Using P19 Embryonal Carcinoma Cells

Paweł Leszczyński[1], Magdalena Śmiech[1], Aamir S. Teeli[1], Aleksandra Zołocińska[2], Anna Słysz[2], Zygmunt Pojda[2], Mariusz Pierzchała[3], Hiroaki Taniguchi[1]

[1]Department of Experimental Embryology, Institute of Genetics and Animal Breeding, Polish Academy of Sciences

[2]Department of Regenerative Medicine, Maria Skłodowska-Curie Institute - Oncology Center

[3]Department of Genomics and Biodiversities, Institute of Genetics and Animal Breeding, Polish Academy of Sciences

Correspondence to: Hiroaki Taniguchi at h.taniguchi@ighz.pl

URL: https://www.jove.com/video/58225
DOI: doi:10.3791/58225

Keywords: Developmental Biology, Issue 146, neurogenesis, P19 cell line, aggregates, retinoic acid, neurons, differentiation.

Date Published: 4/27/2019

Citation: Leszczyński, P., Śmiech, M., Teeli, A.S., Zołocińska, A., Słysz, A., Pojda, Z., Pierzchała, M., Taniguchi, H. Neurogenesis Using P19 Embryonal Carcinoma Cells. *J. Vis. Exp.* (146), e58225, doi:10.3791/58225 (2019).

Abstract

The P19 cell line derived from a mouse embryo-derived teratocarcinoma has the ability to differentiate into the three germ layers. In the presence of retinoic acid (RA), the suspension cultured P19 cell line is induced to differentiate into neurons. This phenomenon is extensively investigated as a neurogenesis model in vitro. Therefore, the P19 cell line is very useful for molecular and cellular studies associated with neurogenesis. However, protocols for neuronal differentiation of P19 cell line described in the literature are very complex. The method developed in this study are simple and will play a part in elucidating the molecular mechanisms in neurodevelopmental abnormalities and neurodegenerative diseases.

Video Link

The video component of this article can be found at https://www.jove.com/video/58225/

Introduction

During embryonal development, a single cell layer is transformed into three separate germ layers[1,2,3]. To increase the research possibilities of phenomena occurring in vivo, generation of three-dimensional aggregates (embryonic bodies) have been developed as a convenient model. Cellular aggregates formed in this way can be exposed to various conditions causing cell differentiation, which reflect development of the embryo[4,5]. The P19 murine embryonic carcinoma cell line (P19 cell line) is commonly used as a cellular model for neurogenesis studies in vitro[6,7,8]. The P19 cell line exhibits typical pluripotent stem cell features and can differentiate into neurons in the presence of retinoic acid (RA) during cell aggregation followed by neurite outgrowth under adherent conditions. Moreover, the undifferentiated P19 cell line is also capable of forming muscle- and cardiomyocyte-like cells under the influence of dimethyl sulfoxide (DMSO)[9,10,11,12].

Many methods[13,14,15,16] have been reported for neuronal differentiation, but the methodology is sometimes complicated and not easy to grasp by only reading the descriptions. For example, protocols sometimes require a combination of Dulbecco's Modified Eagle Medium (DMEM) medium supplemented with a mixture of calf serum (CS) and fetal bovine serum (FBS)[13]. Moreover, media used for neuronal development are often composed of Neurobasal and B27 supplements[13,14,15,16]. As such, existing methods contain complexity in their preparation and our goal here is to simplify the protocols. In this study, we demonstrated that DMEM with FBS can be utilized for maintaining the P19 cell line (DMEM + 10% FBS) as well as for neuronal development (DMEM + 5% FBS + RA). This simplified method for neurogenesis using the P19 cell line allows us to study the molecular mechanism of how neurons are developed. Moreover, research on neurodegenerative diseases such as Alzheimer's disease is also conducted using P19 cell line[17,18], and we believe that the method developed in this study will play a part in elucidating the molecular mechanisms in neurodevelopmental abnormalities and neurodegenerative diseases.

Protocol

1. Culture Maintenance

1. Culture the P19 cell line in Maintenance Medium (Dulbecco's modified Eagle's medium with 4,500 mg/L of glucose supplemented with 10% FBS, 100 units/mL penicillin and 100 units/mL streptomycin). Incubate at 37 °C and 5% CO_2.

2. Sub-culturing Cells

1. When cells reach approximately 80% confluence, remove the spent medium from the cell culture flasks (surface area 25 cm^2).
2. Wash the cells with 2 mL of phosphate buffered saline (PBS) free of calcium and magnesium.
3. Add 1 mL of 0.25% trypsin-EDTA (ethylenediaminetetraacetic acid) onto the cell monolayer.

Copyright © 2019 Journal of Visualized Experiments

4. Put the flask in the CO_2 incubator (37 °C and 5% CO_2) for 2-3 min.
5. Assess the cell attachment to the flask surface. Ensure that all of the cells are detached and floating in the medium.
6. Add 9 mL of Maintenance Medium to stop the enzymatic activity of trypsin.
7. Resuspend the cells in Maintenance Medium.
8. Transfer cells to a 15 mL tube and centrifuge for 5 min at 200 x *g* and room temperature (RT).
9. Discard the supernatant and add 10 mL of fresh Maintenance Medium into the 15 mL tube.
10. Use the cell suspension to determine the cell number using a cell counter according to manufacturer's instructions.
11. Seed cells at 2 x 10^4 cells/cm2 in a new 25 cm^2 flask.
12. Add the Maintenance Medium up to 10 mL.
13. Put the flask with cells in the CO_2 incubator (37 °C and 5% CO_2) for 2-3 days.

3. Trypsin Digestion

1. Aspirate Maintenance Medium from the cell flask. Wash the cells once with 2 mL of calcium and magnesium-free PBS.
2. Add 1 mL of 0.25% trypsin-EDTA.
3. Put the flask with cells into the CO_2 incubator at 37 °C for 2-3 min.
4. Use 1 mL pipette to dissociate the cells by pipetting cells ten times.
5. Neutralize trypsin by adding 9 mL of Differentiation Medium (Dulbecco's modified Eagle's medium with 4500 mg/L of glucose supplemented with 5% FBS, 100 units/mL penicillin and 100 units/mL streptomycin) without RA to the cells.
6. Transfer cells to a 15 mL tube and centrifuge for 5 min at 200 x *g* and RT.
7. Discard the supernatant and add 1 mL of Differentiation Medium without retinoic acid (RA). Resuspend the cell pellet.
8. Use the cell suspension to determine the cell number using a cell counter according to manufacturer's instruction.

4. Aggregate Generation

1. Add 5 µL of RA (1 mM stock dissolved in 99.8% ethanol, stored at -20 °C) to the 10 mL of Differentiation Medium and mix well (final concentration of 0.5 µM RA).
   NOTE: RA is light sensitive. Low concentration of EtOH does not affect cell differentiation[19,20,21].
2. Add 10 mL of Differentiation Medium (with RA) to the 100 mm non-treated culture dish (dedicated to suspension culture).
3. Seed the 1 x 10^6 cells in the 100 mm dish (Dish surface area 56.5 cm^2).
4. Put the flask with cells into the incubator at 37 °C and 5% CO_2 for 2 days in order to promote aggregates formation.
5. After 2 days, exchange the Differentiation Medium. Aspirate medium containing aggregates using a 10 mL pipette and transfer to a 15 mL tube at RT.
6. Allow the aggregates to settle by gravity for 1.5 min at RT.
7. Discard the supernatant.
8. Add a fresh 10 mL of Differentiation Medium with 0.5 µM RA using a 10 mL serological pipette.
   CAUTION: Do not pipette the cell aggregates up and down.
9. Seed the aggregates into new 100 mm non-treated culture dish (dedicated to suspension culture).
10. Place the plate in the incubator (at 37 °C and 5% CO_2) for 2 days.

5. Aggregates Dissociation

1. Aspirate the cell aggregates using a 10 mL pipette.
2. Transfer the aggregates to a 15 mL tube. Allow the cell aggregates to settle by gravity for 1.5 min.
3. Remove the supernatant.
4. Wash the aggregates with DMEM alone (serum- and antibiotic- free).
5. Allow the cell aggregates to settle by gravity sedimentation for 1.5 min at RT.
6. Aspirate the supernatant and add 2 mL of trypsin-EDTA (0.25%).
7. Place the cell aggregates into a water bath (37 °C) for 10 min. Agitate the aggregates gently every 2 min by tapping with a hand.
8. Stop the trypsinization process by adding 4 mL of Maintenance Medium.
9. Pipette aggregates up and down 20 times using 1 mL pipette.
10. Centrifuge cells for 5 min at 200 x *g* and RT.
11. Remove the supernatant and resuspend the cell pellet in 5 mL of Maintenance Medium.
12. Determine the cell number with a cell counter.

6. Plating Cells

1. Add 3 mL per well of Maintenance Medium to a 6-well plate.
2. Seed cells in the 6-well culture plate at a density of 0.5 x 10^6/well.
3. Incubate at 37 °C with 5% CO_2 concentration.
4. Seed the cells on cover glass in 6 well culture plate and perform immunostaining with anti-MAP2 antibody (20% confluence). Use 6-well plate to isolate RNA and perform RT-PCR for *Map2*, *NeuN*, *Oct4*, *Nanog*, and *Gapdh* (20% confluence).

Copyright © 2019 Journal of Visualized Experiments

Representative Results

The simplified scheme of protocol for neurogenesis induction in P19 cell line is presented in **Figure 1**. In order to define the character of the P19 cell line in an undifferentiated state and during neurogenesis, the RT-PCR (reverse transcription-polymerase chain reaction) method was used. The undifferentiated P19 cell line expressed the pluripotency genes such as organic cation/carnitine transporter4 *(Oct4)* and Nanog homeobox *(Nanog)*. Neurogenesis induced by cells aggregation in suspension culture in the presence of RA led to a rapid decrease of *Oct4* and *Nanog* expression. In contrary, expression of neuron markers: microtubule-associated protein 2 (*Map2)*, *NeuN* (also known as RNA binding protein, fox-1 homolog 3 *(Rbfox3))* increased after triggered neurogenesis (**Figure 2**)[6,14,15,22]. The primers used for each gene are indicated along with nucleotide sequencesand the size of the product in **Table 1.** A microscopic image of the undifferentiated P19 cell line presented a round-shaped morphology (**Figure 3A**). After induction of neurogenesis, the neuronal structure of the cells was clearly visible 4 days after plating (**Figure 3B**). Additionally, **Figure 4** represents the fluorescence image of MAP2 expression in the differentiated P19 cell line (4 days after plating cells)[14].

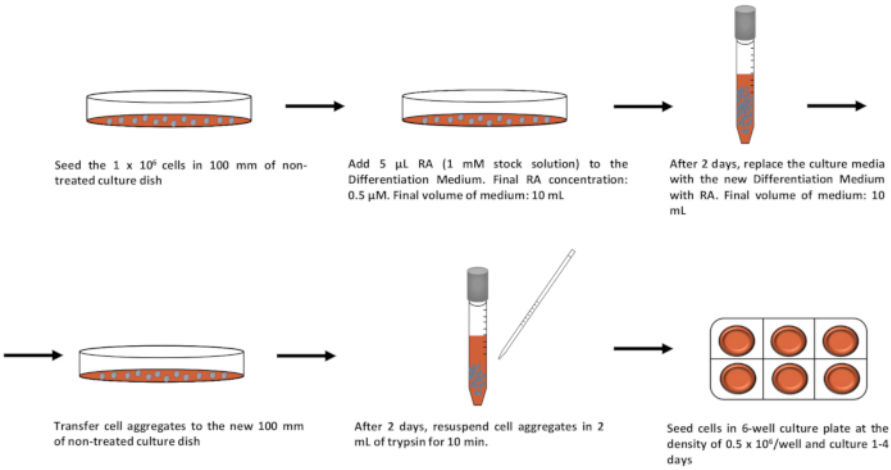

Figure 1: Protocol schematic for induction of neurogenesis in P19 embryonal carcinoma cells. Neurogenesis is induced by culturing the P19 cell line in a 100 mm non-treated culture dish with 5% of FBS and 0.5 µM RA. After 4 days, the cell aggregates are dissociated with trypsin and seeded on adherent cell culture plate for following next 4 days. Please click here to view a larger version of this figure.

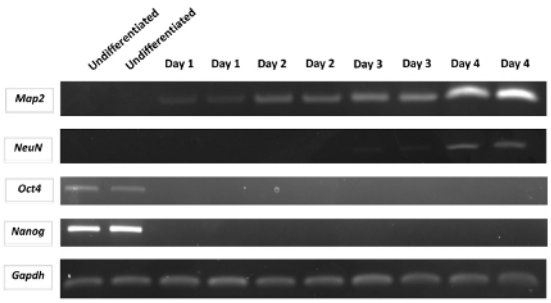

Figure 2: Changes of gene expression in P19 cell line. The band graph represents gene expression for undifferentiated P19 cell line (*Oct4, Nanog*) and during neurogenesis (*Map2, NeuN*). Glyceraldehyde-3-phosphate dehydrogenase *(Gapdh)* was used as the reference gene. Samples are loaded in the agarose gel (1.5%) in double replications. Abbreviations: Undifferentiated represents the undifferentiated P19 cell line without RA treatment; Day 1-4 represents subsequent days after cell plating- following 4 days after RA treatment and cell aggregation stage. Please click here to view a larger version of this figure.

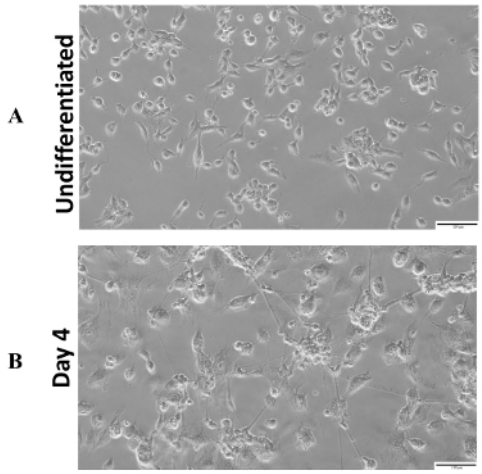

Figure 3: Representative images of analysis of P19 cell line. (**A**) Light microscopic images of undifferentiated P19 cell line. (**B**) Light microscopic images of P19 cell line after 4 days of neurogenesis- following 4 days after RA treatment and cell aggregation stage. Scale bar = 100 µm. Please click here to view a larger version of this figure.

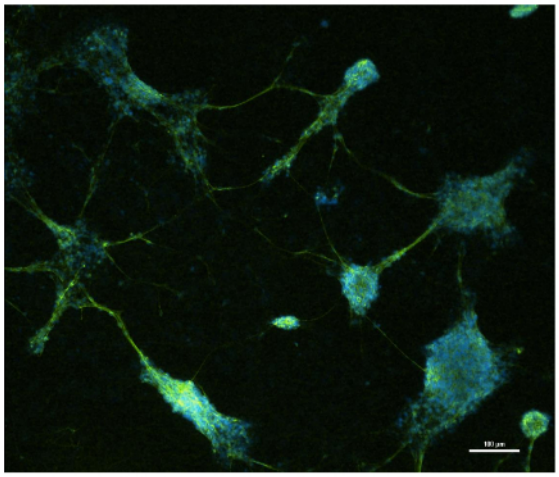

Figure 4: Representative immunofluorescence image of differentiated P19 cell line. Merged immunofluorescence image of P19 cell line stained with anti-MAP2 and DAPI at 4 days after plating. Scale bar = 100 µm. Please click here to view a larger version of this figure.

Primer	Primer sequence	Product size (bp)
Gapdh	F: TGACCTCAACTACATGGTCTACA R: CTTCCCATTCTCGGCCTTG	85
Map2	F: GCTGAGATCATCACACAGTC R: TCCTGCCAAGAGCTCATGCC	211
Oct4	F: GGCGTTCTCTTTGGAAAGGTGTTC R: CTCGAACCACATCCTTCTCT	313
NeuN	F: GGCAAATGTTCGGGCAATTCG R: TCAATTTTCCGTCCCTCTACGAT	160
Nanog	F: AAAGGATGAAGTGCAAGCGGTGG R: CTGGCTTTGCCCTGACTTTAAGC	520

Table 1: Primers used for RT-PCR.

Discussion

Here, we describe a simple protocol for neurogenesis using the P19 cell line. Although many reports have been published in this regard, a detailed methodology for neurogenesis induction using P19 cell line remains unclear. Moreover, we utilized a simple high glucose (4,500 mg/L) DMEM medium with 10% FBS for the entire experiment. This allowed us to perform the neurogenic experiment in a user-friendly manner and expand the usage of this method for the future.

The most critical points within this protocol are the RA concentration as well as the generation of cell aggregates in the suspension culture. The stimulation of neurogenesis in the P19 cell line can be carried out without the formation of aggregates, but the number of neuronal cells produced will be reduced by two-thirds in the cell culture[22]. Monzo et al. have shown neurogenesis induction in P19 cell line by culturing them in monolayer[15]. Although their method is quite convenient as we can eliminate suspension culture process, further studies are required to compare their method with other well-described methods.The RA concentration of 0.5 µM in the medium produced a high number of cell aggregates as well as neurons after plating as compared to 1 µM of RA. It is also important to note that we could not observe an efficient neurogenesis when most of the aggregates are attached to the bottom of the suspension culture dish during RA treatment. The optimal number of the P19 cell line to be used at the beginning of the procedure is 1 x 10^6 for every 10 mL of Differentiation Medium. During the induction of neurogenesis, the P19 cell line forms varying sized aggregates and even single cells are found in the culture. To overcome this problem, we collected the cell aggregates after 1.5 min of free fall in a 15 mL tube. We found that this approach allows the exclusion of contamination of single cells. It is also recommended to perform neuronal enrichment with the cell culture using anti-mitotic drugs (e.g., cytosine arabinoside) for long term culture to inhibit extensive proliferation of glial cells[23].

Neurons derived from the P19 cell line express ionotropic glutamate receptors of both N-methyl-D-aspartate (NMDA) and alpha-amino-3-hydroxy-5-methyl-4-isoxazole propionate (AMPA)/kainite (KA) types[24,25], as well as functional γ-aminobutyric acid (GABA) receptors[25]. Therefore, the P19 cell line is widely used in the studies on molecular mechanisms governing neuronal differentiation[26,27,28]. More importantly, the tumor development was not observed after cell transplantation[29,30].

To this end, research on neurodegenerative diseases such as Alzheimer's disease[17,18] is also conducted using P19 cell line, and we believe that the method developed in this study will thus play a part in elucidating the molecular mechanisms in neurodevelopmental abnormalities and neurodegenerative diseases.

Disclosures

The authors have nothing to disclose.

Acknowledgments

The study was financially supported by National Science Centre, Poland (grant no. UMO-2017/25/N/NZ3/01886) and KNOW (Leading National Research Centre) Scientific Consortium "Healthy Animal - Safe Food", decision of Ministry of Science and Higher Education No. 05-1/KNOW2/2015

References

1. Ramkumar, N., Anderson, K. V. SnapShot: mouse primitive streak. *Cell.* **146** (3), 488-488.e2 (2011).
2. Solnica-Krezel, L., Sepich, D. S. Gastrulation: making and shaping germ layers. *Annual Review of Cell and Developmental Biology.* **28**, 687-717 (2012).
3. Tam, P. P. L., Gad, J. M. Chapter 16: Gastrulation in the Mouse Embryo. Gastrulation: From Cells to Embryo. Stern, C. D. *Cold Spring Harbor Laboratory Press, Cold Spring Harbor. New York.* 233-262 (2004).
4. Sajini, A. A., Greder, L. V., Dutton, J. R., Slack, J. M. W. Loss of Oct4 expression during the development of murine embryoid bodies. *Developmental Biology.* **371** (2), 170-179 (2012).
5. ten Berge, D. *et al.*Wnt Signaling Mediates Self-Organization and Axis Formation in Embryoid Bodies. *Cell Stem Cell.* **3** (5), 508-518 (2008).
6. Bain, G., Ray, W. J., Yao, M., & Gottlieb, D. I. From embryonal carcinoma cells to neurons: the P19 pathway. *Bioessays.* **16** (5), 343-348 (1994).
7. Lin, Y. T. *et al.* YAP regulates neuronal differentiation through Sonic hedgehog signaling pathway. *Experimental Cell Research.* **318** (15), 1877-1888 (2012).
8. Neo, W. H. *et al.* MicroRNA miR-124 controls the choice between neuronal and astrocyte differentiation by fine-tuning Ezh2 expression. *Journal of Biological Chemistry.* **289** (30), 20788-20801 (2014).
9. Jones-Villeneuve, E., McBurney, M. W., Rogers, K. A., & Kalnins, V. I. Retinoic acid induces embryonal carcinoma cells to differentiate into neurons and glial cells. *The Journal of Cell Biology.* **94** (2), 253-262 (1982).
10. McBurney, M. W., & Rogers, B. J. Isolation of male embryonal carcinoma cells and their chromosome replication patterns. *Developmental Biology.* **89** (2), 503-508 (1982).
11. Jones-Villeneuve, E., Rudnicki, M. A., Harris, J. F., & McBurney, M. Retinoic acid-induced neural differentiation of embryonal carcinoma cells. *Molecular and Cellular Biology.* **3** (12), 2271-2279 (1983).
12. Jasmin, Spray, D. C., Campos de Carvalho, A. C., & Mendez-Otero, R. Chemical induction of cardiac differentiation in P19 embryonal carcinoma stem cells. *Stem Cells and Development.* **19** (3), 403-412 (2010).
13. Solari, M., Paquin, J., Ducharme, P., & Boily, M. P19 neuronal differentiation and retinoic acid metabolism as criteria to investigate atrazine, nitrite, and nitrate developmental toxicity. *Toxicological Sciences.* **113** (1), 116-126 (2010).
14. Babuska, V. *et al.* Characterization of P19 cells during retinoic acid induced differentiation. *Prague Medical Report.* **111** (4), 289-299 (2010).

Copyright © 2019 Journal of Visualized Experiments

15. Monzo, H. J. *et al.* A method for generating high-yield enriched neuronal cultures from P19 embryonal carcinoma cells. *Journal of Neuroscience Methods.* **204** (1), 87-103 (2012).
16. Popova, D., Karlsson, J., & Jacobsson, S. O. P. Comparison of neurons derived from mouse P19, rat PC12 and human SH-SY5Y cells in the assessment of chemical- and toxin-induced neurotoxicity. *BMC Pharmacology and Toxicology.* **18** (1), 42 (2017).
17. Woodgate, A., MacGibbon, G., Walton, M., & Dragunow, M. The toxicity of 6-hydroxydopamine on PC12 and P19 cells. *Molecular Brain Research.* **69** (1), 84-92 (1999).
18. Tsukane, M., & Yamauchi, T. Ca2+/calmodulin-dependent protein kinase II mediates apoptosis of P19 cells expressing human tau during neural differentiation with retinoic acid treatment. *Journal of Enzyme Inhibition and Medicinal Chemistry.* **24** (2), 365-371 (2009).
19. Adler, S., Pellizzer, C., Paparella, M., Hartung, T., & Bremer, S. The effects of solvents on embryonic stem cell differentiation. *Toxicology in Vitro.* **20** (3), 265-271 [pii] (2006).
20. Jones-Villeneuve, E.M., McBurney, M.W., Rogers, K.A., & Kalnins, V.I. Retinoic acid induces embryonal carcinoma cells to differentiate into neurons and glial cells. *The Journal of Cell Biology.* **94** (2), 253-262 (1982).
21. Roy, B., Taneja, R., & Chambon, P. Synergistic activation of retinoic acid (RA)-responsive genes and induction of embryonal carcinoma cell differentiation by an RA receptor alpha (RAR alpha)-, RAR beta-, or RAR gamma-selective ligand in combination with a retinoid X receptor-specific ligand. *Molecular and Cellular Biology.* **15** (12), 6481-6487 (1995).
22. Hamada-Kanazawa, M. *et al.* Sox6 overexpression causes cellular aggregation and the neuronal differentiation of P19 embryonic carcinoma cells in the absence of retinoic acid. *FEBS Letters.* **560** (1-3), 192-198 (2004).
23. Tangsaengvit, N., Kitphat,i W., Tadtong, S., Bunyapraphatsara, N., Nukoolkarn, V. Neurite Outgrowth and Neuroprotective Effects of Quercetin from Caesalpinia mimosoides Lamk. on Cultured P19-Derived Neurons. *Evidence-Based Complementary and Alternative Medicine.* 2013: 838051 (2013).
24. Magnuson, D. S., Morassutti, D. J., McBurney, M. W., & Marshall, K. C. Neurons derived from P19 embryonal carcinoma cells develop responses to excitatory and inhibitory neurotransmitters. *Developmental Brain Research.* **90** (1-2), 141-150 (1995).
25. MacPherson, P., Jones, S., Pawson, P., Marshall, K., & McBurney, M. P19 cells differentiate into glutamatergic and glutamate-responsive neurons in vitro. *Neuroscience.* **80** (2), 487-499 (1997).
26. Hong, S. *et al.* Methyltransferase-inhibition interferes with neuronal differentiation of P19 embryonal carcinoma cells. *Biochemical and Biophysical Research Communications.* **377** (3), 935-940 (2008).
27. Wenzel, M. *et al.* Identification of a classic nuclear localization signal at the N terminus that regulates the subcellular localization of Rbfox2 isoforms during differentiation of NMuMG and P19 cells. *FEBS Letters.* **590** (24), 4453-4460 (2016).
28. Harada, Y. *et al.* Overexpression of Cathepsin E Interferes with Neuronal Differentiation of P19 Embryonal Teratocarcinoma Cells by Degradation of N-cadherin. *Cellular and Molecular Neurobiology.* **37** (3), 437-443 (2017).
29. Morassutti, D. J., Staines, W. A., Magnuson, D. S., Marshall, K. C., & McBurney, M. W. Murine embryonal carcinoma-derived neurons survive and mature following transplantation into adult rat striatum. *Neuroscience.* **58** (4), 753-763 (1994).
30. Magnuson, D. S., Morassutti, D. J., Staines, W. A., McBurney, M. W., & Marshall, K. C. In vivo electrophysiological maturation of neurons derived from a multipotent precursor (embryonal carcinoma) cell line. *Developmental Brain Research.* **84** (1), 130-141 (1995).

Copyright © 2019 Journal of Visualized Experiments

International Journal of
Molecular Sciences

MDPI

Article

Deletion of the *Prdm3* Gene Causes a Neuronal Differentiation Deficiency in P19 Cells

Paweł Leszczyński [1], Magdalena Śmiech [1], Aamir Salam Teeli [1], Effi Haque [1], Robert Viger [2,3], Hidesato Ogawa [4], Mariusz Pierzchała [5] and Hiroaki Taniguchi [1,*]

1 Institute of Genetics and Animal Biotechnology, Laboratory for Genome Editing and Transcriptional Regulation, Polish Academy of Sciences, 05-552 Jastrzębiec, Poland; p.leszczynski@ighz.pl (P.L.); m.smiech@ighz.pl (M.Ś.); teeliaamir7@gmail.com (A.S.T.); e.haque@ighz.pl (E.H.)
2 Reproduction, Mother and Child Health, Centre de Recherche du CHU de Québec-Université Laval and Centre de Recherche en Reproduction, Développement et Santé Intergénérationnelle (CRDSI), Quebec, QC GIV4G2, Canada; robert.viger@crchudequebec.ulaval.ca
3 Department of Obstetrics, Gynecology, and Reproduction, Université Laval, Quebec, QC G1V0A6, Canada
4 Graduate School of Frontier Biosciences, Osaka University, 1-3 Yamadaoka, Suita 565-0871, Japan; hidesato@fbs.osaka-u.ac.jp
5 Institute of Genetics and Animal Biotechnology, Department of Genomics and Biodiversity, Polish Academy of Sciences, 05-552 Jastrzębiec, Poland; m.pierzchala@ighz.pl
* Correspondence: h.taniguchi@ighz.pl; Tel.: +48-22-736-70-95

Received: 4 July 2020; Accepted: 22 September 2020; Published: 29 September 2020

Abstract: PRDM (PRDI-BF1 (positive regulatory domain I-binding factor 1) and RIZ1 (retinoblastoma protein-interacting zinc finger gene 1) homologous domain-containing) transcription factors are a group of proteins that have a significant impact on organ development. In our study, we assessed the role of *Prdm3* in neurogenesis and the mechanisms regulating its expression. We found that *Prdm3* mRNA expression was induced during neurogenesis and that *Prdm3* gene knockout caused premature neuronal differentiation of the P19 cells and enhanced the growth of non-neuronal cells. Interestingly, we found that *Gata6* expression was also significantly upregulated during neurogenesis. We further studied the regulatory mechanism of *Prdm3* expression. To determine the role of GATA6 in the regulation of *Prdm3* mRNA expression, we used a luciferase-based reporter assay and found that *Gata6* overexpression significantly increased the activity of the *Prdm3* promoter. Finally, the combination of retinoic acid receptors α and β, along with *Gata6* overexpression, further increased the activity of the luciferase reporter. Taken together, our results suggest that in the P19 cells, PRDM3 contributed to neurogenesis and its expression was stimulated by the synergism between GATA6 and the retinoic acid signaling pathway.

Keywords: P19 cells; Prdm3; Gata6; retinoic acid; neurogenesis; CRISPR; gene knockout

1. Introduction

PRDM3 is a transcription factor belonging to the PRDM (PRDI-BF1 (positive regulatory domain I-binding factor 1) and RIZ1 (retinoblastoma protein-interacting zinc finger gene 1) homologous domain-containing) protein family. A characteristic feature of this group of proteins is the PR-SET domain at the N-terminus, the zinc finger C_2H_2 motif group, and the acidic domain at the C-terminus [1–3]. Mice embryos lacking the *Prdm3* gene exhibit disturbed cardiovascular and nervous system development and die at 10.5 days post coitum [4]. In adult tissues, *Prdm3* is expressed in the lungs, ovaries, kidneys, and brain structures [5,6]. The Hamlet protein (*Drosophila melanogaster* homolog of both PRDM3 and PRDM16) belongs to the molecular machinery involved in the cell fate determination of external sensory organs [7,8] and olfactory receptor neuron diversification [9]. EGL-43

(the PRDM3 homolog in *Caenorhabditis elegans*) is required for the migration of hermaphrodite-specific motor neurons in nematodes [10]. Interestingly, ectopic overexpression of *Prdm3* results in neuronal differentiation [11]. In primary neurons, *Prdm3* mediates transcriptional suppression via histone deacetylase 1 (HDAC1 deacetylase) and controls the synaptic plasticity by inhibiting miR-124 expression [12]. However, despite the importance of PRDM3 in determining the cellular identity [7,13], a clear understanding of the mechanism controlling its expression during neuronal differentiation has yet to be documented.

A possible candidate mechanism that may control *Prdm3* expression is the retinoic acid (RA) signaling pathway. RA is known to be important in the induction of progenitor cell maturation toward neuronal identity [14,15]. RA governs molecular signaling during early neurogenesis in developing brain structures [16–18]. In this regard, several studies have demonstrated that *Prdm3* expression is induced during neurogenesis [11,19,20]. Interestingly, it has been reported that crosstalk between GATA proteins and RA signaling exhibits a significant impact on body development [21], suggesting that there are synergistic roles for the GATA factors and RA signaling in cellular differentiation. The GATA family of zinc finger proteins are transcription factors that bind to the WGATAR consensus nucleotide motifs in the regulatory regions of several target genes, and therefore modulate the target gene expression [22]. The role of GATA factors in the development of organs of endodermal origin has been well studied [23]. However, research on their neuronal-specific function remains incomplete. Nevertheless, GATA2 and GATA3 were reported to be involved in the glutamatergic and serotonergic development of the neuronal subtype [24].

In the present study, we investigated the role of PRDM3 in neurogenesis based on the differentiation of P19 cells [25]. Undifferentiated P19 cells can differentiate into neurons through RA stimulation during cell aggregation [25,26]. Hence, P19 cells are commonly used as a model for studying the genetic mechanisms of neuronal development [27–29]. We observed a significant increase in *Prdm3* expression during RA-induced cell differentiation. To assess the effect of PRDM3 on neurogenesis, we generated a *Prdm3* knockout (KO) in P19 cells. P19 cells lacking PRDM3 displayed earlier neuronal maturation with a rapid proliferation of non-neuronal cells. Additionally, we identified that RA-dependent signaling and *Gata6* overexpression synergistically increased the activity of the *Prdm3* promoter. Importantly, this study has initiated new directions for the further exploration of PRMD3-dependent mechanisms in neurogenesis.

2. Results

2.1. The Neural Differentiation of P19 Cells Was Accompanied by an Increased Expression of Prdm3

To investigate the role of PRDM3 during the neuronal differentiation, we utilized RA-induced P19 embryonic carcinoma stem cells. Neuronally differentiated P19 cells are morphologically and functionally similar to primary neurons. Hence, the cells are considered to be a convenient and simple model for studying the molecular mechanisms orchestrating neurogenesis [25]. Fully developed neuron-like cells were present 9 days after induction (DAI) with RA following cell plating (Figure 1a). *Prdm3* expression was upregulated during the RA-induced neurogenesis using the Northern blot method [11]. Therefore, we decided to determine the exact expression profile with a greater threshold sensitivity using RT-qPCR. During neuronal differentiation, *Prdm3* was continuously expressed, suggesting a significant role in the transition from a pluripotent state to mature postmitotic neurons (Figure 1b).

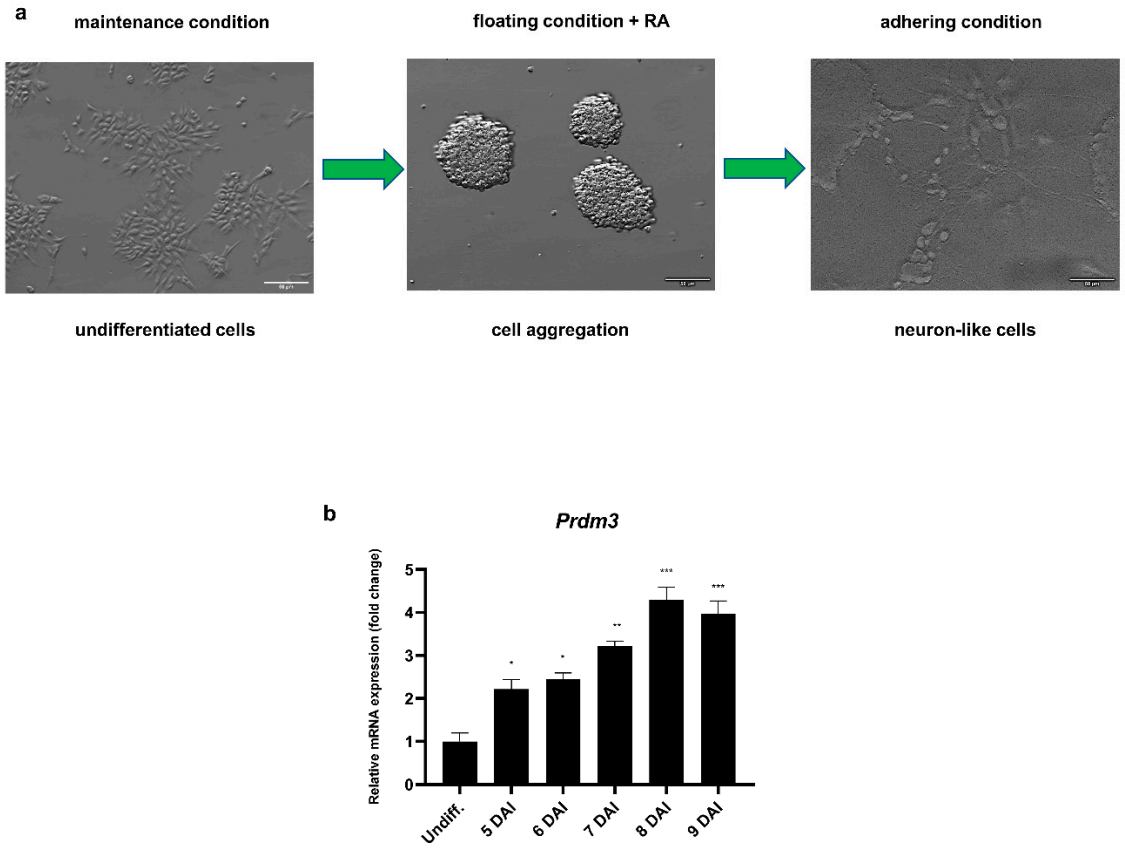

Figure 1. *Prdm3* gene expression was increased during the neurogenesis. (**a**) The undifferentiated P19 cell morphology (left panel), generation of the cell aggregates in a nonadherent dish in the presence of retinoic acid for 4 days (middle panel), and the neuronally differentiated P19 cells 9 days after induction (DAI) with retinoic acid (RA) following cell plating (right panel). The scale bar represents 50 µm. (**b**) The RT-qPCR analysis of the *Prdm3* mRNA expression during neurogenesis. The control group consisted of undifferentiated P19 cells (Undiff.), which were compared with the treated cells 5–9 DAI. *Gapdh* was used as the reference gene. The error bars are shown as the mean ± standard error of the mean (S.E.M.), $n = 3$ per group. * $p < 0.05$, ** $p < 0.01$, and *** $p < 0.001$.

2.2. Generation of the Prdm3 Knockout P19 Cells

To assess the role of *Prdm3* in neuronal differentiation, we used the clustered, regularly interspaced short palindromic repeats/CRISPR-associated protein 9 (CRISPR/Cas9) method to generate P19 cells that had a disrupted *Prdm3* gene. Our workflow for the CRISPR/Cas9-mediated generation of a cell clone with the desired *Prdm3* mutation is illustrated in Figure 2a. We designed our experiment to target exon 4 of the *Prdm3* gene. Disruption of the gene sequence in this location is sufficient to generate mice with a PRDM3 deficiency [30]. Using the lipotransfection method, the Cas9 protein, along with the crRNA:tracrRNA-ATTO-550 (ribonucleoprotein complex, RNP), were delivered to the undifferentiated P19 cells. Next, we enriched the cell population with an ATTO-550-positive signal via fluorescence-activated cell sorting (FACS). Fluorescent-positive P19 cells were expanded as single-cell clones. After 14 days, only the individual colonies were selected for DNA extraction, followed by high-resolution melting (HRM) curve analysis. The HRM curve analysis enabled us to discriminate between the wild-type (control) and *Prdm3* KO cell clones. A rapid assessment allowed us to choose samples with a highly diverse profile compared to the wild-type DNA (Figure 2b). To confirm the deletion, we sequenced selected samples. A cell clone named P19_C5 (a *Prdm3* KO) showed a 59 bp deletion with a 2 bp insertion in the *Prdm3* gene sequence (Figure 2c). The targeted *Prdm3* gene region was also amplified using PCR and validated using agarose gel electrophoresis. The gel image

indicated the faster migration of the shorter amplicon (*Prdm3* KO) relative to the wild-type cells on a 3% agarose gel (Figure 2d). Additionally, we evaluated the PRDM3 protein levels using Western blotting. The result indicated that PRDM3 was not present in the *Prdm3* KO cells, whereas the wild-type cells exhibited an abundance of PRDM3 proteins (Figure 2e).

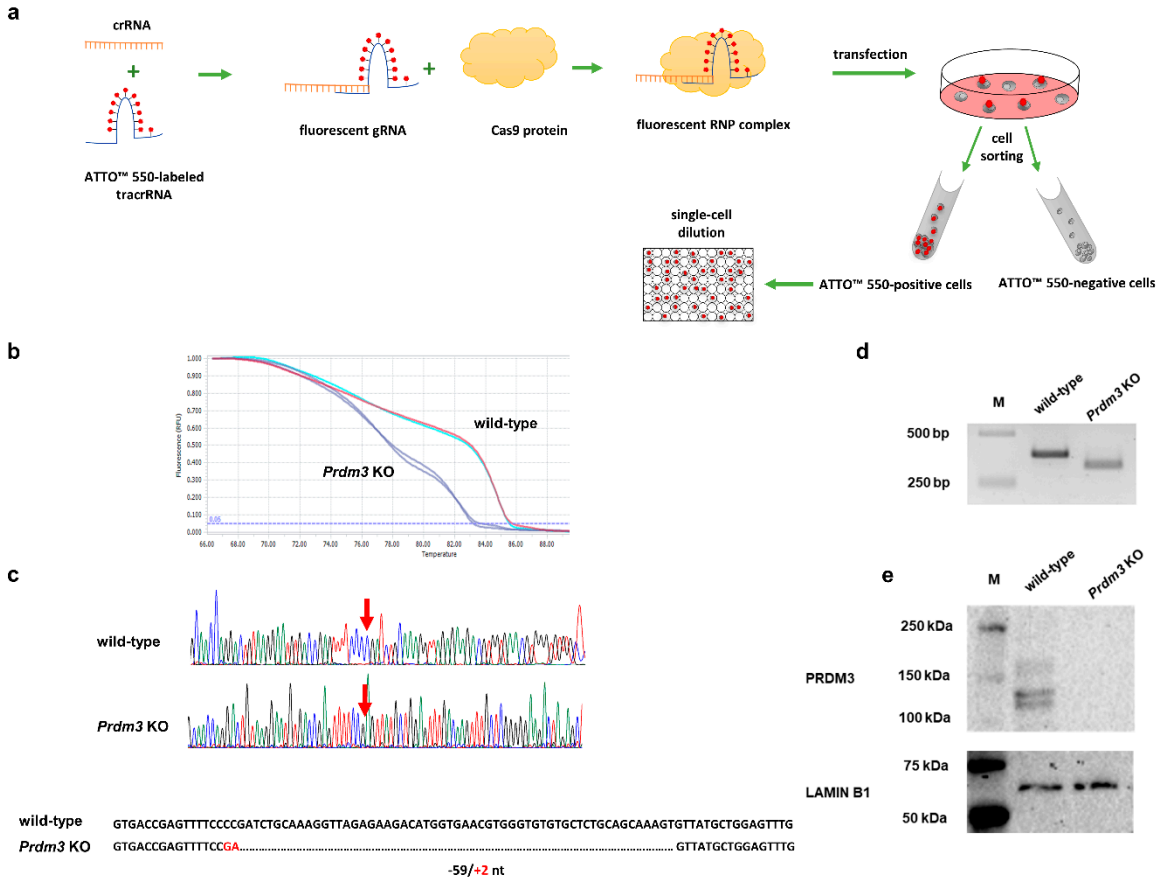

Figure 2. Workflow for the identification of the clustered, regularly interspaced short palindromic repeats/CRISPR-associated protein 9 (CRISPR/Cas9)-mediated *Prdm3* gene deletion in the P19 cells. (**a**) Graphic illustration of the CRISPR/Cas9 genome editing approach for the enrichment and propagation of the cell clones. (**b**) High-resolution melting (HRM) curve analysis of the wild-type (control) and CRISPR/Cas9-edited P19 cells. The curve shift indicates that there were deletions in the CRISPR/Cas9-edited genome sequence. (**c**) A comparison of the sequencing results confirmed that the genome editing was efficient. The edited cells displayed a 59 bp deletion and a 2 bp insertion in the exon 4 sequence compared to the wild-type cells. (**d**) The gel image indicated the faster migration of the shorter amplicon size (*Prdm3* KO) relative to the wild-type cells on a 3% agarose gel. M: DNA-sized ladder. (**e**) The absence of the PRDM3 (PRDI-BF1 (positive regulatory domain I-binding factor 1) and RIZ1 (retinoblastoma protein-interacting zinc finger gene 1) homologous domain-containing transcription factor 3) protein in the *Prdm3* KO cells was confirmed using Western blotting. LAMIN B1 was used as a loading control.

Finally, we assessed whether the P19 cells carrying the *Prdm3* knockout had any undesirable mutations in the genome (off-targets). Using Sanger sequencing, we evaluated the potential genome sites predicted by CHOPCHOP v2, where the binding RNP complex was designed to generate *Prdm3* KO cells with a high probability. We did not observe any off-target mutations in the *Prdm3* KO P19 cells (Figure S1).

2.3. The Prdm3 Gene Disruption Interfered with Neurogenesis in the RA-Induced P19 Cells

Next, we sought to evaluate the role of PRDM3 in neuronal differentiation. First, we investigated the expression of the pluripotency markers *Oct3/4* and *Nanog* using RT-qPCR. Total RNA was isolated from the CRISPR-edited P19 cells and wild-type cells. Undifferentiated P19 cells (Undiff.) expressed stem cell markers (*Oct4* and *Nanog*) at a similar level in the control and *Prdm3* KO cells. Although *Oct4* and *Nanog* expressions were absent in the control cells during neuronal differentiation, the *Prdm3* KO cells exhibited a significant upregulation of *Oct4* and *Nanog* at 5, 7, and 9 DAI. This observation suggested the high proliferation of non-neuronal cells in the *Prdm3* KO cells (Figure 3a,b). We analyzed the impact of the PRDM3 deficiency on the expression of known neuronal marker genes [31]. The *Pax6* gene is involved in the proliferation of radial glial progenitor cells and the migration of immature neurons [32]. We found that *Prdm3* KO cells displayed a downregulation of the *Pax6* mRNA level at 7 and 9 DAI compared to the wild-type cells, but this was not statistically significant (Figure 3c). High *Oct4* and *Nanog* expressions after the RA stimulation suggested that there was a disturbance in the neurogenesis in the *Prdm3* KO cells. To evaluate this observation, we assessed the expression profile of *β-III tubulin* (a neuronal-specific marker) [33]. The analysis revealed that the PRDM3-deficient P19 cells expressed a higher *β-III tubulin* level at 5 DAI compared to the wild-type cells. Surprisingly, in the succeeding days of the neuronal differentiation, the *Prdm3* KO cells displayed a large decrease in their *β-III tubulin* expression, while a gradual upregulation was observed in the wild-type cells (Figure 3d), suggesting that the P19 cells lacking PRDM3 entered into a phase of neuronal maturation earlier than the wild-type cells, though further development was arrested.

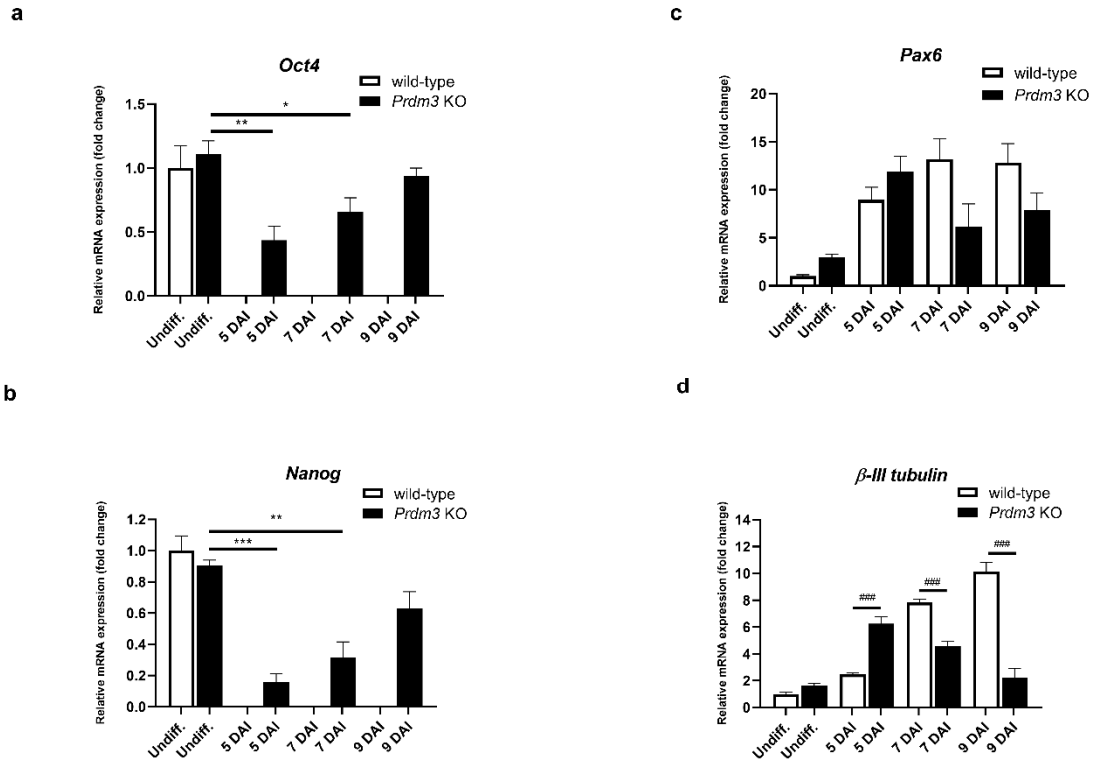

Figure 3. *Prdm3* knockout impeded the RA-induced neurogenesis in the P19 cells, as seen via the qRT-PCR analysis of the (**a**) *Oct4*, (**b**) *Nanog*, (**c**) *Pax6*, and (**d**) *β-III tubulin* mRNA levels during the neurogenesis in the PRDM3-deficient versus wild-type P19 cells. The undifferentiated P19 cells represent the control group and the 5–9 DAI labels signify the days following the cell plating and the RA induction. *Gapdh* was used as the reference gene. The error bars are shown as the mean ± S.E.M., $n = 3$ per group. * $p < 0.05$, ** $p < 0.01$, and *** $p < 0.001$ versus the undifferentiated cells, and ### $p < 0.001$ compared to the wild-type cells within the individual DAI.

Additionally, we validated a cytoskeleton protein specific for mature neurons, microtubule-associated protein 2 (MAP2) [34], and β-III TUBULIN [33] using immunofluorescence staining (Figure 4). The PRDM3-deficient cells were highly MAP2- and β-III TUBULIN-positive at 5 DAI compared to the control cells, but they were barely detectable at 9 DAI. Conversely, the wild-type cells displayed enhanced MAP2 and β-III TUBULIN protein expression with a well-defined neuronal morphology at 9 DAI (Figure 4a,b).

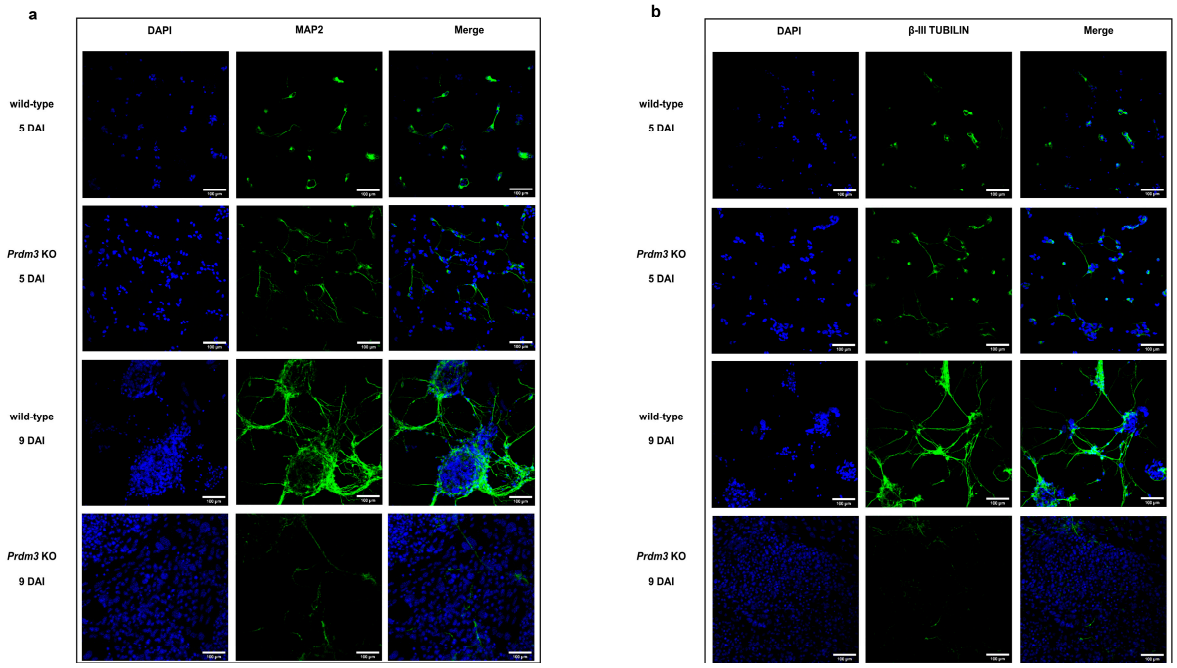

Figure 4. Immunofluorescence microscopy images demonstrating the difference in the microtubule-associated protein 2 (MAP2) and β-III TUBULIN detection in PRDM3-deficient and wild-type P19 cells during neuronal maturation. (**a**,**b**) The MAP2 and β-III TUBULIN staining (green) showed that the *Prdm3* KO P19 cells were relatively well differentiated at 5 DAI, while the MAP2 and β-III TUBULIN in the wild-type cells were barely detectable. On the final day of the RA induction (9 DAI), an overrepresentation of MAP2- and β-III-TUBULIN-negative cells was observed in the PRDM3-deficient group compared to that in the highly MAP2- and β-III TUBULIN-stained wild-type cells. The cell nuclei were stained with 4′,6-diamidino-2-phenylindole (DAPI; blue). The scale bar represents 100 μm.

2.4. GATA Transcription Factors and Retinoic Acid Exerted a Synergistic Effect on the Activity of the Prdm3 Promoter

To explore the possible regulatory mechanism involved in *Prdm3* gene expression during neurogenesis, we used the Eukaryotic Promoter Database (EPD) [35] to identify a *Prdm3*-promoting region. The software identified a sequence (1700 bp) that potentially controlled *Prdm3* expression, which was located in the 5′ upstream region from noncoding exon 1. We focused on the potential role played by the GATA proteins due to the presence of multiple GATA-binding consensus sequences within the *Prdm3* promoter. To identify which GATA factors were involved in the regulation of the *Prdm3* expression, we first evaluated the expression profiles of *Gata1*, *Gata3*, *Gata4*, and *Gata6* in the P19 cells during neurogenesis. The mRNA for *Gata3* showed a transitory increase at 5 DAI (Figure 5a), while *Gata4* (Figure 5b) and *Gata6* (Figure 5c) were significantly upregulated at 9 DAI during neurogenesis. We were unable to detect *Gata1* mRNA at any stage of the cell differentiation (data not shown).

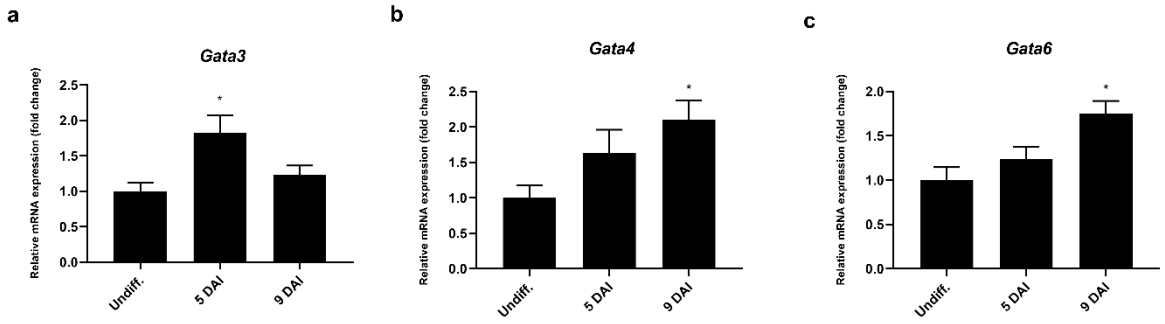

Figure 5. The *Gata3*, *Gata4*, and *Gata6* mRNA expressions were upregulated during the neurogenesis in the P19 cells, as seen in the RT-qPCR analysis of the (**a**) *Gata3*, (**b**) *Gata4*, and (**c**) *Gata6* mRNA expressions. *Gapdh* was used as the reference gene. The control group is abbreviated as Undiff., which represents the gene expression in undifferentiated P19 cells; 5–9 DAI represents the days after the RA induction. The error bars are shown as the mean ± S.E.M., $n = 3$ per group, * $p < 0.05$.

We identified several consensus binding sites for the GATA proteins (Figure S2). To determine whether the GATA factors modulated the activity of the *Prdm3* promoter, we generated a plasmid carrying a luciferase reporter gene under the control of the *Prdm3* promoter. As shown in Figure 6a, the overexpression of the GATA factors increased the activity of the *Prdm3* promoter more than 3-fold. However, the strongest effect was observed for the *Gata6* overexpression (approximately 4.5-fold) (Figure 6a). To determine the mechanism by which GATA proteins influenced the activity of the *Prdm3* promoter, we used a truncated GATA4 protein construct (a dominant-negative competitor, DN), consisting solely of its zinc finger DNA-binding domain [36]. Since the DN protein is devoid of its transactivation domains, it can bind to, but not activate, GATA-dependent target promoters [36]. The structure of the DN construct is based on the GATA4 sequence, but due to the high conservation of the zinc finger domains within the GATA protein family, it can be used as a general competitor for GATA binding [37]. In our study, the DN construct was used to examine the contribution of GATA6 proteins to the activity of the *Prdm3* promoter in P19 cells. We cotransfected the *Gata6* plasmid along with increasing doses of the DN construct (50, 150, and 300 ng). The DN competitor significantly decreased the promoter activity in a dose-independent manner but did not stop the promoter activity (Figure S3). This indicated that the *Prdm3* promoter may have been partially dependent on the direct binding of GATA proteins to the GATA consensus elements found in the *Prdm3* promoter. To assess the potential functional relationship between GATA factors and RA in the neurogenesis, we first tested the effect of RA stimulation on the activity of the *Prdm3* promoter. Compared to the control cells, a concentration of 0.5 μM RA (control + RA) increased the luciferase activity by approximately 40-fold (Figure 6b). Next, we investigated whether the selected GATA factors and the RA treatment could synergistically activate the *Prdm3* promoter. For this purpose, the P19 cells were co-transfected with a control plasmid, along with plasmids encoding *Gata1*, *Gata3*, *Gata4*, or *Gata6*. After one day post-transfection, the same set of cells was treated with RA (0.5 μM) for 24 h and then harvested for a luciferase assay. The combination of the RA stimulation and overexpression of the GATA factors led to a strong synergistic upregulation in the activity of the *Prdm3* promoter. The most pronounced synergism was observed with the combination of *Gata6* and RA treatment, where the increase in the luciferase activity was approximately 140-fold (Figure 6b). To better understand the molecular basis of the RA-dependent stimulation, we focused on the RA receptors (RARs). RARs mediate the molecular effects of RA by interacting with the retinoic acid response elements (RAREs) in the gene regulatory regions [38]. It was also reported that RA stimulates *RARα* and *RARβ* mRNA expression in P19 cells [39,40]. Therefore, we tested the effect of pCMX-VP16-*RARα* and pCMX-VP16-*RARβ* on the activity of the *Prdm3* promoter. VP16-*RAR* is a constitutively active form of the RA receptor that is fused to a VP16 activation domain. In the luciferase assay, the overexpression of VP16-*RARα* and VP16-*RARβ* triggered a significant increase in the activity of the *Prdm3* promoter (Figure 6c). The most

potent activation was observed in the case of the VP16-*RARβ* overexpression. Next, in an attempt to explain the synergistic effect between the GATA factors and the RA stimulation, we validated the additive effects of RARα/RARβ with GATA6 on the activity of the *Prdm3* promoter. Cotransfection of both plasmids showed a large increase in luciferase activity, but the result was not synergistic (Figure 6c). Instead, the observed effect showed an additive tendency regarding the combination of RARα or RARβ with GATA6. These data suggest that the *Prdm3* expression could be partially under the control of RARs, but the molecular mechanism underlying the synergistic effect of the GATA factors and the RA stimulation remains to be defined.

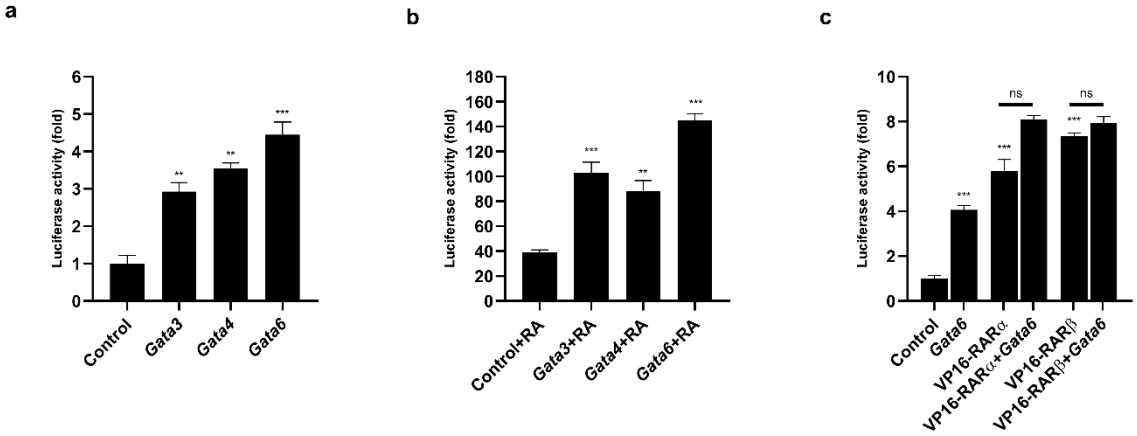

Figure 6. The GATA factors and RA synergistically regulated the *Prdm3* promoter. (**a**) The GATA factors stimulated the activity of the *Prdm3* promoter. The cells were transfected with a plasmid encoding a luciferase reporter gene that was driven by the *Prdm3* promoter with expression plasmids for either *Gata1*, *Gata3*, *Gata4*, *Gata6*, or an empty plasmid (pcDNA3) as a control. (**b**) The RA and GATA factors synergistically activated the *Prdm3* promoter. The P19 cells were cotransfected with pcDNA3 or *Gata* expression vectors, along with the *Prdm3* promoter fused to the luciferase reporter. The cells were cultured with RA (0.5 μM) for 24 h. (**c**) The effect of the retinoic acid receptors (RARs) on the *Prdm3* promoter activity. The P19 cells were transfected with the *Prdm3* promoter, along with pcDNA3, or with *RARα*, *RARβ*, and *Gata6* expression vectors that were used alone or in combination. The luciferase activity is shown as a fold change. Error bars are shown as the mean ± S.E.M., $n = 3$ per group. ** $p < 0.01$, *** $p < 0.001$, and ns (not statistically significant).

Finally, we identified an inverted RARE consensus sequence (CGACCT*ttttg*TGACCT) within the *Prdm3* promoter, where the RAREs consisted of two sequence domains separated by five nucleotides (marked in italics) [41]. We mutated each domain separately to assess the importance of this element in the RARα- and RARβ-dependent activation of the *Prdm3* promoter. We observed that each mutation of the RARE domain did not eliminate the *Prdm3* promoter activity after the RARs' stimulation (Figure S4). This suggested that the RARs regulated, at least in part, the *Prdm3* promoter activity through their binding to the RARE domain in the *Prdm3* promoter.

3. Discussion

We determined the role of PRDM3 in neuronal differentiation using P19 cells, which is a well-established model that is used to study the early stages of mammalian nervous system development [26–29]. Disruption of PRDM3 expression has been shown to lead to slow brain and spinal development [4]. A repressive function of PRDM3 in *Drosophila melanogaster* was also suggested, where Hamlet (the *Drosophila* homolog of PRDM3 and PRDM16 in mammals) was shown to have a crucial involvement in sensory neuron differentiation [2]. Although PRDM3 and PRDM16 share a similar structure and probably have analogous functions [42], the number of reports on the role of PRDM16 in the nervous system is constantly increasing [43–46]. However, the function of PRDM3 remains enigmatic and poorly characterized. Our current findings suggest that PRDM3 was

required to maintain normal neurogenesis in mammals. Additionally, we found that GATA factors and activation of the RA-dependent molecular pathway might have been involved in the *Prdm3* gene expression during neuronal differentiation.

During the early development of zebrafish, Prdm3 proteins are expressed in brain structures [47]. Furthermore, *Prdm3* expression was also reported in adult mouse brains [48], where its expression was found specifically in the postmitotic neurons [12]. Nevertheless, the precise expression pattern during neuronal development is not well known. In our study, we showed that *Prdm3* expression was upregulated during neurogenesis using the P19 cells (Figure 1b). Increased *Prdm3* expression was observed in the global gene expression analysis during the neuronal differentiation of human embryonic cells and mouse P19 cells [19]. These findings collectively point to a possible role for PRDM3 in mammalian neurogenesis. However, this possibility has so far been based only on circumstantial gene expression profiling evidence and not on the direct effect of PRDM3 in neuronal differentiation. For this reason, we generated PRDM3-deficient P19 cells using a CRISPR/Cas9 strategy. Surprisingly, the PRDM3-deficient P19 cells displayed an increased expression of *Oct4* and *Nanog* at 7 and 9 days after the RA induction (Figure 3a,b), suggesting a significant retainment of cell stemness and an impairment of the neurogenic potential of the deficient cells. PAX6 (paired box 6) plays a fundamental role during the early stage of neurogenesis, where it maintains the balance between the self-renewal of neural stem cells and neuronal maturation [31]. Consistent with this function, *Pax6* mRNA levels were upregulated during neurogenesis in wild-type P19 cells, but this upregulation was hindered in the PRDM3-deficient P19 cells during neuronal differentiation (Figure 3c). Interestingly, we found that the expression of mature neuron-specific markers, namely, β-III TUBULIN and MAP2, in the PRDM3-deficient cells was substantially different than that in the control cells (Figure 4a,b). At 5 DAI, *β-III tubulin* was highly upregulated in the modified cells but this effect was lost by 9 DAI (Figure 3d). A similar observation was found for the anti-MAP2 and β-III TUBULIN staining (Figure 4a,b). The gradual loss of the *β-III tubulin* expression in the days following the cell seeding might be explained by the non-neuronal cell overgrowth, where this observation was also consistent with the increased *Oct4* and *Nanog* expression (Figure 3a,b). On the other hand, the expression level of *β-III tubulin* at 5 DAI was significantly higher in the PRDM3-deficient P19 cells than that in the wild-type cells. Thus, the P19 cells lacking PRDM3 appeared to enter neural maturation earlier than the wild-type cells but could not continue this process in the absence of PRDM3. PRDM3 may have a stepwise involvement in the regulation of neurogenesis. Therefore, our data show that during RA stimulation, PRDM3 was part of the molecular machinery controlling the stage-dependent neuronal maturation, at least in the P19 cells.

It has been suggested that GATA2 and GATA3 affect the specialization of neuronal differentiation into glutamatergic and serotonergic subtypes [24]. This suggestion prompted us to evaluate the effect of GATA factors on the regulation of *Prdm3* expression. *Gata3*, *Gata4*, and *Gata6* upregulation were observed in the days following the RA-induced differentiation (Figure 5a–c). Moreover, each of the tested GATA factors stimulated the activity of the *Prdm3* promoter, where the strongest effect was observed with *Gata6* (Figure 6a). It was reported that *Prdm3* expression is stimulated by RA in NTERA-2 human teratocarcinoma cells and acute myeloid leukemia cells [49,50]. In our study, RA increased the activity of the *Prdm3* promoter by approximately 40-fold in luciferase assays, but along with *Gata6* overexpression, we observed a particularly high synergy of both factors (Figure 6b). Moreover, it was reported that there is a functional interaction between an RA-dependent pathway and GATA2 in an embryonic stem cell model of hematopoietic differentiation [21]. These results are consistent with our findings and suggest that there is a close relationship between the *Prdm3* expression, GATA factors, and the RA-dependent molecular pathway. Additionally, we assessed whether the involvement of GATA proteins with the *Prdm3* promoter was the result of direct GATA binding. The *Prdm3* promoter nucleotide sequence contains multiple potential GATA-binding consensus motifs, which makes assessing the individual motifs challenging. To overcome this problem, we used a truncated GATA4 protein, which acted as a DN for all GATA proteins [36]. The GATA DN significantly decreased, but did not stop, the GATA6-induced *Prdm3* promoter activity. This suggested the influence of GATA proteins

on Prdm3 expression during neurogenesis. However, the effect of the GATA proteins could have been mediated by the regulation of other transcriptional factors or by affecting the differentiation state of the neurons. Accordingly, further studies are needed to elucidate how GATA proteins regulate *Prdm3* expression during neurogenesis. Taken together, our results provide an additional functional example of the close relationship between *Prdm3* expression, GATA factors, and RA-induced molecular signaling. RA stimulates a vast number of molecular pathways [51,52], which can coincide with GATA factors during neuronal differentiation, and thus, might orchestrate *Prdm3* expression.

We also tested whether *Prdm3* expression could be regulated through the interaction of RARs and GATA proteins. RARs are activated by RA binding and act as transcription factors that contribute to the diversification of the neuronal cell types [53–55]. We found a RARE within the *Prdm3* promoter. We confirmed that the RARs stimulated the *Prdm3* promoter activity through the binding of the RARs to the RARE (Figure S4). Moreover, the functional synergism between GATA2 and RARα through protein–protein interaction was demonstrated in human KG1 myeloid cells [21]. In our study, the overexpression of *Gata6* and the *RAR*s was only additive and did not exceed the effect observed with the RA-dependent stimulation (Figure 6c). Thus, it appears that the synergism between GATA- and RA-dependent pathways could only be partially explained by the participation of the RARs. RA is well recognized for its ability to promote neuronal development in embryos [56], but many of the molecular targets remain largely unidentified. Even less is known about the GATAs' downstream targets in mouse and human nervous systems [57]. In our study, we could not determine the exact molecular mechanism underlying the synergism effect between the RA signaling and the GATA factors observed in the P19 cells. As such, we could not exclude the influence of other factors on the activity of the *Prdm3* promoter, especially those whose expression is stimulated by RA and/or GATA factors. Further studies are needed to clarify this point.

4. Materials and Methods

4.1. Cell Culture

The P19 cells (donated by Katsuhiko Mikoshiba, RIKEN Center for Brain Science, Wako, Japan) were cultured in Dulbecco's modified Eagle medium (DMEM) supplemented with 4.5 g/L of glucose (Lonza, Basel, Switzerland), 10% of fetal bovine serum (FBS) (EURx, Gdansk, Poland), 100 units/mL of penicillin, and 100 units/mL of streptomycin (Lonza, Basel, Switzerland). The cells were maintained in an incubator at 37 °C and 5% CO_2. Briefly, the P19 cells (1×10^6 cells) were cultured on a 10 cm bacterial-grade Petri dish (Corning, Corning, NY, USA) in media containing DMEM/5% FBS and 0.5 μM all-*trans* retinoic acid (Sigma, St. Louis, MO, USA) for 4 days. During this period, the cells aggregated and resembled the structure of an embryonic body (EB). To induce neuronal differentiation, the P19 cells were trypsinized and plated into adherent culture dishes in DMEM/10% FBS for the next 5 days [25].

4.2. Quantitative RT-PCR (RT-qPCR)

Total RNA was isolated from cultured cells using a fenozol reagent (A&A Biotechnology, Gdynia, Poland). For the reverse transcription, 0.5 μg of total RNA was used and the reactions were performed according to the manufacturer's instructions (EURx, Gdansk, Poland). Next, the RT-qPCR was performed with using a Fast SG qPCR Master Mix (EURx, Gdansk, Poland), and the gene expression was examined using a LightCycler 96 Instrument (Roche, Mannheim, Germany) under the following conditions: incubation at 95 °C for 5 min, followed by 40 cycles of 95 °C for 10 s, 60 °C for 10 s, and 72 °C for 10 s. The expression of the target gene was normalized against glyceraldehyde-3-phosphate dehydrogenase (*Gapdh*). The sequences of primers used for the RT-qPCR are presented in Table 1.

Table 1. Primers used for the RT-qPCR.

Gene Name	Primer Sequence	Product Size (bp)
Gapdh	F: TGACCTCAACTACATGGTCTACA R: CTTCCCATTCTCGGCCTTG	85
β-III tubulin	F: CCCAGCGGCAACTATGTAGG R: CCAGACCGAACACTGTCCA	144
Oct4	F: GGCGTTCTCTTTGGAAAGGTGTTC R: CTCGAACCACATCCTTCTCT	313
Pax6	F: TAGCCCAGTATAAACGGGAGTG R: CCAGGTTGCGAAGAACTCTG	131
Prdm3	F: TTGTTTCACCCGCAATTC R: CGTGTTAGGTTCGCAGACC	235
Gata3	F: CCCCATTACCACCTATCCGC R: CCTCGACTTACATCCGAACCC	106
Gata4	F: CTCTGGAGGCGAGATGGGAC R: CGCATTGCAAGAGGCCTGGG	254
Gata6	F: TTGCTCCGGTAACAGCAGTG R: GTGGTCGCTTGTGTAGAAGGA	105

4.3. Generation of the Prdm3 Gene-Inactivated P19 Cells

The PRDM3-deficient P19 cells were generated using the CRISPR/Cas9-mediated gene editing method. The sequence of crRNA (5′-TCTCTAACCTTTGCAGATCG-3′) was designed to target the mouse *Prdm3* gene in the location of exon 4 using CHOPCHOP v2 [58]. Selected crRNA and ATTO-550-labeled tracrRNA were purchased from Integrated DNA Technologies (Coralville, IA, USA). Briefly, the cells were plated 24 h before transfection (3.5×10^4 cells/well in 24-well plates). A duplex of crRNA and tracrRNA-ATTO-550 was prepared in equimolar concentrations (1 µM), heated at 95 °C for 5 min, and cooled down to room temperature (RT). The formation of the ribonucleoprotein (RNP) complex was generated via the assembly of 1 µM of Cas9 protein (Integrated DNA Technologies, Coralville, IA, USA) with a crRNA:tracrRNA-ATTO-550 duplex in Opti-MEM (Thermo Fisher Scientific, Waltham, MA, USA) and incubated for 10 min at RT. Next, 1.5 µL of Lipofectamine CRISPRMAX (Thermo Fisher Scientific, Waltham, MA, USA) was added to the RNP complex, mixed, and incubated at RT for 10–15 min. Finally, the mixture was added dropwise onto the cell medium. To address the potential off-target effects of the CRISPR/Cas9 method, we used the CHOPCHOP v2 program to select sites in the genome that had a high sequence similarity to the crRNA binding site in the *Prdm3* gene [58]. We designed a primer set to amplify the potential off-target regions (Table S1) and performed PCR amplification. Next, we verified the selected fragments using Sanger sequencing (Genomed, Warsaw, Poland) (Figure S1).

4.4. Western Blotting

The nuclear protein concentrations from the wild-type and PRDM3-deficient P19 cells were determined using the Pierce BCA Protein Assay Kit (Thermo Fisher Scientific, Waltham, MA, USA). Protein extracts (20 µg) were separated on 4–15% precast gel (Bio-Rad, Hercules, CA, USA) and transferred to a PVDF membrane (Merck Millipore, Burlington, MA, USA) using a wet transfer. Blots were probed overnight with a primary antibody for PRDM3 (1:1000, Cell Signaling Technology, Danvers, MA, USA) in 5% skim milk in TBS (tris-buffered saline, Sigma-Aldrich, Saint Louis, MO, USA) supplemented with 0.1% tween-20 (Sigma-Aldrich, Saint Louis, MO, USA), followed by incubation with HRP-conjugated anti-rabbit IgG produced in goats (1:5000, Sigma-Aldrich, Saint Louis, MO, USA) in 5% skim milk in TBST for 1 h at RT. Proteins were visualized using the ECL Western Blotting Analysis System (Amersham, Illinois, CA, USA) and ChemiDoc XRS+ System (Bio-Rad, Hercules, CA, USA). The molecular weight of the proteins was estimated using the Precision Plus Protein WesternC

Standards (Bio-Rad, Hercules, CA, USA). Lamin B1 (1:1000, Santa Cruz Biotechnology, Dallas, TX, USA) was used as a loading control for the Western blotting.

4.5. FACS Analysis

After the transfection (24 h), the P19 cells labeled with tracrRNA-ATTO-550 (Integrated DNA Technologies, Coralville, IA, USA) were isolated using fluorescence-activated cell sorting (FACS). Cells treated with a fluorescence RNP complex, but without a transfection reagent, were used as a control to set the gate during the cell sorting. The flow cytometric analysis was performed on a FACSAria (BD Biosciences, San Jose, CA, USA) using Cell Quest software (BD Biosciences, San Jose, CA, USA) in the Department of Immunology at the University of Warsaw, Poland.

4.6. Establishment of the Edited P19 Cells from Single-Cell Clones

FACS-sorted P19 cells were diluted to 1 cell/100 µL by adding 100 cells into 10 mL DMEM/10% FBS. Then, 100 µL of the cell suspension was distributed into each well of the 96-well plate and incubated for 1 week. The wells with a visible single-cell colony were washed with 100 µL of PBS (Phosphate Buffered Saline) without calcium and magnesium (Lonza, Basel, Switzerland) and then detached by adding 20 µL of trypsin-EDTA (0.25%) (Biosera, Nuaille, France). Next, the cells were split in the same arrangement into two 96-well plates. After one week, the cells reached an approximately 80% confluence and were used for further analysis.

4.7. Genomic DNA Isolation, HRM PCR, and Sanger Sequencing

The genomic DNA was isolated using the Genomic Mini kit (A&A Biotechnology, Gdynia, Poland) following the manufacturer's instructions. The HRM PCR reaction was prepared by mixing 5 µL of RT HS-PCR Mix EvaGreen (A&A Biotechnology, Gdynia, Poland) 0.25 µL of each primer (10 µM), and 1 µL of isolated DNA (10 ng), and then adjusted with water up to 10 µL. The primers used for the HRM PCR and PCR are presented in Table 2. The HRM PCR reaction was carried out in a LightCycler 96 (Roche, Mannheim, Germany) using the following HRM PCR conditions: 95 °C for 5 min, then 40 cycles of 95 °C for 15 s and 60 °C for 15 s, 72 °C for 20 s, followed by one cycle of 95 °C for 30 s and 60 °C for 60 s. The melting analysis was performed by preheating the PCR product to 95 °C. Then, the mixture was cooled down to 40 °C for 1 min, followed by heating to 65 °C. A continuous fluorescent signal was acquired from 65 to 97 °C. The amplified curves were analyzed using LightCyler 96 software (Roche, Mannheim, Germany). The sequence of the PCR products was assayed using Sanger sequencing (Genomed, Warsaw, Poland).

Table 2. Primers used for the high-resolution melting (HRM) PCR and PCR.

Primer Name	Primer Sequence	Product Size (bp)
E4A_HRM_PCR	F: TCTCCGAGAGATCCATGGCA R: TCTTCCCCCGAGCAAACTTG	149
E4A_PCR	F: GGACTTTTGGATCCCACCTT R: GGCCAGTTGTTTTGAAGCTC	375

4.8. Plasmid Construction

To amplify the *Prdm3* promoter sequence located in the 5′ region upstream from noncoding exon 1, we isolated the genomic DNA from P19 cells using a Genomic Mini kit (A&A Biotechnology, Gdynia, Poland). The primers for the selected region were designed based on the sequence located on chromosome 3, namely, 30,014,710 to 30,013,010. KpnI and HindIII restriction sites were incorporated into the forward and reverse primers, respectively. The primers used for cloning the *Prdm3* promoter are depicted in Table 3. The *Prdm3* promoter was amplified via PCR using PrimeSTAR Max DNA Polymerase (TaKaRa, Shiga, Japan) according to the manufacturer's instructions. A pGL3 basic-vector -coding luciferase gene (Promega, Madison, WI, USA) was digested with KpnI and HindIII enzymes

(Thermo Fisher Scientific, Waltham, MA, USA) and ligated with a PCR product using the Gibson assembly method. In brief, the purified DNA fragments (1:9 molar ratio of pGL3 vector to the insert) were resuspended in nuclease-free water. An OverLap™ Assembly (A&A Biotechnology, Gdynia, Poland) kit was used for the cloning. The components used were 4 µL of OverLap Assembly Buffer, 2 µL of nucleotides, 2 µL of OverLap™ Assembly Enzyme Mix, and DNA fragments; the components were mixed on ice and adjusted with water to a final volume of 20 µL. The assembly reaction was carried out at 50 °C for 15 min. Positive bacterial clones were selected for the plasmid isolation and then sequenced. VP16-*RARα* and VP16-*RARβ* were cloned into the pCMX plasmid. pcDNA3-*Gata1*, pcDNA3-*Gata3*, pcDNA3-*Gata4*, pcDNA3-*Gata6*, and GATA DN plasmids were reported [36,59]. The RARE site located in the *Prdm3* promoter was mutated using a Site-Directed Mutagenesis Kit (Agilent Technologies, Santa Clara, CA, USA) according to the manufacturer's instructions. Specific primers for the reaction were designed using the QuikChange Primer Design tool (Agilent Technologies, Santa Clara, CA, USA). Mutated sequences of the receptor binding sites were confirmed using Sanger sequencing. The primer sequences used for the mutagenesis of the RARE site are depicted in Table S2.

Table 3. Primers used for cloning.

Primer Name	Primer Sequence	Product Size (bp)
Gibson_PCR	F: TTTCTCTATCGATAGGTACCGCCACCAAAATGAATTAGTCACC R: CCGGAATGCCAAGCTTAGCTCCAGGGGCAAGACC	1700

4.9. Cell Transfection and the Luciferase Assays

For the luciferase assays, 3×10^4 cells were seeded into 24-well plates. After 24 h, the cells were transfected using Lipofectamine 3000 (Thermo Fisher Scientific, Waltham, MA, USA). The cells were harvested after 48 h and the luciferase activity was assayed using a Luciferase Assay Kit (Promega, Madison, WI, USA) according to the enclosed protocol with a Synergy LX luminometer (Biotek, Winooski, VT, USA).

4.10. Immunofluorescence

During the RA-induced neurogenesis, the P19 cells were fixed with 4% paraformaldehyde in PBS (Sigma-Aldrich, Saint Louis, MO, USA) for 15 min at RT. The fixed cells were then permeabilized with 0.5% Triton x-100 (Sigma-Aldrich, Saint Louis, MO, USA) for 10 min and incubated for 20 min with non-fat milk (1%) to block the non-specific binding of antibodies. After the blocking, the cells were incubated separately with anti-MAP2 rabbit antibody (Thermo Fisher Scientific, Waltham, MA, USA, diluted 1:200) and β-III TUBULIN (Cell Signaling Technology, Danvers, MA, USA, diluted 1:200) rabbit antibody in 1% non-fat milk overnight at 4 °C. The next day, the cells were washed with 0.1% Triton x-100 in PBS. A goat anti-rabbit IgG secondary antibody, namely, Alexa Fluor Plus 488 (Thermo Fisher Scientific, Waltham, MA, USA, diluted 1:500), was used for the detection of MAP2 and β-III TUBULIN (1 h incubation at RT). The cell nuclei were counterstained with 1 µg/mL of 4',6-diamidino-2-phenylindole (DAPI) (Thermo Fisher Scientific, Waltham, MA, USA) for 10 min. The cells were finally washed with PBS and mounted on slides with ProLong™ Gold Antifade Mountant (Thermo Fisher Scientific, Waltham, MA, USA). The samples were imaged with a 20× objective using a Nikon A1R confocal microscope (Nikon, Tokyo, Japan). The microscopic pictures were analyzed using Nikon Instruments and ImageJ software (version 1.52q, NIH, Bethesda, MD, USA).

4.11. Statistical Analysis

Data are presented as the mean ± standard error of the mean (S.E.M.) of each group in the experiment. The statistical analysis was done using a one-way analysis of variance (ANOVA), followed by Tukey's post hoc tests. Any p-value < 0.05 was considered statistically significant. GraphPad PRISM software version 6 (GraphPad Software, La Jolla, CA, USA) was used for the statistical analysis.

Supplementary Materials: The following are available online at http://www.mdpi.com/1422-0067/21/19/7192/s1, Figure S1: Sanger sequencing shows no mutations in putative off-target sites, Figure S2: Sequence of *Prdm3* promoter with indicated GATA binding sites and RARE consensus sequence, Figure S3: A GATA dominant negative competitor decreases GATA6-dependent activation of *Prdm3* promoter activity, Figure S4: Effect of a RARE mutation in the Prdm3 promoter on RARs stimulation, Table S1: Putative off-target sites for CRISPR-mediated *Prdm3* gene knock-out, Table S2: Sequence of the primers used for mutagenesis of RARE sites.

Author Contributions: Conceptualization, P.L. and H.T.; methodology, P.L., M.Ś., and H.T.; validation, P.L. and M.Ś.; formal analysis, P.L. and M.Ś.; investigation, P.L. and M.Ś.; resources, P.L., M.Ś., A.S.T., R.V., H.O., and H.T.; data curation, P.L.; writing—original draft preparation, P.L., M.Ś., and H.T.; writing—review and editing, M.Ś., H.T., E.H., M.P., R.V., and H.O.; visualization, P.L.; supervision, H.T.; project administration, P.L. and H.T.; funding acquisition, P.L. All authors have read and agreed to the published version of the manuscript.

Funding: This study was supported by the National Science Center, Poland (grant no. 2017/25/N/NZ3/01886).

Acknowledgments: The authors are grateful to Aneta Jończy and Rafał Mazgaj (Iron Molecular Biology Team, Institute of Genetics and Animal Biotechnology of the Polish Academy of Sciences) for help with the confocal microscopy imaging.

Conflicts of Interest: The authors declare no conflict of interest.

Abbreviations

EB	Embryonic body
Gapdh	Glyceraldehyde-3-phosphate dehydrogenase
CRISPR	Clustered, regularly interspaced short palindromic repeats
Cas9	CRISPR-associated proteins 9
tracrRNA	*Trans*-activating CRISPR RNA
crRNA	CRISPR RNA
FACS	Fluorescence-activated cell sorting
RNP	Ribonucleoprotein
HRM	High-resolution melting curve
PCR	Polymerase chain reaction
MAP2	Microtubule-associated protein 2
Oct4	Octamer-binding transcription factor 4
RARα	Retinoic acid receptor alpha
RARβ	Retinoic acid receptor beta
Pax6	Paired box 6
β-III tubulin	Tubulin beta 3 class III
DAI	Days after induction
GATA6	GATA-binding factor 6
Prdm3	(positive regulatory domain I-binding factor 1) and RIZ1 (retinoblastoma protein-interacting zinc finger gene 1) homologous domain containing transcription factor 3
RA	Retinoic acid
RARE	Retinoic acid response element

References

1. Fumasoni, I.; Meani, N.; Rambaldi, D.; Scafetta, G.; Alcalay, M.; Ciccarelli, F.D. Family expansion and gene rearrangements contributed to the functional specialization of PRDM genes in vertebrates. *BMC Evol. Boil.* **2007**, *7*, 187. [CrossRef] [PubMed]
2. Kinameri, E.; Inoue, T.; Aruga, J.; Imayoshi, I.; Kageyama, R.; Shimogori, T.; Moore, A.W. Prdm proto-oncogene transcription factor family expression and interaction with the Notch-Hes pathway in mouse neurogenesis. *PLoS ONE* **2008**, *3*, e3859. [CrossRef] [PubMed]
3. Yoshida, M.; Nosaka, K.; Yasunaga, J.; Nishikata, I.; Morishita, K.; Matsuoka, M. Aberrant expression of the MEL1S gene identified in association with hypomethylation in adult T-cell leukemia cells. *Blood* **2004**, *103*, 2753–2760. [CrossRef]
4. Hoyt, P.R.; Bartholomew, C.; Davis, A.J.; Yutzey, K.; Gamer, L.W.; Potter, S.S.; Ihle, J.N.; Mucenski, M.L. The Evi1 proto-oncogene is required at midgestation for neural, heart, and paraxial mesenchyme development. *Mech. Dev.* **1997**, *65*, 55–70. [CrossRef]

5. Morishita, K.; Parganas, E.; Parham, D.M.; Matsugi, T.; Ihle, J.N. The Evi-1 zinc finger myeloid transforming gene is normally expressed in the kidney and in developing oocytes. *Oncogene* **1990**, *5*, 1419–1423. [PubMed]
6. Fears, S.; Mathieu, C.; Zeleznik-Le, N.; Huang, S.; Rowley, J.D.; Nucifora, G. Intergenic splicing of MDS1 and EVI1 occurs in normal tissues as well as in myeloid leukemia and produces a new member of the PR domain family. *Proc. Natl. Acad. Sci. USA* **1996**, *93*, 1642–1647. [CrossRef]
7. Moore, A.W.; Jan, L.Y.; Jan, Y.N. Hamlet, a binary genetic switch between single- and multiple- dendrite neuron morphology. *Science* **2002**, *297*, 1355–1358. [CrossRef]
8. Moore, A.W.; Roegiers, F.; Jan, L.Y.; Jan, Y.N. Conversion of neurons and glia to external-cell fates in the external sensory organs of Drosophila hamlet mutants by a cousin-cousin cell-type respecification. *Genes Dev.* **2004**, *18*, 623–628. [CrossRef]
9. Endo, K.; Karim, M.R.; Taniguchi, H.; Krejci, A.; Kinameri, E.; Siebert, M.; Ito, K.; Bray, S.J.; Moore, A.W. Chromatin modification of Notch targets in olfactory receptor neuron diversification. *Nat. Neurosci.* **2011**, *15*, 224–233. [CrossRef]
10. Garriga, G.; Guenther, C.; Horvitz, H.R. Migrations of the Caenorhabditis elegans HSNs are regulated by egl-43, a gene encoding two zinc finger proteins. *Genes Dev.* **1993**, *7*, 2097–2109. [CrossRef]
11. Kazama, H.; Kodera, T.; Shimizu, S.; Mizoguchi, H.; Morishita, K. Ecotropic viral integration site-1 is activated during, and is sufficient for, neuroectodermal P19 cell differentiation. *Cell Growth Differ. Mol. Boil. J. Am. Assoc. Cancer Res.* **1999**, *10*, 565–573.
12. Hou, Q.; Ruan, H.; Gilbert, J.; Wang, G.; Ma, Q.; Yao, W.D.; Man, H.Y. MicroRNA miR124 is required for the expression of homeostatic synaptic plasticity. *Nat. Commun.* **2015**, *6*, 10045. [CrossRef] [PubMed]
13. Harms, M.J.; Ishibashi, J.; Wang, W.; Lim, H.W.; Goyama, S.; Sato, T.; Kurokawa, M.; Won, K.J.; Seale, P. Prdm16 is required for the maintenance of brown adipocyte identity and function in adult mice. *Cell Metab.* **2014**, *19*, 593–604. [CrossRef] [PubMed]
14. Okada, Y.; Shimazaki, T.; Sobue, G.; Okano, H. Retinoic-acid-concentration-dependent acquisition of neural cell identity during in vitro differentiation of mouse embryonic stem cells. *Dev. Boil.* **2004**, *275*, 124–142. [CrossRef] [PubMed]
15. Bonnet, E.; Touyarot, K.; Alfos, S.; Pallet, V.; Higueret, P.; Abrous, D.N. Retinoic acid restores adult hippocampal neurogenesis and reverses spatial memory deficit in vitamin A deprived rats. *PLoS ONE* **2008**, *3*, e3487. [CrossRef] [PubMed]
16. Yu, S.; Levi, L.; Siegel, R.; Noy, N. Retinoic acid induces neurogenesis by activating both retinoic acid receptors (RARs) and peroxisome proliferator-activated receptor β/δ (PPARβ/δ). *J. Boil. Chem.* **2012**, *287*, 42195–42205. [CrossRef]
17. Haushalter, C.; Asselin, L.; Fraulob, V.; Dollé, P.; Rhinn, M. Retinoic acid controls early neurogenesis in the developing mouse cerebral cortex. *Dev. Boil.* **2017**, *430*, 129–141. [CrossRef]
18. Sandell, L.L.; Sanderson, B.W.; Moiseyev, G.; Johnson, T.; Mushegian, A.; Young, K.; Rey, J.P.; Ma, J.X.; Staehling-Hampton, K.; Trainor, P.A. RDH10 is essential for synthesis of embryonic retinoic acid and is required for limb, craniofacial, and organ development. *Genes Dev.* **2007**, *21*, 1113–1124. [CrossRef]
19. Elkabetz, Y.; Panagiotakos, G.; Al Shamy, G.; Socci, N.D.; Tabar, V.; Studer, L. Human ES cell-derived neural rosettes reveal a functionally distinct early neural stem cell stage. *Genes Dev.* **2008**, *22*, 152–165. [CrossRef]
20. Delile, J.; Rayon, T. Single cell transcriptomics reveals spatial and temporal dynamics of gene expression in the developing mouse spinal cord. *Development* **2019**, *146*. [CrossRef]
21. Tsuzuki, S.; Kitajima, K.; Nakano, T.; Glasow, A.; Zelent, A.; Enver, T. Cross talk between retinoic acid signaling and transcription factor GATA-2. *Mol. Cell. Boil.* **2004**, *24*, 6824–6836. [CrossRef]
22. Engels, M.; Span, P.N.; Mitchell, R.T.; Heuvel, J.; Marijnissen-van Zanten, M.A.; van Herwaarden, A.E.; Hulsbergen-van de Kaa, C.A.; Oosterwijk, E.; Stikkelbroeck, N.M.; Smith, L.B.; et al. GATA transcription factors in testicular adrenal rest tumours. *Endocr. Connect.* **2017**, *6*, 866–875. [CrossRef] [PubMed]
23. Tremblay, M.; Sanchez-Ferras, O.; Bouchard, M. GATA transcription factors in development and disease. *Development* **2018**, *145*. [CrossRef]
24. Haugas, M.; Tikker, L.; Achim, K.; Salminen, M.; Partanen, J. Gata2 and Gata3 regulate the differentiation of serotonergic and glutamatergic neuron subtypes of the dorsal raphe. *Development* **2016**, *143*, 4495–4508. [CrossRef] [PubMed]
25. Leszczyński, P.; Śmiech, M.; Teeli, A.S.; Zołocińska, A.; Słysz, A.; Pojda, Z.; Pierzchała, M.; Taniguchi, H. Neurogenesis Using P19 Embryonal Carcinoma Cells. *J. Vis. Exp.* **2019**. [CrossRef]

26. Jones-Villeneuve, E.M.; McBurney, M.W.; Rogers, K.A.; Kalnins, V.I. Retinoic acid induces embryonal carcinoma cells to differentiate into neurons and glial cells. *J. Cell Boil.* **1982**, *94*, 253–262. [CrossRef]
27. Kobayashi, T.; Komori, R.; Ishida, K.; Kino, K.; Tanuma, S.; Miyazawa, H. Tal2 expression is induced by all-trans retinoic acid in P19 cells prior to acquisition of neural fate. *Sci. Rep.* **2014**, *4*, 4935. [CrossRef]
28. Liu, X.; Chen, M.; Li, L.; Gong, L.; Zhou, H.; Gao, D. Extracellular Signal-regulated Kinases (ERKs) Phosphorylate Lin28a Protein to Modulate P19 Cell Proliferation and Differentiation. *J. Boil. Chem.* **2017**, *292*, 3970–3976. [CrossRef]
29. Ankö, M.L.; Morales, L.; Henry, I.; Beyer, A.; Neugebauer, K.M. Global analysis reveals SRp20- and SRp75-specific mRNPs in cycling and neural cells. *Nat. Struct. Mol. Boil.* **2010**, *17*, 962–970. [CrossRef]
30. Goyama, S.; Yamamoto, G.; Shimabe, M.; Sato, T.; Ichikawa, M.; Ogawa, S.; Chiba, S.; Kurokawa, M. Evi-1 is a critical regulator for hematopoietic stem cells and transformed leukemic cells. *Cell Stem Cell* **2008**, *3*, 207–220. [CrossRef]
31. Sansom, S.N.; Griffiths, D.S.; Faedo, A.; Kleinjan, D.J.; Ruan, Y.; Smith, J.; van Heyningen, V.; Rubenstein, J.L.; Livesey, F.J. The level of the transcription factor Pax6 is essential for controlling the balance between neural stem cell self-renewal and neurogenesis. *PLoS Genet.* **2009**, *5*, e1000511. [CrossRef] [PubMed]
32. Osumi, N.; Shinohara, H.; Numayama-Tsuruta, K.; Maekawa, M. Concise review: Pax6 transcription factor contributes to both embryonic and adult neurogenesis as a multifunctional regulator. *Stem Cells* **2008**, *26*, 1663–1672. [CrossRef] [PubMed]
33. Lyu, J.; Costantini, F.; Jho, E.H.; Joo, C.K. Ectopic expression of Axin blocks neuronal differentiation of embryonic carcinoma P19 cells. *J. Boil. Chem.* **2003**, *278*, 13487–13495. [CrossRef] [PubMed]
34. Matus, A.; Bernhardt, R.; Hugh-Jones, T. High molecular weight microtubule-associated proteins are preferentially associated with dendritic microtubules in brain. *Proc. Natl. Acad. Sci. USA* **1981**, *78*, 3010–3014. [CrossRef]
35. Database, E.P. Eukaryotic Promoter Database. Available online: https://epd.epfl.ch//index.php (accessed on 10 October 2018).
36. Tremblay, J.J.; Robert, N.M.; Viger, R.S. Modulation of endogenous GATA-4 activity reveals its dual contribution to Müllerian inhibiting substance gene transcription in Sertoli cells. *Mol. Endocrinol.* **2001**, *15*, 1636–1650. [CrossRef]
37. Viger, R.S.; Guittot, S.M.; Anttonen, M.; Wilson, D.B.; Heikinheimo, M. Role of the GATA family of transcription factors in endocrine development, function, and disease. *Mol. Endocrinol.* **2008**, *22*, 781–798. [CrossRef]
38. Pozzi, S.; Rossetti, S.; Bistulfi, G.; Sacchi, N. RAR-mediated epigenetic control of the cytochrome P450 Cyp26a1 in embryocarcinoma cells. *Oncogene* **2006**, *25*, 1400–1407. [CrossRef]
39. Jonk, L.J.; de Jonge, M.E.; Kruyt, F.A.; Mummery, C.L.; van der Saag, P.T.; Kruijer, W. Aggregation and cell cycle dependent retinoic acid receptor mRNA expression in P19 embryonal carcinoma cells. *Mech. Dev.* **1992**, *36*, 165–172. [CrossRef]
40. Pratt, M.A.; Crippen, C.A.; Ménard, M. Spontaneous retinoic acid receptor beta 2 expression during mesoderm differentiation of P19 murine embryonal carcinoma cells. *Differ. Res. Biol. Divers.* **2000**, *65*, 271–279. [CrossRef]
41. Bastien, J.; Rochette-Egly, C. Nuclear retinoid receptors and the transcription of retinoid-target genes. *Gene* **2004**, *328*, 1–16. [CrossRef]
42. McGlynn, K.A.; Sun, R.; Vonica, A.; Rudzinskas, S.; Zhang, Y.; Perkins, A.S. Prdm3 and Prdm16 cooperatively maintain hematopoiesis and clonogenic potential. *Exp. Hematol.* **2020**. [CrossRef] [PubMed]
43. Inoue, M.; Iwai, R.; Tabata, H.; Konno, D.; Komabayashi-Suzuki, M.; Watanabe, C.; Iwanari, H.; Mochizuki, Y.; Hamakubo, T.; Matsuzaki, F.; et al. Prdm16 is crucial for progression of the multipolar phase during neural differentiation of the developing neocortex. *Development* **2017**, *144*, 385–399. [CrossRef]
44. Shimada, I.S.; Acar, M.; Burgess, R.J.; Zhao, Z.; Morrison, S.J. Prdm16 is required for the maintenance of neural stem cells in the postnatal forebrain and their differentiation into ependymal cells. *Genes Dev.* **2017**, *31*, 1134–1146. [CrossRef] [PubMed]
45. Baizabal, J.M.; Mistry, M.; García, M.T.; Gómez, N.; Olukoya, O.; Tran, D.; Johnson, M.B.; Walsh, C.A.; Harwell, C.C. The Epigenetic State of PRDM16-Regulated Enhancers in Radial Glia Controls Cortical Neuron Position. *Neuron* **2018**, *98*, 945–962.e948. [CrossRef] [PubMed]
46. Su, L.; Lei, X.; Ma, H.; Feng, C.; Jiang, J.; Jiao, J. PRDM16 orchestrates angiogenesis via neural differentiation in the developing brain. *Cell Death Differ.* **2020**. [CrossRef] [PubMed]

47. Sun, X.J.; Xu, P.F.; Zhou, T.; Hu, M.; Fu, C.T.; Zhang, Y.; Jin, Y.; Chen, Y.; Chen, S.J.; Huang, Q.H.; et al. Genome-wide survey and developmental expression mapping of zebrafish SET domain-containing genes. *PLoS ONE* **2008**, *3*, e1499. [CrossRef] [PubMed]
48. Perkins, A.S.; Mercer, J.A.; Jenkins, N.A.; Copeland, N.G. Patterns of Evi-1 expression in embryonic and adult tissues suggest that Evi-1 plays an important regulatory role in mouse development. *Development* **1991**, *111*, 479–487.
49. Verhagen, H.J.; Smit, M.A.; Rutten, A.; Denkers, F.; Poddighe, P.J.; Merle, P.A.; Ossenkoppele, G.J.; Smit, L. Primary acute myeloid leukemia cells with overexpression of EVI-1 are sensitive to all-trans retinoic acid. *Blood* **2016**, *127*, 458–463. [CrossRef]
50. Bingemann, S.C.; Konrad, T.A.; Wieser, R. Zinc finger transcription factor ecotropic viral integration site 1 is induced by all-trans retinoic acid (ATRA) and acts as a dual modulator of the ATRA response. *FEBS J.* **2009**, *276*, 6810–6822. [CrossRef]
51. Mishra, S.; Kelly, K.K.; Rumian, N.L.; Siegenthaler, J.A. Retinoic Acid Is Required for Neural Stem and Progenitor Cell Proliferation in the Adult Hippocampus. *Stem Cell Rep.* **2018**, *10*, 1705–1720. [CrossRef]
52. Lee, K.; Skromne, I. Retinoic acid regulates size, pattern and alignment of tissues at the head-trunk transition. *Development* **2014**, *141*, 4375–4384. [CrossRef] [PubMed]
53. Purton, L.E.; Bernstein, I.D.; Collins, S.J. All-trans retinoic acid enhances the long-term repopulating activity of cultured hematopoietic stem cells. *Blood* **2000**, *95*, 470–477. [CrossRef] [PubMed]
54. Purton, L.E.; Dworkin, S.; Olsen, G.H.; Walkley, C.R.; Fabb, S.A.; Collins, S.J.; Chambon, P. RARgamma is critical for maintaining a balance between hematopoietic stem cell self-renewal and differentiation. *J. Exp. Med.* **2006**, *203*, 1283–1293. [CrossRef] [PubMed]
55. Cabezas-Wallscheid, N.; Buettner, F.; Sommerkamp, P.; Klimmeck, D.; Ladel, L.; Thalheimer, F.B.; Pastor-Flores, D.; Roma, L.P.; Renders, S.; Zeisberger, P.; et al. Vitamin A-Retinoic Acid Signaling Regulates Hematopoietic Stem Cell Dormancy. *Cell* **2017**, *169*, 807–823.e819. [CrossRef] [PubMed]
56. Janesick, A.; Wu, S.C.; Blumberg, B. Retinoic acid signaling and neuronal differentiation. *Cell. Mol. Life Sci.* **2015**, *72*, 1559–1576. [CrossRef] [PubMed]
57. Kamnasaran, D.; Guha, A. Expression of GATA6 in the human and mouse central nervous system. *Dev. Brain Res.* **2005**, *160*, 90–95. [CrossRef] [PubMed]
58. CHOPCHOPv2. CHOPCHOPv2. Available online: https://chopchop.cbu.uib.no/ (accessed on 22 October 2018).
59. Tremblay, J.J.; Viger, R.S. GATA factors differentially activate multiple gonadal promoters through conserved GATA regulatory elements. *Endocrinology* **2001**, *142*, 977–986. [CrossRef]

© 2020 by the authors. Licensee MDPI, Basel, Switzerland. This article is an open access article distributed under the terms and conditions of the Creative Commons Attribution (CC BY) license (http://creativecommons.org/licenses/by/4.0/).

Supplementary Materials

Table S1. Putative off-target sites for CRISPR-mediated *Prdm3* gene knock-out. Sequence of the primers used to check putative top two off-target sites are indicated below. Mismatched nucleotides in sequence for crRNA binding are marked in red.

Off-target site no.	Target sequence	Number of mismatches	Primer sequence	Product size
1	TCTCTAACCTTTGCAcAggGtGG	4	**F**: GGGACACTTGTGTGCATGAT **R**: GCAAATGCCCTTCCAATCTA	543 bp
2	TCTCTAACtTTTGCAcATCtTGG	3	**F**: TACTTGGTCGCAAGCTGATG **R**: GCCAACTGTCTGCAAGTGAA	629 bp

Table S2. Sequence of the primers used for mutagenesis of RARE sites.

RARE site	Primer sequence
RARE_mut1	**F**: GGCGGGAGAGGAAACAAAAAGGTCGCCAAGACCC **R**: GGGTCTTGGCGACCTTTTTGTTTCCTCTCCCGCC
RARE_mut2	**F**: GGAGAGGTCACAAAAAGGAAGCCAAGACCCAAGTCCTA **R**: TAGGACTTGGGTCTTGGCTTCCTTTTTGTGACCTCTCC

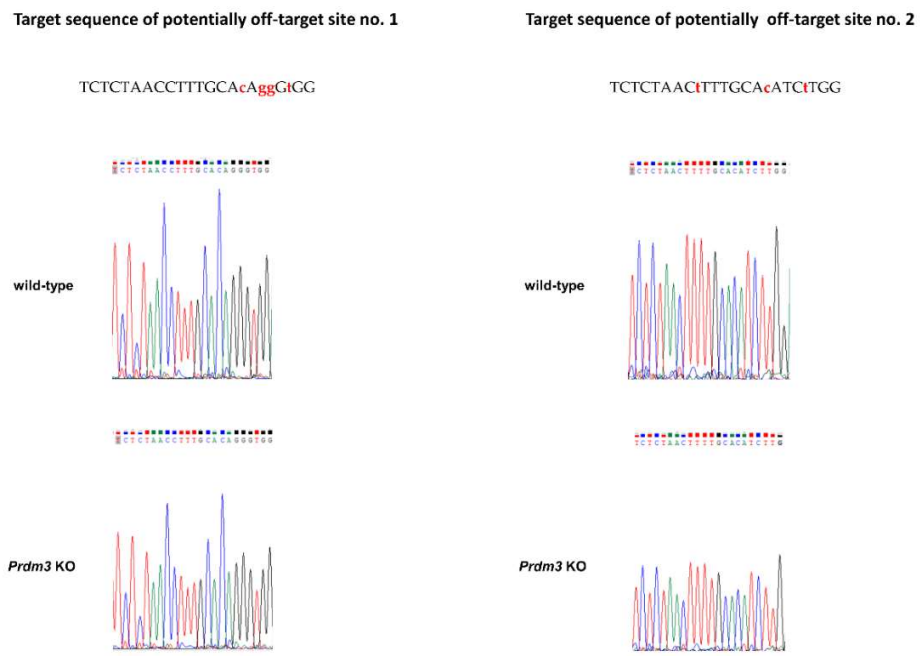

Figure S1. Sanger sequencing shows no mutations in putative off-target sites. Mismatched nucleotides in the crRNA binding sequence are highlighted in red.

GCCACCAAAATGAATTAGTCACCACCTCTAGTCATTTACTGTCACCTGCTTCCTTGTCTTCTGACACTATTTTTGTTTTTTGATCAGCATTTTGGGGAAAATAAAGA

GATA-box

TCTACTGGATTTTCACATTAACTTGCCCTTGGAGAGAAAGAAATGTGGGTGGTACTGTGAGTCCTGATTCATAGATAAAAGTTTAATGTCAGCACACATTCTAAG

CCTGTGAGCTGGCTCCACCCCTCCCAAGTACCTGTTCCTAGACCTAGGCATTTTACTAAATTTTCCATTGTTGAGTTGAGAATAAATTGGATCTGAGGGCTGGCGA

TTTAGCTCAGAGGCAGTTCTCTTGCCTAGTGGGGGTTGGGGGTGGTTGTCCTGGAGGTGTTTCTGTCTTCTCTTGGTGGGTAGGTGAGCTGTATCTTTCTATTTG

GATA-box

CTTTTATAAATGGAGTTTTCTCATCAAAAGCATTTATTCTCAATTAAGCGGTGGGTTTAACATTTTTTTTTCCAAATTTATCTACAAATAAACACATGGATTCTTATA

GATA-box GATA-box

TTTTGCCATCCTCTATCCAAATTCTTTCACCCAATGTCATCTCTGCATTGTATTGATAGAAAGTGCCCAAACTTATTATAAAGTTATCTAATATATAAAATATGAATC

ACTAAAAGCAACCACTTGCATAACTTGACTCTGGGGAAGTCATGGCCTTTTGAATAACTTAGAAAATATTCTCAATCTACTACAATCTATTTGTGAGAGAGATATG

AAAATAATGCTTTAGATTTTAAGATTTGTTCTTGTGTGTGTGTGTGTGTGTGTGTGTGTGTGTGTGTGTGTAGGGGTATTTTTAAAATGTACACATTTCTGGGG

ACCTAACTATAAAAAGGAAAGGAATAAATTTAAGTAGAAACTTAAATTATATTTTATTTTAAAATATGCTTAACTGGAAACTGGAAATGTGTGTTAGTTTTCACTT

TTGAAGCTGCTGTCTTGAGACTTTTAATGCGAGCCAGTATCTCTTTATCCTAAGAGTTGCCCTGGCCCTCTTCAGAGCTTCCAAACTACCAGCCTGCCTGGGGAGG

GATA-box

CACCCTCACACCCCTGAAAGCAATTCTCCACCCTATCTTTCCCATCCCCCACCCAACTCTAACACAGACTCTCTCTCTCTCTCTCTCTCTCTCTCTCTCTCTCT

CTCTCTCTCTCACACACACACACACACACACACACACACACACACACACACACACCCTTGTGCTCAGGACATCAAAACCAAAGAGATTTCCCTGGGGAAACAAAT

CCTGCCTGGAGAAATTTCCCCATTGGTTGTTTATCGGCAGAAATCTACATGTTTCTGGGGATGGTGCATCTATAATCAGTCTGTCCCTATAGGACTTGGGTCTTGG

RARE consensus sequence

CGACCTTTTTGTGACCTCTCCCGCCAGAGGAGGCTGCTGTCACTTTAAAAATTTACTGAAAGAGGAGCCCGTCGTCTGGCTTCCGACCACTCTGGAGATAGCTCC

GATA-box

CTTTCTCCCTCGCCCCGGTTTCTTTCTGGATGGCCGAGCAGATCCCCTTTAAAGAGACAGTTCATGAAATAGAAACCCT

Figure S2. Sequence of *Prdm3* promoter with indicated GATA binding sites and RARE consensus sequence

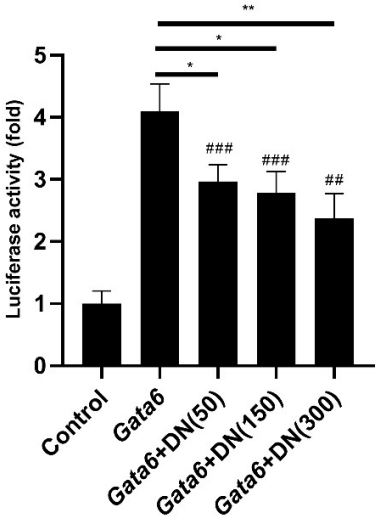

Figure S3. A GATA dominant negative competitor decreases GATA6-dependent activation of *Prdm3* promoter activity. *Prdm3* promoter along with pcDNA3 or GATA6 expression vector in combination with increasing dose of DN (50, 150, 300ng) were transfected in P19 cells. All transfections were performed using a constant amount of DNA (500 ng per culture well). Luciferase activity is shown as a fold change over control. Error bars are shown as mean ± S.E.M., n=4 per group. *p<0.05, **p<0.01, compared to *Gata6* group. ##p<0.01 ### p<0.001 compared to Control.

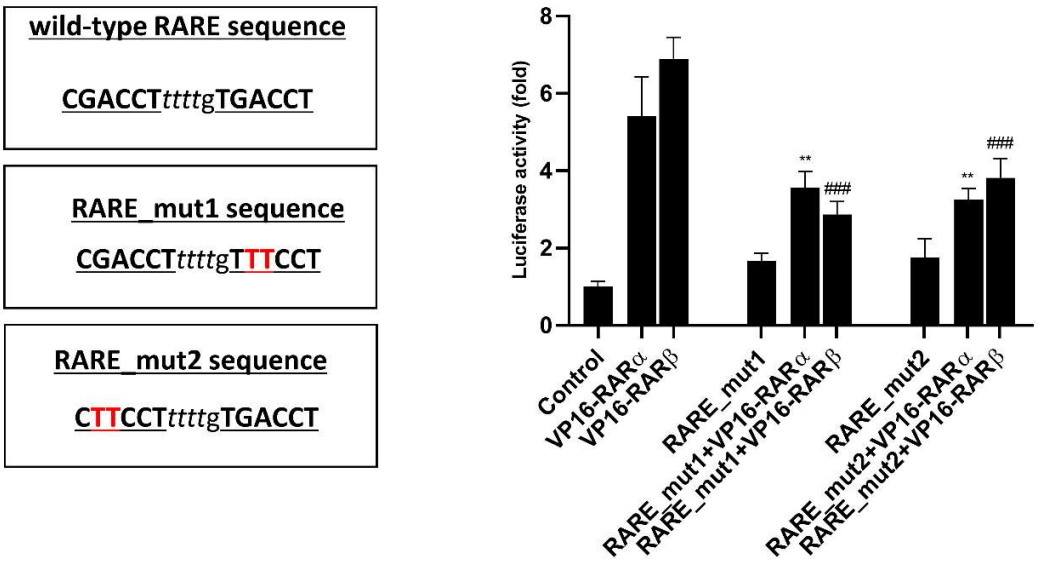

Figure S4. Effect of a RARE mutation in the *Prdm3* promoter on RARs stimulation. P19 cells were transfected with the *Prdm3* promoter carrying RARE wild-type, RARE_mut1, and RARE_mut2 sequences in combination with pcDNA3 (Control), RARα, or RARβ. Luciferase activity is shown as a fold change over control. Error bars are shown as mean ± S.E.M., n=4 per group. **p<0.01 compared to VP16-RARα and ### p<0.001 compared to VP16-RARβ.

cells

MDPI

Review

Emerging Roles of PRDM Factors in Stem Cells and Neuronal System: Cofactor Dependent Regulation of PRDM3/16 and FOG1/2 (Novel PRDM Factors)

Paweł Leszczyński [1], Magdalena Śmiech [1], Emil Parvanov [2], Chisato Watanabe [3,4], Ken-ichi Mizutani [4] and Hiroaki Taniguchi [1,*]

1 Department of Experimental Embryology, Laboratory for Genome Editing and Transcriptional Regulation, Institute of Genetics and Animal Biotechnology of the Polish Academy of Sciences, 05-552 Jastrzębiec, Poland; p.leszczynski@igbzpan.pl (P.L.); m.smiech@igbzpan.pl (M.Ś.)
2 Department of Mouse Molecular Genetics, Institute of Molecular Genetics of the Czech Academy of Science, 142 20 Vestec, Prague, Czech Republic; eparvanov@gmail.com
3 Department of Stem Cells and Human Disease Models, Research Center for Animal Life Science, Shiga University of Medical Science, Shiga 520-2192, Japan; cwatanab@belle.shiga-med.ac.jp
4 Laboratory of Stem Cell Biology, Graduate School of Pharmaceutical Sciences, Kobe Gakuin University, Kobe 650-8586, Japan; mizutani@pharm.kobegakuin.ac.jp
* Correspondence: h.taniguchi@igbzpan.pl; Tel.: +48-22-736-70-95

Received: 13 October 2020; Accepted: 25 November 2020; Published: 4 December 2020

Abstract: PRDI-BF1 (positive regulatory domain I-binding factor 1) and RIZ1 (retinoblastoma protein-interacting zinc finger gene 1) (PR) homologous domain containing (PRDM) transcription factors are expressed in neuronal and stem cell systems, and they exert multiple functions in a spatiotemporal manner. Therefore, it is believed that PRDM factors cooperate with a number of protein partners to regulate a critical set of genes required for maintenance of stem cell self-renewal and differentiation through genetic and epigenetic mechanisms. In this review, we summarize recent findings about the expression of PRDM factors and function in stem cell and neuronal systems with a focus on cofactor-dependent regulation of PRDM3/16 and FOG1/2. We put special attention on summarizing the effects of the PRDM proteins interaction with chromatin modulators (NuRD complex and CtBPs) on the stem cell characteristic and neuronal differentiation. Although PRDM factors are known to possess intrinsic enzyme activity, our literature analysis suggests that cofactor-dependent regulation of PRDM3/16 and FOG1/2 is also one of the important mechanisms to orchestrate bidirectional target gene regulation. Therefore, determining stem cell and neuronal-specific cofactors will help better understanding of PRDM3/16 and FOG1/2-controlled stem cell maintenance and neuronal differentiation. Finally, we discuss the clinical aspect of these PRDM factors in different diseases including cancer. Overall, this review will help further sharpen our knowledge of the function of the PRDM3/16 and FOG1/2 with hopes to open new research fields related to these factors in stem cell biology and neuroscience.

Keywords: PRDM; FOG; stem cells; neurons; NuRD; CtBP

1. Introduction

PRDI-BF1 (positive regulatory domain I-binding factor 1) and RIZ1 (retinoblastoma protein-interacting zinc finger gene 1) (PR) homologous-domain-containing (PRDM) transcription factors have received considerable attention recently due to their importance in regulating the development and function of various tissues and organ systems. The PRDM protein family is a group of 19 poorly studied factors that are involved in a wide range of cellular processes [1–4]. The PR domain is associated with the catalytic SET

(suppressor of variegation 3–9, enhancer of zeste and trithorax) domain, which possesses histone lysine methyltransferase (HMT) activity [5]. Although some PRDM proteins have not been shown to have intrinsic HMTase activity [6–8], several studies have confirmed that PRDM2, PRDM3, PRDM8, PRDM9, and PRDM16 possess this capability [9–14].

Depending on the cellular or tissue context, PRDM proteins mediate either transcriptional repression or activation. As several PRDM proteins appear to be enzymatically inactive, they achieve transcriptional regulation through interaction with transcription factors and histone-modifying enzymes. Interacting proteins include the Polycomb repressive complex 2 (PRC2), HMTs, histone acetyltransferases (HATs), histone deacetylases (HDACs), protein arginine N-methyltransferase 5 (PRMT5), and lysine-specific demethylase 1 (LSD1) [7,10,15–20]. For instance, the interplay between PRDM3 and the Suv39H1 HMT [21] leads to gene repression through H3K9 methylation. PRDM1, PRDM5, PRDM6 and PRDM12 are also known to interact with G9a HMT and repress gene expression through methylation of H3 lysine 9 [6–8,12,22]. PRDM proteins are involved in several developmental processes such as stem cell maintenance (Figure 1, Table 1), hematopoiesis, and adipogenesis [12,23]. Recent studies have highlighted the importance of these factors during neuronal development [24–26], including brain or spinal cord formation [26,27].

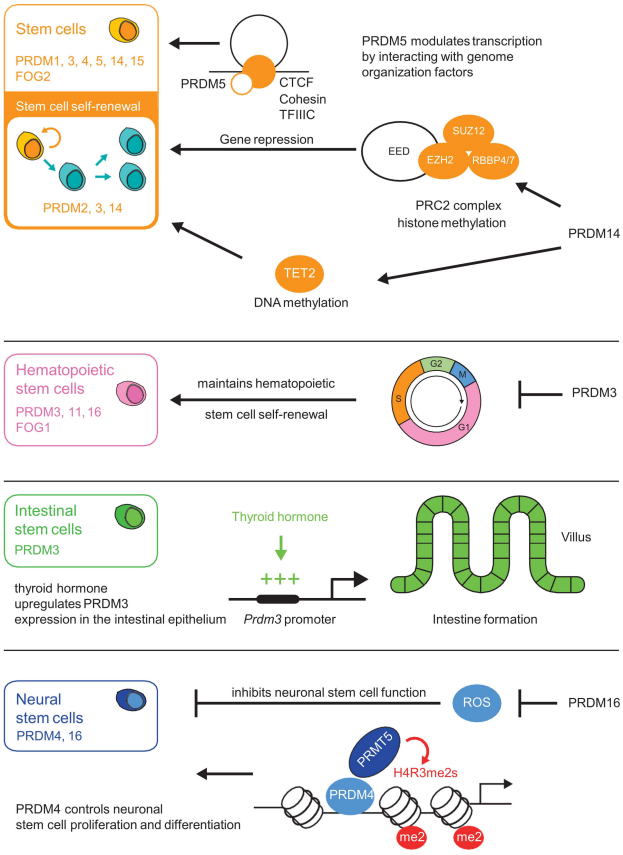

Figure 1. PRDI-BF1 (positive regulatory domain I-binding factor 1) and RIZ1 (retinoblastoma protein-interacting zinc finger gene 1) (PR) homologous domain containing (PRDM) factors play important roles in stem cell maintenance. PRDM3 and PRDM16 exhibit a crucial regulatory role in hematopoietic stem cell (HSC) and progenitor cell maintenance during fetal development [28–33]. PRDM1 determines the fate of embryonic stem cells and their progenitors [34,35]. PRDM14 plays an important role in governing the gene machinery responsible for maintaining the pluripotent state of embryonic stem cells. PRDM14 reprograms somatic cells to induce pluripotent stem cells through epigenetic pathways [36,37]. PRDM15 is also a transcriptional regulator of key genes involved in the maintenance of naive pluripotency of embryonic stem cells [38].

Table 1. Roles of PRDM factors in stem cell system.

PRDM Protein	Role in Stem Cells	References
PRDM1/BLIMP-1	Expression level predicts embryonic stem cells and progenitors' fate (mechanism partially dependent on PRL family members).	[34,35]
	Defines a mammary stem cell subpopulation with specific phenotype (mechanism unknown).	[39]
PRDM2/RIZ1	Maintains the key features of the quiescent state and affects the self-renewal of stem cells (interacts with the PRC2 complex and regulates the level of H3K9me2 within the promoter of *CCNA2A*).	[40,41]
PRDM3/EVI1	Inhibits a cell cycle and a differentiation of hematopoietic progenitor cells (indirectly upregulates genes related to keeping long-term hematopoietic stem cells like *Abca1*, *Cdkn1b*, and *Epcam*).	[42]
	Indispensable for intestinal stem cell formation during development (mechanism unknown).	[28,29]
	Induction of *Danio rerio* hematopoietic stem cell emergence by regulation of Notch pathway.	[43]
	Keeps long-term hematopoietic stem cell function during adult hematopoiesis by regulation of *Gata2*, *Sall2*, and *Pbx1* gene expression.	[44–46]
	Implicated in genesis of leukemia stem cells (precise mechanism unknown, putative target genes: *Gata1*, *Gata2*, *Mpl*, *Jag2*, *Setbp1*, and *Pbx1*).	[47,48]
PRDM4/PFM1	Regulates gene expression in embryonic stem cells mainly by binding proximally to transcription start sites of *Nodal* and *Klf5.*	[49]
	Controls the neural stem cells differentiation and proliferation by recruiting an arginine methyltransferase 5 (PRMT5).	[50]
PRDM5	Interacts with insulator proteins and modulates transcription program in embryonic stem cells.	[51]
	Transient expression with *Run1t1*, *Lmo2*, *Zfp37*, *Hlf* and *Pbx1* allows it to reprogram blood cells to hematopoietic cells.	[52]
PRDM11	Function unknown, expression in hematopoietic stem.	[53]
PRDM12	Overexpression stops cell proliferation in P19 cell line (direct mechanism unknown, upregulates p27 protein and increases the cell population in the G1 phase of the cell cycle).	[22]
PRDM14	Maintains pluripotency and self-renewal of embryonic stem (effect partially executed by recruiting repressive PRC2 complex and active DNA demethylation mediated via ten-eleven translocation (TET) proteins).	[36,54–57]
	Implicated in stem cell reprogramming (downregulates *Rnf12* gene expression via PRC2).	[58]
PRDM15	Maintains pluripotency of mouse embryonic stem cells by regulation of MAPK-ERK and WNT signaling.	[38]
PRDM16/MEL1	Supports maintenance of hematopoietic and neural stem cells (upregulates expression of *Hgf*, and *Foxj1* and regulates levels of reactive oxygen species).	[30–33]
FOG1/ZFPM-1	Increase erythropoietic differentiation rate in human hematopoietic stem cells (direct mechanism unknown, partially dependent on GATA-1, *c-myc*, and *c-myb* expression).	[59]
	Expressed in early hematopoietic cells in zebrafish and influences megakaryocytic and erythroid maturation.	[60]
	Interaction with NuRD promotes hematopoiesis.	[61]
	Required for the generation of erythroid- megakaryocytic progenitors in mice (putative mechanism addressed to Trib2-dependent C/EBPα and C/EBPβ degradation).	[62]
FOG2/ZFPM-2	Human bone marrow mesenchymal stem cells with high FOG2 expression display cardiomyogenic potency (mechanism unknown).	[63]

The PR domain is followed by repeated zinc fingers (proline-rich domains) mediating sequence-specific DNA binding and protein-protein interactions with other histone-modifying enzymes, and plays a role in nuclear import [23,64–69]. PRDM3 and PRDM16 display 63% nucleotide and 56% amino acid homology [70]. They exhibit intrinsic HMT activity towards histone 3 lysine 9 (H3K9), a mark typically associated with repressed transcription [9]. Other in vitro studies show that PRDM3 and 16 are involved in gene expression activation via methylation of histone 3 lysine 4 (H3K4) [9,24,71,72].

An additional pathway by which PRDM3 and PRDM16 govern gene expression through modification of chromatin structure is via the formation of protein complexes, such as the CtBP and NuRD [73–75]. Interestingly, FOG proteins, recently defined as PRDM factors, have also been confirmed to exert their function through the interaction with the NuRD complex and the CtBP protein [76–78], and it has been proposed that these factors may control cell fate decisions in stem cells and neuronal cells through the CtBP and NuRD complexes in a similar fashion to PRDM3 and PRDM16 [73,79]. In this review we will discuss the possible mechanism for their function in stem cell and neuronal systems through the interaction with their cofactors.

2. PRDM Factors Are Substantial Players in Stem Cells

In recent years, the number of studies on the role of PRDM proteins in stem cells and cell differentiation has increased significantly. In this section we discuss studies on the role of PRDM proteins in maintaining self-renewal and pluripotency of stem cells, and in the neuronal system with potential molecular mechanisms that regulate the action of PRDM proteins. Highly pluripotent stem cells derived from the inner cell mass (ICM) are generated from precursors with high PRDM1 expression. Moreover, PRDM1-positive cells display a gene expression profile associated with the early specification of embryonic cells toward germ cell identity [35]. Additionally, the silencing of PRDM1 in human embryonic stem cells (hESCs) changes germline potential and directs cell differentiation towards neuronal specification by increasing SOX2 expression [80], suggesting that PRDM1 acts as a switch for neural or germline cell fate by inhibiting SOX2 expression during human development. The pluripotent state in stem cells can also be controlled by epigenetic regulation. PRDM14 is an important player regulating the epigenetic state and the transcription network in stem cells [56,81]. A genome-wide RNAi screen study revealed that PRDM14 colocalizes with stemness transcription factors such as OCT3/4, SOX2 and NANOG to maintain stem cell identity [37]. Moreover, it has been shown that the recruitment of OCT3/4 to the demethylated regulatory regions of pluripotency genes is driven by PRDM14 [36]. PRDM14-dependent pluripotency is mediated by reducing *Dnmt3a/b* and *Dnmt3l* expression and globally correlates with the CpG methylation landscape [55,82,83]. PRDM14 also maintains an active DNA demethylation status in the embryonic stem cells via TET (ten-eleven translocation) proteins [54]. These results suggest that the demethylation status observed during the induction of pluripotency is controlled by PRDM14. Besides PRDM14, PRDM15 was shown to be highly expressed in the embryo inner cell mass (ICM) [84] and plays a role as a safeguard of pluripotency in stem cells by regulating MAPK–ERK and WNT signaling [38]. Stimulation of the MAPK–ERK pathway triggers ESC lineage commitment [85], whereas the WNT pathway prevents differentiation of embryonic stem cells [86]. Stem cells with PRDM15 depletion showed a marked rise in nucleosome occupancy along with increased methylation and decreased acetylation at lysine 27 on histone H3 (H3K27ac to H3K27me3) at the promoter region of *Rspo1* (R-spondin 1) and *Spry1* (protein sprouty homolog 1), which are regulators of WNT signaling and MAPK–ERK pathways [38]. In order to maintain pluripotency and self-renewal of ESC, PRDM15 increases *Spry1* and *Rspo1* expression by decreasing nucleosome occupancy at the promoter sequence and allows RNA polymerase II recruitment [38].

3. An Overview of the Roles of PRDM Factors in the Neuronal System

Newly generated cortical neurons are derived from the division of radial glia progenitors in the ventricular zone (VZ). During neuronal maturation, progenitor cells move from VZ to the subventricular zone (SVZ) and then to the intermediate zone (IZ), where they adopt multipolar morphology (MP). In the subplate (SP) zone they acquire a bipolar shape and then settle in the cortical plate (CP) as mature neurons with defined characteristics [87,88]. Role of the PRDM factors and their expression in central nervous system (CNS) is depicted in Figure 2, Table 2. PRDM8 was shown to play a role in the development of brain structures. High expression of PRDM8 is found in the upper part of the IZ where it regulates the transition from multipolar to bipolar morphology of cortical neurons [89]. Moreover, mice carrying a *Prdm8* gene deletion displayed a significant reduction of brain growth along with a

decreased number of neocortical neurons, indicating its essential role in neocortical development [26]. It has also been shown that basic helix-loop-helix family member E22 (BHLHB5), another cofactor of PRDM8, can significantly influence the formation of neuronal plasticity. PRDM8 and BHLHB5 form a repressor complex that orchestrates the neuronal circuit [90]. Mice with PRDM8 or BHLHB5 deficiency display highly similar axonal mistargeting and behavioral abnormalities [90], indicating the inherent spatiotemporal role of these factors in the formation of the nervous system. Much like their functions in stem cell maintenance, PRDM proteins tune progenitors of neuronal proliferation and differentiation through epigenetic modifications. For instance, PRDM4 is part of an epigenetic complex regulating the proliferative capacity and modulating cell cycle progression in neural stem cells (NSCs). PRDM4 interacts with PRMT5 through the PR/SET domain and the latter modifies chromatin structure by symmetric dimethylation on arginine 3 of histone H4 (H4R3me2s), specifically in the undifferentiated NSCs. Furthermore, a decrease in PRDM4 expression in NSC demonstrated precocious neurogenesis [50].

It is interesting to note that PRDM12 is involved in the development of nociceptors. Mutation in human *PRDM12* has been found in patients with congenital pain insensitivity (CIP) [91]. This mutation was found to be located in His289 of PRDM12 and it disrupts the interaction between PRDM12 and HMT G9a (EHMT2). PRDM12 has been reported to interact with G9a (EHMT2) and leads to dimethylation of histone H3 on lysine 9 (H3K9me2) in P19 cells [22]. On the other hand, it was shown that PRDM12 ablation negatively affects the Ngn1/2-TrkA pathway which interferes with nociceptor maturation [92]. These observations suggest that PRDM12 functions through epigenetic mechanisms and could serve as a molecular target in the therapeutic treatment of pain.

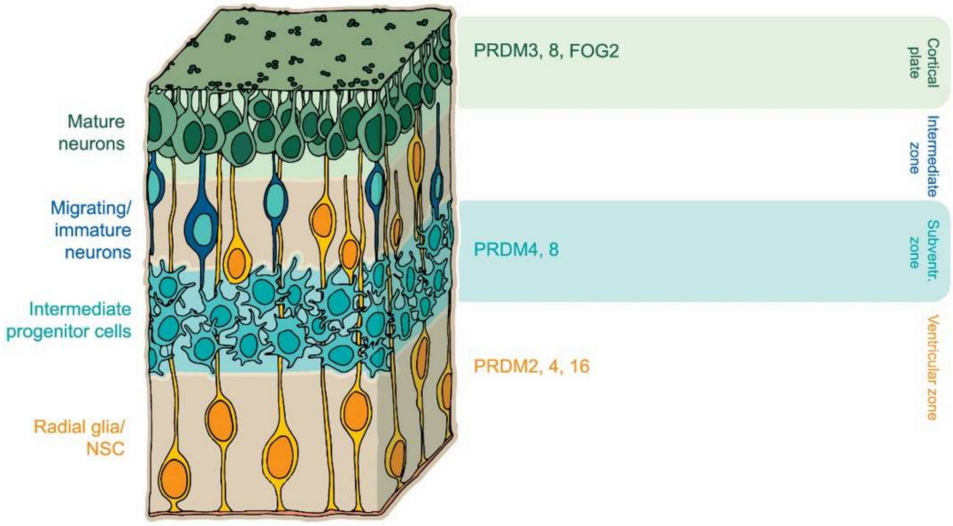

Figure 2. PRDM factors play multiple roles during central nervous system (CNS) development. PRDM16 controls the migration and differentiation of neuronal progenitors during cortical development [24,25]. FOG2 arranges a neuronal subtype identity [93] whereas PRDM8 controls axonal targeting [90].

Table 2. The roles of PRDM factors in the neuronal system.

PRDM Protein	Nervous System Function	References
PRDM1/BLIMP-1	Leads to specialization and identity of photosensory neurons (directly reduces *Chx10* expression).	[94–97]
PRDM2	Monomethylates H3K9 in neurons of the rat dorsomedial prefrontal cortex and is involved in alcohol dependence.	[98]
PRDM3/EVI1	*Caenorhabditis elegans* egl-43 protein (ortholog of PRDM3) is required for the proper development of phasmid neurons (mechanism unknown).	[99]
	Knock-out mice exhibit malformation of neuronal development during mouse embryo growth (mechanism unknown).	[100]
	The overexpression of *Prdm3* triggers neurogenesis in P19 cell line (direct mechanism unknown, high expression of *Mash1*, *Ngn1*, *NeuroD1* observed).	[101]
	Gene knock-out leads to precocious neuronal differentiation in the P19 cells (direct mechanism unknown, increased expression of MAP2 and β-III TUBULIN).	[102]
	Hamlet (*Drosophila melanogaster* PRDM3 and PRDM16 homolog) removes notch-dependent fate signature during neuronal-class diversification via direct chromatin-modification.	[103]
	Regulates homeostatic synaptic plasticity by downregulation of miR-124.	[104]
PRDM4	Controls neural stem cell proliferation and differentiation by protein arginine methyltransferase 5 (PRMT5).	[50]
PRDM5	Enhances neuronal apoptosis triggered by lipopolysaccharide (direct mechanism unknown) .	[105]
	Low expression associated with neurotherapeutic effects of miR-182/7a in spinal cord injury (SCI) model.	[106]
	Overexpression increases abnormalities mediated by WNT signaling during the development of anterior neural structures in *Danio rerio*.	[107]
PRDM8	Along with BHLHB5 creates a transcriptional repressor complex required for normal development of specific neural circuits.	[90]
	Regulates promoter activity of *Prkca* and thus retinal bipolar cell development and survival.	[108]
	Controls the morphological changes at the multipolar phase during neocortex development by indirect repression of guidance molecules, like EPHA6, NRP2, and EBF3.	[89]
	Gene knock-out impairs development of neocortical neurons (direct mechanism unknown, deregulation of *Fgf5*, *Hmcn1*, *Antxr2*, and *Slc15a2* gene expression).	[26]
PRDM12	Orchestrates sensory neuron development and specification in part by dimethylation of H3K9 (target genes unknown).	[91,109]
PRDM13	Generates neuronal specification by repression of bHLH transcriptional activators.	[110]
	Inhibits glutamatergic and promotes GABAergic neuronal development in the neural tube by repressing *Ascl1* activation of *Tlx3* gene expression.	[71,111]
PRDM14	Regulates axon growth of primary motoneurons in *Danio rerio* by regulation of *islet2* promoter activity.	[112]
PRDM15	Gene knock-out causes brain malformations via deregulation of NOTCH- and WNT-dependent pathway.	[113]
PRDM16/MEL1	Coordinates neuronal-dependent brain vascularization via SMOC1 protein.	[114]
	Involved in cortical neuron migration and positioning in part by repressing PDZRN3 expression.	[24,89]
FOG2/ZFPM-2	Controls axonal targeting and differentiation of corticothalamic projection neurons (by interaction with COUPTF1, GATA2, and GATA4 to reduce *Citp2* expression).	[93]
	Together with GATA4 and GATA6 increases *Kv4.2* gene (a subunit of somatodendritic A-type potassium channels) expression in PC12 neuron-like cell line.	[115]

4. The Function of PRDM3 and 16 in Stem Cells

Among the PRDM factors, emerging roles of PRDM3 and PRDM16 in diverse systems, including stem cells and the neuronal system, have been proposed [25,33,46,103]. Mouse embryos with *Prdm3* deletion exhibit various developmental defects and caused lethality at 10.5 days post coitum [100]. This is mainly attributed to impaired hematopoietic stem cell (HSC) proliferation.

PRDM3 regulates hematopoietic stem cell proliferation by activating the *Gata2* promoter [46], and *Gata2* gene expression is greatly reduced in *Prdm3* mutant mice [100]. Interestingly, mice lacking GATA2 expression showed a phenotype similar to PRDM3-deficient embryos. This suggests that these factors cooperate in HSC gene regulation [46,116]. Moreover, PRDM3 plays important roles in long-term HSC self-renewal [45]. These findings suggest that PRDM3 is one of the major regulators of *GATA2* gene expression and that it is also important for HSC maintenance. In *Xenopus tropicalis*, Prdm3 is required for adult intestinal formation and for the maintenance of epithelial stem cell proliferation [28]. PRDM3 has been reported as a histone 3 lysine 9 mono-methyltransferase (H3K9me1) in mammals and controls heterochromatin integrity [9]. In zebrafish, Prdm3 controls the chromatin landscape by influencing H3K9me3 and H3K4me3 marks. Furthermore, Prdm3-deficient zebrafish embryos display a 40% reduction in H3K4me3 marks [117]. These findings imply that PRDM3 plays a crucial role in stem cell self-renewal and differentiation through histone methylation. Further investigation to elucidate how PRDM3 impacts global methylation patterns to regulate the stem cell state is warranted.

Much like *Prdm3*, *Prdm16* expression is required for HSC maintenance [32,33]. PRDM16 is also responsible for many developmental processes in brown fat tissue [118,119], heart [120] and craniofacial formation [121–123]. *Prdm16* deletion in mice induces dysregulation of HSC renewal and increases apoptosis [32]. Moreover, mutation of *Prdm16* causes a disturbance in gene expression related to hematopoietic stem cell function [32]. As mentioned previously, studies in mouse embryonic fibroblasts have identified that PRDM3 is an H3K9me1 methyltransferase. PRDM16 displays similar characteristics to PRDM3. Both proteins methylate histone H3 in the cytoplasm. SUV39H1 and SUV39H2 enzymes then convert H3K9me1 to H3K9me3 in the nucleus. These modifications reinforce the heterochromatin to be assembled in pericentric DNA and the nuclear lamina [9]. The integrity of heterochromatin is important for spatial genome organization and gene expression programs [9]. Thus, PRDM16 could be involved in the modification of epigenetic markers, thereby regulating the differentiation of stem cells and progenitor cells. Indeed, this phenomenon is observed in a myoblast differentiation model, suggesting a significant role for PRDM16 in cellular transformation. Ectopic overexpression of *Prdm16* reprograms C2C12 myoblasts into brown fat cells [119]. Direct reprogramming induced by PRDM16 is accompanied by hypermethylation of myogenin and *MyoD* promoters [124]. Taken together, PRDM3 and PRDM16 both play important roles in stem cell maintenance in several systems through epigenetic mechanisms.

5. A Novel PRDM Factors, Friend of GATA (FOG) and its Function in Stem Cells

Recent studies have revealed that FOG1 is a PRDM family member [125]. FOG1/2 and PRDM3/16, carry a CtBP-binding sequence in their protein structure and repress transcription. Both proteins also contain a PR domain [64,125]. Historically, it was known that FOG1 regulates GATA1 transcription factor function and FOG2 governs GATA2 function. The interaction between the FOG family and GATA transcription factors is crucial in various tissues [126–129] where FOG proteins repress the transcriptional activity of GATA factors. Serious problems, such as failure in heart development, occur as a result of blocking the interaction between GATA4 and FOG2 [130]. Moreover, mutations in FOG2 hinder integration with GATA4 leading to congenital heart disease [131,132]. While FOG2 interacts with GATA4-6, little is known about its role in stem cells and the nervous system. Interestingly, much like AML1-PRDM3 [133], the AML1-FOG2 fusion protein have implications in myelodysplasia [134]. In this regard, the FOG2 protein may also regulate hematopoietic stem cell function. Human bone marrow mesenchymal stem cells (BM-MSC) are a heterogeneous population and only some have cardiomyogenic potential. BM-MSC subpopulations with high cardiomyogenic potential display high FOG2 gene expression [63]. This suggests that FOG2 is involved in cardiomyocyte progenitor cell function. Moreover, since the FOG family's major role is to inhibit GATA factors, FOGs may be involved in regulatory processes in stem cells and progenitors in which GATA factors play major roles.

It is known that *Fog1* deficiency is lethal for mice. Mouse embryos with this deficiency die between days 10.5 and 12.5 of gestation [135]. In these mice, erythropoiesis is highly disrupted and

megakaryocytes are absent. Intriguingly, GATA1 acts as a hematopoietic transcription factor that induces erythrocyte and megakaryocyte differentiation. These findings suggest similar phenotypes in FOG1 and GATA1-deficiencies. Another study has clearly shown that GATA1 and FOG1 interaction is essential to promote megakaryocyte/erythrocyte lineage differentiation [135]. Moreover, FOG1 is considered a reprogramming factor that stimulates the stemness state in differentiated cells. In avian eosinophils, FOG1 overexpression leads to the dedifferentiation and generation of multipotent cells [136]. Furthermore, overexpression of *Fog1* in mouse hematopoietic lineages resulted in a decreased number of eosinophils [137]. Thus, FOG1 is likely an important factor that controls the stem cell state and its function is tightly associated with GATA1.

6. The Function of PRDM3 and PRDM16 in Neuronal Cells

In *Caenorhabditis elegans*, it has been suggested that *Egl-43* (the PRDM3 and PRDM16 orthologue in *C. elegans*) has a significant influence on nervous system development. During embryonic growth, two serotonergic hermaphrodite specific neurons migrate from the caudal position to the central part of the body. Disruption of *Egl-43* gene expression stops neuronal migration and further development [99]. Follow-up reports in higher organisms highlighted the importance of PRDM3 in the formation of neuronal identity. The cellular specification of olfactory receptor neurons in *Drosophila melanogaster* is coordinated by a context-dependent response to Notch signaling. Hamlet (the PRDM3 and PRDM16 orthologue in *Drosophila*) mediates this pathway and contributes to the development of a specific type of neuron [103]. During the initiation of olfactory receptor neuron (ORN) development, Hamlet proteins erase the Notch-active state in differentiating cells. This phenomenon provides new insights into the Notch-dependent signaling pathway. The activity of Hamlet protein influences gene expression by altering the methylation profiles at promoter regions, histone packing density and chromatin organization. Hamlet alters chromatin accessibility by enabling Su(H) (suppressor of hairless protein) binding to Notch-specific enhancers. Mouse embryos with *Prdm3* deletion displayed severe defects in nervous system development, but detailed studies on brain structures were not conducted [100]. In mammals, *Prdm3* transcription is strongly activated by retinoic acid (RA) in murine embryonal carcinoma P19 cells [101]. Moreover, *Prdm3* gene expression is upregulated in NSCs compared to human embryonic stem cells [138]. Additionally, ectopic overexpression of *Prdm3* induces neurogenesis in P19 cells without RA stimulation [101]. However, the neuronal-specific role of PRDM3 remains to be addressed in mammals, and PRDM3 could be implicated in the onset of neurogenesis. Recently, our study showed that P19 cells with *Prdm3* gene knock-out displayed earlier maturation of neurons along with the rapid proliferation of non-neuronal cells [102]. These findings strongly showed the significant role of PRDM3 in the formation of the mammalian nervous system in vivo. Chromatin structure and epigenetic modifications have been reported to be crucial for regulating gene expression during brain development [139]. In this regard, PRDM3 plays a role in the formation of synaptic plasticity via epigenetic regulation of gene transcription. Investigation of synaptic plasticity using an in vitro model demonstrated that PRDM3 is expressed in the nucleus of hippocampal neurons and may be implicated in neuronal activity associated with α-amino-3-hydroxy-5-methyl-4-isoxazolepropionic acid receptor (AMPAR) regulation [104]. miR-124 expression has been strongly associated with a homeostatic response during neuronal activity [104]. Interestingly, miR-124 transcription is directly dependent on the active complex of PRDM3 and HDAC1. Regulation of miR-124 expression in hippocampal and cortical neurons is partially explained by PRDM3-dependent reduction of mir-124 promoter activity [104]. It is known that gene expression in neurons highly depends on chromatin remodeling factors [140]. Therefore, the PRDM3–HDAC1 complex could be part of a bigger, specific chromatin remodeling complex involved in the fine-tuning of synaptic plasticity. PRDM3 activates genes associated with the self-renewal mechanism in hematopoietic stem cells in mouse myelodysplastic syndrome through an increase in methylation level at the miR-124 promoter [141]. As such, the relationship between PRDM3 and miR-124 is clearly supported in two different cellular models. Therefore, further studies are

needed to determine whether PRDM3 directly affects the promoter status of other target genes in the neuronal system.

In the developing nervous system, PRDM16 is expressed in the SVZ of the neocortex and is crucial for neural stem cell maintenance. PRDM16 is a key player in maintaining neural stem cell and progenitor cells in the brain by controlling their temporal and spatial gene regulation networks [31]. In the mouse embryo, PRDM16 is mainly expressed in the VZ and SVZ but its expression decreases during brain maturation [114]. A conditional *Prdm16* deletion exhibits significant depletion of mouse neural stem cells in the SVZ as well as a limited ability to form self-renewing neurospheres in vitro [31]. Moreover, reduced *Prdm16* expression and complementary upregulation of the proneural gene *NeuroD1* in embryonic neural stem cells is crucial for the regulation of peroxisome proliferative activated receptor 1 (PGC1)-mediated changes in reactive oxygen species (ROS) levels, and this mechanism has been suggested to be important for neural migration in the developing cortex [25]. On the other hand, PRDM16 is preferentially expressed in adult neural stem cells and is required for their maintenance, partly by suppressing oxidative stress through the promotion of hepatocyte growth factor (HGF) expression [33]. Another study revealed that PRDM16 is involved in the migration and differentiation of neurons during embryonic cerebral cortex development [24]. Here, it was shown that epigenetic status during the early stages of neuronal differentiation is closely related to PRDM16-dependent mechanisms. Interestingly, the association of gene expression level with H3K27ac modification in radial cells (PRDM16 positive) is also found in mature cortical neurons where PRDM16 is not expressed. This phenomenon suggests that the previously acquired epigenetic memory remains during cortical neuronal development [24]. It has been suggested that the determination of neuronal position in the upper layer of the cerebral cortex is controlled by PRDM16-mediated repression of the gene encoding E3 ubiquitin ligase PDZ domain-containing RING finger protein 3 (PDZRN3). PRDM16 significantly reduces PDZRN3 expression in brain progenitor cells. This can be partially explained by the reduction in H3K27ac levels at the enhancer and promoter regions of *Pdzrn3*. Conversely, a significant increase in H3K27ac levels is observed in cortical cells in the absence of PRDM16. Impaired PRDM16 expression causes a significant increase in PDZRN3 expression in newly formed neurons, but the consequence of this genetic deregulation is the decreased ability of these cells to migrate to the upper brain layers. Moreover, a lack of PRDM16 in neuronal progenitors leads to abnormal dendritic morphology of mature neurons [24]. *Prdm16* deletion in neuronal stem cells causes dysregulation of angiogenesis. It was found that neurovascular communication depends in part on SMOC1, which is secreted by certain types of neurons. Neuronal SMOC1 interacts with TGFBR1 and activates the TGF-β-SMAD signaling pathway in endothelial cells. The loss of PRDM16 in neural progenitor disrupts this process and significantly impairs vascular growth in the developing brain [114]. The PRDM16 influence on neuronal cell migration and angiogenesis during central nervous system development is illustrated in Figure 3. Interestingly, RNA sequencing data show that disabling PRDM16 in progenitor cells (radial glia) resulted in a seven-fold increase in *Prdm3* expression [24]. Therefore, crosstalk between PRDM16 and PRDM3 during neuronal differentiation merits further investigation. Taken together, although functional studies in the neuronal system have just started, PRDM3 and PRDM16 most likely play paramount roles in neuronal cell fate decision and function.

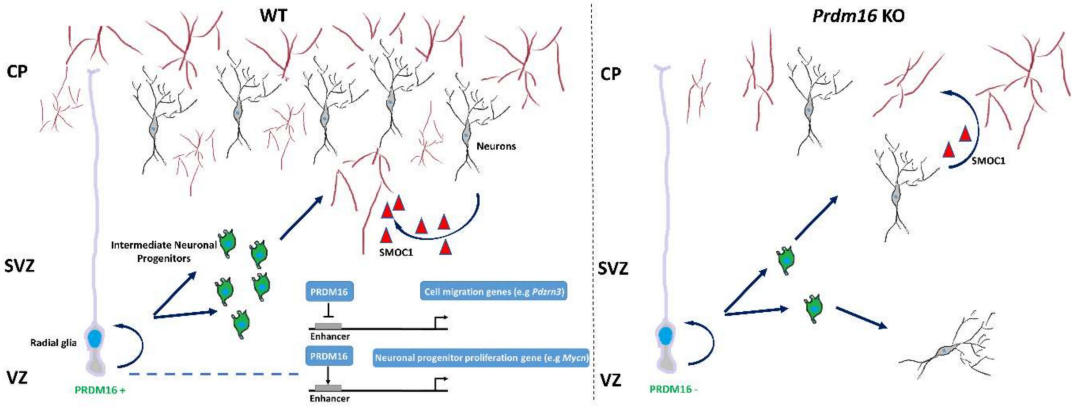

Figure 3. PRDM16 orchestrates neuronal migration and angiogenesis in the developing brain. PRDM16 organizes the migration of cortical neurons through enhancer-dependent silencing of *Pdzrn3* gene expression. In addition, PRDM16 controls the expression of genes associated with the amplification of neuronal progenitors (e.g., *Mycn*) [24]. PRDM16 positively regulates neuronal angiogenesis by enhancing the TGF-β signaling pathway via neuronally secreted SMOC1 [114]. VZ (ventricular zone), SVZ (subventricular zone), CP (cortical plate).

7. The Function of FOG1 and FOG2 in Neuronal Cells

FOG1 expression was found in the mouse mid-brain [129] as well as in the *Danio rerio* developing brain [142]. FOG1 affects the heart ventricular wall structure by regulating cardiomyocyte proliferation via the neuregulin (NRG)-ErbB-dependent signaling pathway [143]. NRG is a growth factor involved in the stimulation of ErbB tyrosine kinase receptors and thus affects cell survival, proliferation and differentiation in neuronal and non-neuronal systems. The NRG-ErbB axis is associated with susceptibility to mental illnesses such as bipolar disorder and schizophrenia [144,145]. A tight relationship between disease state and the NRG-ErbB pathway is indicated by the significant dysregulation of synaptic plasticity and neurotransmission (reviewed in [146]). Thus, the FOG1-controlled NRG-ErbB pathway may theoretically be involved in the development of synaptic plasticity and neuronal identity. However, due to the limited number of reports, the role of FOG1 in the nervous system development remains to be clarified.

In the developing brain, FOG-2 expression is detectable from around day 10 of embryonic development (E10.5) [147]. Recent studies have reported that FOG2 may be involved in shaping neuronal identity [93]. FOG2 was found exclusively in postmitotic neurons in the cortex as well as in the thalamic reticular nucleus, the hippocampus, the amygdala and the hypothalamus. These findings strongly suggest that FOG2 plays a role as a transcriptional regulator during the final stage of neuronal maturation [93]. In addition, high expression of GATA transcription factors (e.g., GATA4 and GATA6) was found within the central nervous system in mice and humans, and this expression was mainly observed in post-mitotic neurons of the cerebral cortex and the hippocampus [148,149]. Nevertheless, the function of GATA proteins in shaping the identity of neurons has not been sufficiently investigated. GATA-dependent mechanisms that form neuronal identity could be partly explained through interaction with FOG1 and FOG2 proteins. FOG2, in cooperation with GATA6, significantly increases promoter activity of the *Kv4.2* (KCND2) gene (voltage-dependent potassium channels) in PC12 neuron-like cells. This study highlighted the importance of FOG2 in neuronal function and plasticity [115]. Tying FOG2-GATA6 to the regulation of voltage-gated ion channels could reveal new avenues in investigating the regulation of brain neuroplasticity and thus the formation of memory. Accurate tuning of gene expression during cortical development requires precise regulation of molecular machinery. In this context, FOG2 appears to be a mediator in the process of generating final cellular identities in the brain. FOG2 is involved in the control of corticothalamic projection neuron (CThPN) identity and positioning [93]. CThPNs are a diverse set of neurons that are important for the function of

cortical circuitry. They are responsible for the access of sensory information to the cerebral cortex by modulating thalamic activity [150,151]. Interestingly, regulation of CThPN projection is controlled by the FOG2 and GATA4 complex via *Ctip2* (Coup-Tf interacting protein 1) promoter activity [93]. CTIP2 belongs to a group of factors crucial in postnatal brain development [152]. CTIP2 is also involved in the differentiation of postmitotic neurons and thus in memory and learning [152]. In humans, FOG2 mutations have been recognized primarily in congenital heart disease, but neurological and behavioral abnormalities have also been observed. Patients with a FOG2 deletion exhibit delayed or impaired speech ability, intellectual disability and seizures [153,154]. Based on the above information, it is postulated that FOG2 could be a crucial factor during the assembly of neural circuits and the acquisition of identities in postmitotic neurons. Further research is needed to determine the FOG2 role in brain development and neuronal plasticity.

8. NuRD Interacts with PRDM3, PRDM16, FOG1, and FOG2

Chromatin remodeling complex NuRD (nucleosome remodeling and deacetylase) primarily exhibits histone deacetylase activity and, therefore, exerts a repressor function [155,156]. The base composition of NuRD includes the metastasis-associated proteins MTA1/2/3, the histone deacetylases HDAC1 and HDAC2, the methyl-CpG-binding domain proteins (MBD2 or MBD3), CHD4, and the histone binding proteins RBBP4/7 [157–159]. NuRD regulates gene transcription associated with pluripotency and mediates the cellular response to differentiation signals in mouse embryonic stem cells (ESCs) [160,161]. NuRD activity has been reported to mediate the reduction of H3K27 acetylation facilitating recruitment of PRC2 and subsequent trimethylation of H3K27 in NuRD-dependent promoters [160,161]. The NuRD/MBD3 complex significantly shapes the final developmental stages of the brain. Despite high *Mbd3* expression in neuroepithelial cells (NECs) of the embryonic cortex [162], NuRD/MBD3 has been shown to be particularly important in regulating cell differentiation during neuronal specification [163]. Moreover, the NuRD complex affects synaptic plasticity in the mammalian brain and controls cortical neuron identity [140,164]. A good example of how NuRD influences the shape of terminal neuronal differentiation is by the regulation of the *Satb2-Ctip2* axis. CTIP2 and SATB2 are key transcription factors that define the development of two classes of projection neurons. *Ctip2* expression is terminated by the cooperation of SATB2 and NuRD. This, in turn, induces NuRD recruitment of HDAC1 and finally deacetylation of the *Ctip2* locus. Decreased levels of CTIP2 lead to the formation of a different subclass of projection neuron [165]. Recent studies have demonstrated that both PRDM3 and PRDM16 proteins interact with the chromatin remodeling NuRD complex through the RBBP4 (RB binding protein 4, chromatin remodeling factor; also known as NURF55) protein [73]. RBBP4 is recognized as a mediator that facilitates the association of chromatin with the NuRD complex by binding to histone H3 tails [166]. Amino acids from the N-terminus of PRDM3 and PRDM16 are responsible for binding to RBBP4 [73]. Interestingly, it has been reported that FOG1 and FOG2 also interact with the NuRD complex through their N-terminal amino acid sequence (Figure 4A,B) [76,78]. The N-terminal amino acid residues that interact with NuRD are conserved between PRDM3 and PRDM16 (Figure 4A). The first 12 residues of both proteins show high sequence similarity with histone 3 N-terminal residues [73]. It is known that RBBP4 interacts with LHX2 and regulates the expression of the *Sox11* and *Fezf2* genes; the most important factors determining the identity of neuronal subtype in the mouse cortex [164]. Since PRDM3 and PRDM16 interact with RBBP4 and the NuRD complex, these proteins may play a regulatory role in shaping the identity of neurons and their position in various brain structures. Moreover, since CtBP is also a major PRDM3 and PRDM16 modulator, and controls cell fate decisions (Figure 4B) [74], investigation is needed into how PRDM3 and PRDM16 select their binding to CtBP and NuRD complex.

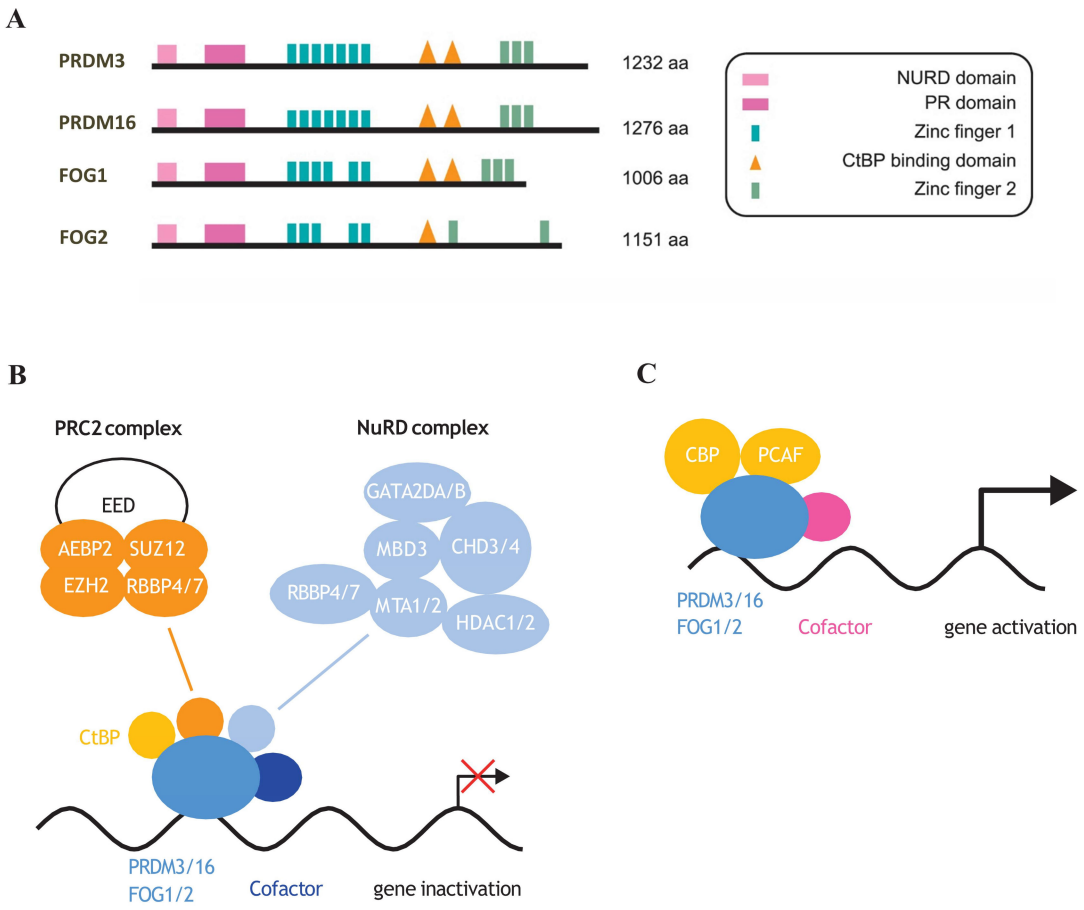

Figure 4. Protein structure of NuRD complex-dependent PRDM factors. (**A**) PR domain, CtBP binding sites, zinc fingers as well as NuRD complex binding elements are indicated. (**B**) PRDM3/16 and FOG1/2 by interaction with CtBP or NuRD complex negatively regulate gene expression during cellular differentiation [15,61,74,167,168]. (**C**) CBP- and PCAF-mediated acetylation of PRDM3 [169,170] increases its transcriptional activity [168].

FOG1/GATA1-dependent transcriptional repression is mediated by the NuRD complex. FOG-1 binds to NuRD via a 12-amino acid N-terminal motif [171]. FOG1 forms an active complex with NuRD to promote hematopoiesis. Depending on the composition of the protein complex, it also regulates cell lineage specification [61,171]. The FOG1/NuRD complex acts as a repressor of GATA1 and GATA2. This repression induces hematopoiesis by inhibiting GATA factors and subsequently halts mast cell differentiation [61]. Similarly, FOG2 modulates cardiomyocyte proliferation and heart morphogenesis by interacting with GATA4 to reduce GATA4-dependent gene expression [167,172]. However, the specific role of FOG2/NuRD interaction remains unknown.

PRDM genes can generate alternative forms of transcripts, which mainly include an isoform without a PR domain and a long product with a PR domain at the N-terminus. These two forms of transcripts can be generated using different promoter sites or by alternative splicing [64,65,67]. It is striking that the PRDM short product almost always acts as an oncogene and the long-form acts as a tumor suppressor [64,65]. PRDM3 is generated by combining two distinct genes- *MDS1* and *EVI1*. The construct without the PR domain is transcribed from one locus and is called EVI1 or sPRDM3 (short PRDM3) [173]. Mutations in the PRDM3 gene are common in acute myeloid leukemia and are related to reduced overall survival [174–176]. High expression of short PRDM3 is relatively often observed in myeloid or solid tumors. Intriguingly, the PR domain in PRDM3 appears to play a tumor suppressor function [177–179]. In addition, sPRDM3 appears to be frequently mutated in skin

melanomas, colon, lung, bladder and endometrial cancers with simultaneous decreased expression of the long PRDM3 form [180]. Moreover, deficiency of the long version of PRDM3 also leads to a decrease in the number of hemopoietic stem cells and a loss of long-term repopulation capacity through deregulation of the p57-kip2 pathway [45]. Apparently, the PR domain of the PRDM16 protein plays a significant role in regulating gene expression through modification of epigenetic signatures. Loss of the PR domain of PRDM16 leads to a reduction in histone H3 acetylation (H3ac), H3K4me3 and H3K27me3 modifications at the *Pparγ* promoter. These changes attenuate the potential of adipogenic transdifferentiation in C2C12 myoblasts [124]. Furthermore, the isoforms of PRDM16 show distinct impact on leukemia hematopoiesis. While full-length PRDM16 suppresses the inflammatory pathway, its short-isoform exhibits the opposite effect in HSC [30]. On the other hand, PRDM16 lacking a PR domain triggers leukemic transformation in mice progenitor cells that carry a *p53* deletion. Hence, it is presumed that the long isoform of PRDM16 conceivably acts as a tumor suppressor [181]. The function of the PR domain in PRDM proteins during neuronal differentiation is unclear due to the small number of related studies, but the PR domain of PRDM16 is known to control epigenetic silencing determining the migration and position of neurons in the brain cortex [24]. In the same study, it was demonstrated that only a long version of PRDM16 is able to reverse the neuronal migration defects in PRDM16-deficient mouse brains [24]. Interestingly, the removal of a PR domain in the PRDM3/16 and FOG1/2 should also eliminate the NuRD domain, which is located at the N-terminus of the protein (Figure 4A). NuRD has shown paramount importance in the maintenance of hematopoietic stem cells [182] and neuronal development [183]. Therefore, it would be interesting to determine whether the effect of loss of PR domain results from the lack of interaction with cofactors such as the NuRD complex.

9. CtBP Controls PRDM3, PRDM16, and FOG Function

CtBP controls the function of PRDM3, 16, and the FOG family through its specific binding sites [74,75,77,126]. CtBP1 and 2 are known as major transcriptional corepressors [184]. Ablation of CtBP proteins in early development is known to cause embryonic lethality [184], and information on the function of CtBP in the neural system is, therefore, limited. However, expression of CtBP1 has been reported in cultured hippocampal neurons, suggesting a potential function of CtBP1 in learning and memory [185]. Moreover, functional roles for CtBP in the neural system have been described in a number of studies in *D. melanogaster*. Drosophila CtBP (dCtBP) can control cell fate decisions in the sensory organ system as its loss of function leads to the formation of extra bristles, whereas flies with mutated dCtBP show a loss of bristles. Hamlet, fly PRDM3/16, loses its repressive activity when both CtBP domain and Zn fingers are deleted [103]. These results suggest that the function of PRDM3/16 and Hamlet is largely dependent on the CtBP protein, and their physical interaction is one of the key mechanisms by which PRDM3/16 orchestrates target gene expressions in stem cells and neuronal systems.

Crosstalk between CtBP and sumoylation has been reported to be important for repressing transcriptional activity of PRDM16 protein [186]. Sumoylation is characterized by the reversible attachment of small ubiquitin-related modifier (SUMO) family members to lysine residue(s) located on target proteins via SUMO-activating enzyme subunit 1/2 (SAE1/2) and the SUMO-1-conjugating enzyme UBC9. The role of sumoylation has been studied in neurodegenerative diseases including Alzheimer's disease [187,188]. *Sumo1*, *2*, and *3* are expressed in the developing mouse brain [189] and sumoylation acts as a modulator of several neural activities and of neuronal stem cell maintenance [190–192]. Among PRDM factors, PRDM3 and PRDM16 are known to be modulated by sumoylation. Sumoylation inhibits the DNA binding activity of PRDM3 to the *Bcl-xL* promoter, which eventually might be involved in mediating apoptosis [193]. Sumoylation of PRDM16 regulates its interaction with CtBP and activates PRDM16's repressor activity. Moreover, the role of sumoylation in the regulation of PRDM16 has been well characterized in adipose tissue thermogenesis [194] and acute myeloid leukemia progression [195]. Thus, it has been proposed that sumoylation plays an

important role in modulating PRDM3 and PRDM16 activity. Still, the role of sumoylation-dependent regulation of PRDM3 and PRDM16 in the nervous system remains to be elucidated. The new PRDM family member FOG1 is also regulated by sumoylation and specifically its interaction with CtBP. Interestingly, the sumoylation of FOG1 is modulated by the presence of phosphorylated residues in its sequence. Yang et al. [196] have proposed that several transcription factors possess a ψKxExxS/T (K = sumoylation target, S/T = phosphorylation target) motif which could be responsible for the interplay between sumoylation and phosphorylation marks on FOG1 activity. Thus, the interplay between post-translational modifications may orchestrate transcriptional repression via CtBP-dependent PRDM factors including PRDM3, 16, FOG1, and FOG2.

10. PRDM3/16 Function as Activators in Gene Regulation

Interestingly, PRDM3 and 16 interact not only with transcriptional repressors but also activators. Therefore, they are considered to be able to bidirectionally control gene expression (gene upregulation and downregulation) to exert their function. Acetylation of proteins acts as a positive regulator of transcription factors. PCAF and CBP acetylate PRDM3 [169,170], which enhances its transcriptional activity at the *GATA2* promoter (Figure 4C) [168]. Accordingly, the active PRDM3-GATA2 axis maintains a pool of hematopoietic stem cells. An interesting example of activation of gene expression by PRDM3 can be depicted by the interaction of PRDM3 with BRG1 in the embryonic fibroblast cell line (NIH 3T3). BRG1 significantly reduces the *E2F1* promoter activity, thus reducing the level of cell proliferation. By binding to BRG1, PRDM3 blocks this repression thereby accelerating the cell cycle [197]. BRG1 is a component of the SWI/SNF complex. SWI/SNF predominantly enhances gene expression by remodeling chromatin structure and making it more accessible to transcription factors but, depending on its protein partners, it may exhibit a repressive effect [198,199]. Interestingly, it has been shown that BRG1 can be also associate with the NuRD complex [200]. Therefore, the functional relationships between PRDM3, BRG1 and NuRD complex [73,197] remain to be clarified. Overexpression of C/EBPβ and PRDM16 reprograms murine and human fibroblasts into fat cells. It is suggested that C/EBP-β acts as a PRDM16 coactivator to enable the interaction of PGC-1α and PPARγ and activates cell differentiation [201]. It is known that C/EBP-β mediates the tuning of the transcription program to induce neurogenesis and to inhibit glial growth [202]. In mice, C/EBP-β has been shown to be involved in the survival and proliferation of neural stem cells in the hippocampus [203]. A similar effect was described by Shimada et al. where PRDM16 was indispensable for the maintenance of neural stem cells in the postnatal brain [31]. These similarities imply that C/EBP-β may also interact with PRDM16 during brain development and thus tune the genetic program in order to generate neuronal precursors.

Table 3 displays the most recognized cofactors interacting with PRDM3/16 and FOG1/2, and their roles.

Table 3. Summary of PRDM3/16 and FOG1/2 interaction with their known cofactors. The PRDM3/16 and FOG1/2 proteins affect the genetic program and cell functions by interaction with their cofactors. This influence may have a positive or negative effect.

Gene Symbol	Interacting Protein	Gene Repression	Refs
PRDM3	CtBP1/2	Increases proliferation of Mv1Lu cell line and (murine hematopoietic precursor cell line) 32Dc13.	[79,168,204–207]
	RUNX1	Blocks the differentiation of 32Dcl3 cells and induce cell death.	[208]
	GATA1	Represses of erythroid-lineage differentiation in murine bone marrow cells.	[209]
	PU.1	Impairs myelopoiesis in bone marrow progenitors.	[210]
	SMAD3	Increase the growth of myeloid cells.	[211]
	JNK	Stops stress-induced cell death in NIH 3T3 cells.	[212]
	SNAIL, HDAC1	Fosters epithelial-to-mesenchymal transition in nasopharyngeal carcinoma cell line (6-10B cells).	[213]

Table 3. *Cont.*

Gene Symbol	Interacting Protein	Gene Repression	Refs
	DNMT3A/B	Represses regulatory regions of miR-124-3, function unknown.	[214]
	SUV39H1, G9a	Bone marrow immortalization and transcription suppression.	[215,216]
	HDAC1	Stops the homeostatic response in cortical neurons.	[56,104,204]
	NuRD complex (RBBP4)	Function unknown.	[73,204]
	PRC2 complex (EZH2, SUZ12, EED)	Myeloid transformation of bone marrow.	[15]
	HIC1	Abolishes the PRDM3-mediated inhibition of apoptosis in HCT116 cells.	[217]
	p65	Represses inflammation via inhibition of NF-κB in middle ear epithelial and airway epithelial cells.	[218]
	P/CAF and CBP	Cell function unknown, changes nuclear localization pattern of PRDM3.	[170]
	BRG1	Increases proliferation of 32Dcl3 cells (murine hematopoietic precursor cell line).	[197]
	P/CAF	Increases proliferation and maintenance of HSC.	[168]
	NuRD complex (MBD3)	Hinders the histone deacetylation activity of NuRD (in vivo function unknown).	[219]
PRDM16	CtBP1/2	Reduces gene expression involved in white fat development.	[74]
	UBC9	Mediates CtBP1/2-dependent blocking of myeloid differentiation of L-G3 cells.	[186]
	EHMT1	Blocks myogenic differentiation.	[220]
	SMAD3	Inhibits the cytostasis in MKN28 gastric cancer cells.	[221]
	LSD1	Diminishes the expression of white fat genes.	[222]
	NuRD complex (RBBP4)	Function unknown.	[73]
	C/EBPβ	Sets up a transformation of myoblastic precursors into brown fat cells.	[201]
	PPARγ	Stimulates a brown adipogenesis.	[119]
	MEDIATOR complex (MED1)	Adjusts a chromatin architecture in key brown fat genes.	[223]
	ZFP516	Promotes brown fat development in white fat cells.	[224]
	PGC-1α	Highly stimulates a transcriptional program of brown fat development.	[74]
FOG1	GATA1	Represses erythroid cell maturation.	[135,225,226]
	NuRD complex (MTA1/2, p66, RBBP4)	Inhibits GATA-1-dependent gene transcription involved in the terminal erythroid maturation.	[128]
	CtBP1/2	Hampers erythropoiesis in *Xenopus*.	[77,227]
	LSD1	Function unknown.	[228]
FOG2	COUP-TF2, COUP-TF3	Specific function unknown, probably involved in cardiac morphogenesis.	[229]
	Art27	Boosts the transcriptional repression of GATA4 and thus gene expression involved in cardiac development.	[230]
	CtBP1/2	Suppresses the adipogenesis of 3T3-L1 cells.	[126]
	NuRD complex (MTA1/RBBP4/7)	Increases cardiomyocyte proliferation mediated via repression of *Cdkn1a* transcription.	[76,167]
	GATA4	Decreases *α-MHC* promoter in primary cardiomyocytes.	[147]
	RXRα	Boosts the transcriptional repression of GATA4 and thus gene expression involved in cardiac development.	[231]
	GATA6	Function unknown.	[172]
	GATA4	Increases the α-MHC promoter activity in Cos cells.	[147]

11. Role of PRDM Proteins in Cancer Development and their Gene Mutations Found in Neuronal Diseases

Although PRDM proteins are recognized as regulators involved in cell differentiation [23], their commitment (suppressive or oncogenic) in the pathogenesis of human diseases such as carcinogenesis is also under investigation. PRDM1 is recognized as a tumor suppressor that inhibits the development of cancer cells, including lymphomas [232–235]. A chromosomal deletion or epigenetic silencing of PRDM1 expression is common in diffuse large B cell lymphoma subtypes [234,236,237]. Abnormal PRDM1 expression is also associated with other nonhematopoietic cancer cells, such as glioblastoma malignancies [238]. It has been identified that the downregulation of PRDM1 correlates with increased malignancy of lung tumors, where *PRDM1* disruption promoted neoplastic invasiveness [235]. The *PRDM*3 is a fused complex of two different transcripts, *MDS1* and *EVI1*. It is a frequent site of viral insertion and is associated with the development of myeloid leukemia [239,240]. PRDM14 overexpression, or retroviral integration in the gene locus, is often found in various types of cancer, and the molecular mechanism is set up to promote pluripotent traits [241]. PRDM14 overexpression is detected in approximately 25% of human lymphoid tumors. Mice bone marrow cells transduced with the PRDM14 expression vector often develop leukemia. The analysis of the gene expression profile indicated that *PRDM14* overexpressing cells showed significant enrichment of pluripotent genes and enhancement of the tumor-initiating pathway (WNT and RAS signaling) [242]. Although PRDM14 seems to be associated with the acquisition of an immortal phenotype, the neoplastic process driven by PRDM14 might depend on the tissue. Assessment of gene methylation levels from cervical scratches positive for human papillomavirus (HPV) at high risk of malignant disease showed an increased methylation level of the *PRDM14* gene [243]. It can, therefore, be assumed that PRDM14 acts as a tumor suppressor in cervical cancer. Hence, the role of PRDM14 in tumor development is enigmatic and requires further research. In lung cancer, the high methylation signature of the PRDM16 gene caused a significant reduction of its expression [244,245]. Another study indicated that relatively high expression of PRDM16 in patients with nonsmall cell lung cancer was associated with a preferable survival score [246–248]. At least in part, the PRDM16-mediated tumor inhibition could be explained by hammering the epithelial-to-mesenchymal transition in lung adenocarcinomas [246]. The role of FOG1 in the development of neoplasms is still ambiguous, albeit mutations within *FOG1* locus are extremely common (approximately 50% of cases) in patients with adrenocortical carcinoma [180]. Moreover, preliminary analysis indicates that *FOG1* is also frequently mutated in colorectal cancer [180]. Despite the small number of studies conducted on the relationship between FOG1 and initiation or tumor progression, the abovementioned findings indicate an unexplored phenomenon of the high frequency of *FOG1* mutations in tumors. FOG2, along with GATA4 and GATA6, is relatively highly expressed in sex cord-derived ovarian tumors [249]. Deregulation of the expression of *FOG2* and its cofactors has also been observed in ovarian granular cell tumors and ovarian stromal tumors in children [250,251]. Moreover, recent studies have shown that FOG2 is one of the most common mutated genes in the PRDM protein family. A high frequency of *FOG2* mutations is found in skin melanomas, uterine cancer, rectal cancer, esophageal cancer, gastric adenocarcinoma and lung tumors [180].

Human *PRDM* gene mutations in the nervous system are poorly recognized. Nevertheless, genetic abnormalities found within *PRDM* genes are significantly associated with neurological disabilities (Table 4). Clinical effects of *PRDM12* mutations in patients within the congenital insensitivity to pain are caused by defects in the development of nociceptors [91]. *FOG2* mutations were found to have a deleterious effect on brain structure development and patients exhibited a motor, linguistic and cognitive delay with seizure events [154,252].

Table 4. Clinical effect of mutation in PRDM genes within the neurological system.

Gene	Mutation Type	Phenotype	References
PRDM8	Homozygous missense mutation	Progressive myoclonus epilepsy.	[253]
PRDM12	Several mutations within gene, autosomal recessive	Neuropathy, congenital insensitivity to pain.	[91]
PRDM13	Heterozygous mutation, tandem duplication	Macular dystrophy, North Carolina type.	[254]
PRDM16	Chromosome 1p36 deletion	Mental retardation.	[255]
FOG2	46XY sex reversal 9	Subtentorial ventricular dilation, major learning and reading difficulties.	[252]
	46,XY,del (1) (q41q42.12)	Atrophy of the right hippocampus, loss of volume in the right side of the brain, seizures.	[154]

12. Conclusions

Emerging evidence has suggested that PRDM factors cooperate with a number of protein partners to regulate a critical set of genes required for the maintenance of stem cell self-renewal and differentiation through multiple mechanisms. In this review, we proposed a NuRD and CtBP-dependent function of PRDM3/16 and FOG1/2 with respect to stem cell maintenance and neuronal differentiation. Moreover, we listed possible mechanisms of how these factors can regulate their target gene expression in a spatiotemporal and bidirectional manner. Although the PR domain that is contained in PRDM factors exerts methylation enzyme activity, our study suggests that cofactor-dependent regulation of PRDM3/16 and FOG1/2 is also one of the most important mechanisms to regulate PRDM factors function. Stem cell and neuronal cell fate are orchestrated by fine-tuned molecular mechanisms in which several transcription factors are encountered and dissociated. Furthermore, dysfunction of these factors causes abnormality in several tissues, and even leads to increased cancer risk. Therefore, identifying their stem cell and neuronal-specific cofactors will help to improve understanding of how they function in healthy and diseased conditions.

Author Contributions: Conceptualization, P.L. and H.T.; writing—original draft preparation, P.L., M.Ś., and H.T.; writing—review and editing, M.Ś., H.T., E.P., C.W., and K.-i.M.; figure design; P.L., M.Ś., and H.T.; funding acquisition, P.L. All authors have read and agreed to the published version of the manuscript.

Funding: This review was financially supported by National Science Centre, Poland (grant no. 2017/25/N/NZ3/01886).

Acknowledgments: The authors thank Tobias Hohenauer for help with editing the manuscript and illustrations.

Conflicts of Interest: The authors declare no conflict of interest.

References

1. Buyse, I.M.; Shao, G.; Huang, S. The retinoblastoma protein binds to RIZ, a zinc-finger protein that shares an epitope with the adenovirus E1A protein. *Proc. Natl. Acad. Sci. USA* **1995**, *92*, 4467–4471. [CrossRef] [PubMed]
2. Huang, S. Blimp-1 is the murine homolog of the human transcriptional repressor PRDI-BF1. *Cell* **1994**, *78*, 9–10. [CrossRef]
3. Keller, A.D.; Maniatis, T. Identification and characterization of a novel repressor of beta-interferon gene expression. *Genes Dev.* **1991**, *5*, 868–879. [CrossRef] [PubMed]
4. Turner, C.A., Jr.; Mack, D.H.; Davis, M.M. Blimp-1, a novel zinc finger-containing protein that can drive the maturation of B lymphocytes into immunoglobulin-secreting cells. *Cell* **1994**, *77*, 297–306. [CrossRef]
5. Xiao, B.; Wilson, J.R.; Gamblin, S.J. SET domains and histone methylation. *Curr. Opin. Struct. Biol.* **2003**, *13*, 699–705. [CrossRef]
6. Duan, Z.; Person, R.E.; Lee, H.H.; Huang, S.; Donadieu, J.; Badolato, R.; Grimes, H.L.; Papayannopoulou, T.; Horwitz, M.S. Epigenetic regulation of protein-coding and microRNA genes by the Gfi1-interacting tumor suppressor PRDM5. *Mol. Cell. Biol.* **2007**, *27*, 6889–6902. [CrossRef]

7. Davis, C.A.; Haberland, M.; Arnold, M.A.; Sutherland, L.B.; McDonald, O.G.; Richardson, J.A.; Childs, G.; Harris, S.; Owens, G.K.; Olson, E.N. PRISM/PRDM6, a transcriptional repressor that promotes the proliferative gene program in smooth muscle cells. *Mol. Cell Biol.* **2006**, *26*, 2626–2636. [CrossRef]
8. Gyory, I.; Wu, J.; Fejer, G.; Seto, E.; Wright, K.L. PRDI-BF1 recruits the histone H3 methyltransferase G9a in transcriptional silencing. *Nat. Immunol.* **2004**, *5*, 299–308. [CrossRef]
9. Pinheiro, I.; Margueron, R.; Shukeir, N.; Eisold, M.; Fritzsch, C.; Richter, F.M.; Mittler, G.; Genoud, C.; Goyama, S.; Kurokawa, M.; et al. Prdm3 and Prdm16 are H3K9me1 methyltransferases required for mammalian heterochromatin integrity. *Cell* **2012**, *150*, 948–960. [CrossRef]
10. Kim, K.C.; Geng, L.; Huang, S. Inactivation of a histone methyltransferase by mutations in human cancers. *Cancer Res* **2003**, *63*, 7619–7623.
11. Hayashi, K.; Yoshida, K.; Matsui, Y. A histone H3 methyltransferase controls epigenetic events required for meiotic prophase. *Nature* **2005**, *438*, 374–378. [CrossRef] [PubMed]
12. Fog, C.K.; Galli, G.G.; Lund, A.H. PRDM proteins: Important players in differentiation and disease. *Bioessays* **2012**, *34*, 50–60. [CrossRef] [PubMed]
13. Eom, G.H.; Kim, K.; Kim, S.M.; Kee, H.J.; Kim, J.Y.; Jin, H.M.; Kim, J.R.; Kim, J.H.; Choe, N.; Kim, K.B.; et al. Histone methyltransferase PRDM8 regulates mouse testis steroidogenesis. *Biochem. Biophys. Res. Commun.* **2009**, *388*, 131–136. [CrossRef] [PubMed]
14. Derunes, C.; Briknarova, K.; Geng, L.; Li, S.; Gessner, C.R.; Hewitt, K.; Wu, S.; Huang, S.; Woods, V.I., Jr.; Ely, K.R. Characterization of the PR domain of RIZ1 histone methyltransferase. *Biochem. Biophys. Res. Commun.* **2005**, *333*, 925–934. [CrossRef]
15. Yoshimi, A.; Goyama, S.; Watanabe-Okochi, N.; Yoshiki, Y.; Nannya, Y.; Nitta, E.; Arai, S.; Sato, T.; Shimabe, M.; Nakagawa, M.; et al. Evi1 represses PTEN expression and activates PI3K/AKT/mTOR via interactions with polycomb proteins. *Blood* **2011**, *117*, 3617–3628. [CrossRef]
16. Su, S.T.; Ying, H.Y.; Chiu, Y.K.; Lin, F.R.; Chen, M.Y.; Lin, K.I. Involvement of histone demethylase LSD1 in Blimp-1-mediated gene repression during plasma cell differentiation. *Mol. Cell Biol.* **2009**, *29*, 1421–1431. [CrossRef]
17. Ancelin, K.; Lange, U.C.; Hajkova, P.; Schneider, R.; Bannister, A.J.; Kouzarides, T.; Surani, M.A. Blimp1 associates with Prmt5 and directs histone arginine methylation in mouse germ cells. *Nat. Cell Biol.* **2006**, *8*, 623–630. [CrossRef]
18. Alliston, T.; Ko, T.C.; Cao, Y.; Liang, Y.Y.; Feng, X.H.; Chang, C.; Derynck, R. Repression of bone morphogenetic protein and activin-inducible transcription by Evi-1. *J. Biol. Chem.* **2005**, *280*, 24227–24237. [CrossRef]
19. Chittka, A.; Arevalo, J.C.; Rodriguez-Guzman, M.; Perez, P.; Chao, M.V.; Sendtner, M. The p75NTR-interacting protein SC1 inhibits cell cycle progression by transcriptional repression of cyclin E. *J. Cell Biol.* **2004**, *164*, 985–996. [CrossRef]
20. Yu, J.; Angelin-Duclos, C.; Greenwood, J.; Liao, J.; Calame, K. Transcriptional repression by blimp-1 (PRDI-BF1) involves recruitment of histone deacetylase. *Mol. Cell Biol.* **2000**, *20*, 2592–2603. [CrossRef]
21. Cattaneo, F.; Nucifora, G. EVI1 recruits the histone methyltransferase SUV39H1 for transcription repression. *J. Cell Biochem.* **2008**, *105*, 344–352. [CrossRef] [PubMed]
22. Yang, C.M.; Shinkai, Y. Prdm12 is induced by retinoic acid and exhibits anti-proliferative properties through the cell cycle modulation of P19 embryonic carcinoma cells. *Cell Struct. Funct.* **2013**, *38*, 197–206. [CrossRef] [PubMed]
23. Hohenauer, T.; Moore, A.W. The Prdm family: Expanding roles in stem cells and development. *Development* **2012**, *139*, 2267–2282. [CrossRef] [PubMed]
24. Baizabal, J.M.; Mistry, M.; Garcia, M.T.; Gomez, N.; Olukoya, O.; Tran, D.; Johnson, M.B.; Walsh, C.A.; Harwell, C.C. The Epigenetic State of PRDM16-Regulated Enhancers in Radial Glia Controls Cortical Neuron Position. *Neuron* **2018**, *98*, 945–962.e8. [CrossRef] [PubMed]
25. Inoue, M.; Iwai, R.; Tabata, H.; Konno, D.; Komabayashi-Suzuki, M.; Watanabe, C.; Iwanari, H.; Mochizuki, Y.; Hamakubo, T.; Matsuzaki, F.; et al. Prdm16 is crucial for progression of the multipolar phase during neural differentiation of the developing neocortex. *Development* **2017**, *144*, 385–399. [CrossRef]
26. Inoue, M.; Iwai, R.; Yamanishi, E.; Yamagata, K.; Komabayashi-Suzuki, M.; Honda, A.; Komai, T.; Miyachi, H.; Kitano, S.; Watanabe, C.; et al. Deletion of Prdm8 impairs development of upper-layer neocortical neurons. *Genes Cells* **2015**, *20*, 758–770. [CrossRef]

27. Eguchi, R.; Yoshigai, E.; Koga, T.; Kuhara, S.; Tashiro, K. Spatiotemporal expression of Prdm genes during Xenopus development. *Cytotechnology* **2015**, *67*, 711–719. [CrossRef]
28. Okada, M.; Shi, Y.B. EVI and MDS/EVI are required for adult intestinal stem cell formation during postembryonic vertebrate development. *FASEB J.* **2018**, *32*, 431–439. [CrossRef]
29. Miller, T.C.; Sun, G.; Hasebe, T.; Fu, L.; Heimeier, R.A.; Das, B.; Ishizuya-Oka, A.; Shi, Y.B. Tissue-specific upregulation of MDS/EVI gene transcripts in the intestine by thyroid hormone during Xenopus metamorphosis. *PLoS ONE* **2013**, *8*, e55585. [CrossRef]
30. Corrigan, D.J.; Luchsinger, L.L.; Justino de Almeida, M.; Williams, L.J.; Strikoudis, A.; Snoeck, H.W. PRDM16 isoforms differentially regulate normal and leukemic hematopoiesis and inflammatory gene signature. *J. Clin. Investig.* **2018**, *128*, 3250–3264. [CrossRef]
31. Shimada, I.S.; Acar, M.; Burgess, R.J.; Zhao, Z.; Morrison, S.J. Prdm16 is required for the maintenance of neural stem cells in the postnatal forebrain and their differentiation into ependymal cells. *Genes Dev.* **2017**, *31*, 1134–1146. [CrossRef] [PubMed]
32. Aguilo, F.; Avagyan, S.; Labar, A.; Sevilla, A.; Lee, D.F.; Kumar, P.; Lemischka, I.R.; Zhou, B.Y.; Snoeck, H.W. Prdm16 is a physiologic regulator of hematopoietic stem cells. *Blood* **2011**, *117*, 5057–5066. [CrossRef] [PubMed]
33. Chuikov, S.; Levi, B.P.; Smith, M.L.; Morrison, S.J. Prdm16 promotes stem cell maintenance in multiple tissues, partly by regulating oxidative stress. *Nat. Cell Biol.* **2010**, *12*, 999–1006. [CrossRef] [PubMed]
34. Mould, A.; Morgan, M.A.; Li, L.; Bikoff, E.K.; Robertson, E.J. Blimp1/Prdm1 governs terminal differentiation of endovascular trophoblast giant cells and defines multipotent progenitors in the developing placenta. *Genes Dev.* **2012**, *26*, 2063–2074. [CrossRef]
35. Chu, L.F.; Surani, M.A.; Jaenisch, R.; Zwaka, T.P. Blimp1 expression predicts embryonic stem cell development in vitro. *Curr. Biol.* **2011**, *21*, 1759–1765. [CrossRef]
36. Okashita, N.; Suwa, Y.; Nishimura, O.; Sakashita, N.; Kadota, M.; Nagamatsu, G.; Kawaguchi, M.; Kashida, H.; Nakajima, A.; Tachibana, M.; et al. PRDM14 Drives OCT3/4 Recruitment via Active Demethylation in the Transition from Primed to Naive Pluripotency. *Stem. Cell Reports* **2016**, *7*, 1072–1086. [CrossRef]
37. Chia, N.Y.; Chan, Y.S.; Feng, B.; Lu, X.; Orlov, Y.L.; Moreau, D.; Kumar, P.; Yang, L.; Jiang, J.; Lau, M.S.; et al. A genome-wide RNAi screen reveals determinants of human embryonic stem cell identity. *Nature* **2010**, *468*, 316–320. [CrossRef]
38. Mzoughi, S.; Zhang, J.; Hequet, D.; Teo, S.X.; Fang, H.; Xing, Q.R.; Bezzi, M.; Seah, M.K.Y.; Ong, S.L.M.; Shin, E.M.; et al. PRDM15 safeguards naive pluripotency by transcriptionally regulating WNT and MAPK-ERK signaling. *Nat. Genet* **2017**, *49*, 1354–1363. [CrossRef]
39. Elias, S.; Morgan, M.A.; Bikoff, E.K.; Robertson, E.J. Long-lived unipotent Blimp1-positive luminal stem cells drive mammary gland organogenesis throughout adult life. *Nat. Commun.* **2017**, *8*, 1–12. [CrossRef]
40. Cheedipudi, S.; Gala, H.P.; Puri, D.; Dhawan, J. Identification of PRDM2 regulated genes in quiescent C2C12 myoblasts. *Genom. Data* **2015**, *6*, 264–266. [CrossRef]
41. Cheedipudi, S.; Puri, D.; Saleh, A.; Gala, H.P.; Rumman, M.; Pillai, M.S.; Sreenivas, P.; Arora, R.; Sellathurai, J.; Schroder, H.D.; et al. A fine balance: Epigenetic control of cellular quiescence by the tumor suppressor PRDM2/RIZ at a bivalent domain in the cyclin a gene. *Nucleic. Acids Res.* **2015**, *43*, 6236–6256. [CrossRef] [PubMed]
42. Kustikova, O.S.; Schwarzer, A.; Stahlhut, M.; Brugman, M.H.; Neumann, T.; Yang, M.; Li, Z.; Schambach, A.; Heinz, N.; Gerdes, S.; et al. Activation of Evi1 inhibits cell cycle progression and differentiation of hematopoietic progenitor cells. *Leukemia* **2013**, *27*, 1127–1138. [CrossRef] [PubMed]
43. Konantz, M.; Alghisi, E.; Muller, J.S.; Lenard, A.; Esain, V.; Carroll, K.J.; Kanz, L.; North, T.E.; Lengerke, C. Evi1 regulates Notch activation to induce zebrafish hematopoietic stem cell emergence. *EMBO J.* **2016**, *35*, 2315–2331. [CrossRef] [PubMed]
44. Fukuda, S.; Hoggatt, J.; Singh, P.; Abe, M.; Speth, J.M.; Hu, P.; Conway, E.M.; Nucifora, G.; Yamaguchi, S.; Pelus, L.M. Survivin modulates genes with divergent molecular functions and regulates proliferation of hematopoietic stem cells through Evi-1. *Leukemia* **2015**, *29*, 433–440. [CrossRef]
45. Zhang, Y.; Stehling-Sun, S.; Lezon-Geyda, K.; Juneja, S.C.; Coillard, L.; Chatterjee, G.; Wuertzer, C.A.; Camargo, F.; Perkins, A.S. PR-domain-containing Mds1-Evi1 is critical for long-term hematopoietic stem cell function. *Blood* **2011**, *118*, 3853–3861. [CrossRef]

46. Yuasa, H.; Oike, Y.; Iwama, A.; Nishikata, I.; Sugiyama, D.; Perkins, A.; Mucenski, M.L.; Suda, T.; Morishita, K. Oncogenic transcription factor Evi1 regulates hematopoietic stem cell proliferation through GATA-2 expression. *EMBO J.* **2005**, *24*, 1976–1987. [CrossRef]
47. Goyama, S.; Yamamoto, G.; Shimabe, M.; Sato, T.; Ichikawa, M.; Ogawa, S.; Chiba, S.; Kurokawa, M. Evi-1 is a critical regulator for hematopoietic stem cells and transformed leukemic cells. *Cell Stem. Cell* **2008**, *3*, 207–220. [CrossRef]
48. Arai, S.; Yoshimi, A.; Shimabe, M.; Ichikawa, M.; Nakagawa, M.; Imai, Y.; Goyama, S.; Kurokawa, M. Evi-1 is a transcriptional target of mixed-lineage leukemia oncoproteins in hematopoietic stem cells. *Blood* **2011**, *117*, 6304–6314. [CrossRef]
49. Bogani, D.; Morgan, M.A.; Nelson, A.C.; Costello, I.; McGouran, J.F.; Kessler, B.M.; Robertson, E.J.; Bikoff, E.K. The PR/SET domain zinc finger protein Prdm4 regulates gene expression in embryonic stem cells but plays a nonessential role in the developing mouse embryo. *Mol. Cell Biol.* **2013**, *33*, 3936–3950. [CrossRef]
50. Chittka, A.; Nitarska, J.; Grazini, U.; Richardson, W.D. Transcription factor positive regulatory domain 4 (PRDM4) recruits protein arginine methyltransferase 5 (PRMT5) to mediate histone arginine methylation and control neural stem cell proliferation and differentiation. *J. Biol. Chem.* **2012**, *287*, 42995–43006. [CrossRef]
51. Galli, G.G.; Carrara, M.; Francavilla, C.; De Lichtenberg, K.H.; Olsen, J.V.; Calogero, R.A.; Lund, A.H. Genomic and proteomic analyses of Prdm5 reveal interactions with insulator binding proteins in embryonic stem cells. *Mol Cell Biol* **2013**, *33*, 4504–4516. [CrossRef] [PubMed]
52. Riddell, J.; Gazit, R.; Garrison, B.S.; Guo, G.; Saadatpour, A.; Mandal, P.K.; Ebina, W.; Volchkov, P.; Yuan, G.C.; Orkin, S.H.; et al. Reprogramming committed murine blood cells to induced hematopoietic stem cells with defined factors. *Cell* **2014**, *157*, 549–564. [CrossRef] [PubMed]
53. Thoren, L.A.; Fog, C.K.; Jensen, K.T.; Buza-Vidas, N.; Come, C.; Lund, A.H.; Porse, B.T. PRDM11 is dispensable for the maintenance and function of hematopoietic stem and progenitor cells. *Stem. Cell Res.* **2013**, *11*, 1129–1136. [CrossRef] [PubMed]
54. Okashita, N.; Sakashita, N.; Ito, K.; Mitsuya, A.; Suwa, Y.; Seki, Y. PRDM14 maintains pluripotency of embryonic stem cells through TET-mediated active DNA demethylation. *Biochem. Biophys. Res. Commun.* **2015**, *466*, 138–145. [CrossRef] [PubMed]
55. Yamaji, M.; Ueda, J.; Hayashi, K.; Ohta, H.; Yabuta, Y.; Kurimoto, K.; Nakato, R.; Yamada, Y.; Shirahige, K.; Saitou, M. PRDM14 ensures naive pluripotency through dual regulation of signaling and epigenetic pathways in mouse embryonic stem cells. *Cell Stem. Cell* **2013**, *12*, 368–382. [CrossRef]
56. Ma, Z.; Swigut, T.; Valouev, A.; Rada-Iglesias, A.; Wysocka, J. Sequence-specific regulator Prdm14 safeguards mouse ESCs from entering extraembryonic endoderm fates. *Nat. Struct. Mol. Biol.* **2011**, *18*, 120–127. [CrossRef] [PubMed]
57. Tsuneyoshi, N.; Sumi, T.; Onda, H.; Nojima, H.; Nakatsuji, N.; Suemori, H. PRDM14 suppresses expression of differentiation marker genes in human embryonic stem cells. *Biochem. Biophys. Res. Commun.* **2008**, *367*, 899–905. [CrossRef]
58. Payer, B.; Rosenberg, M.; Yamaji, M.; Yabuta, Y.; Koyanagi-Aoi, M.; Hayashi, K.; Yamanaka, S.; Saitou, M.; Lee, J.T. Tsix RNA and the germline factor, PRDM14, link X reactivation and stem cell reprogramming. *Mol. Cell* **2013**, *52*, 805–818. [CrossRef]
59. Yang, H.Y.; Kim, S.H.; Kim, S.H.; Kim, D.J.; Kim, S.U.; Yu, D.Y.; Yeom, Y.I.; Lee, D.S.; Kim, Y.J.; Park, B.J.; et al. The suppression of zfpm-1 accelerates the erythropoietic differentiation of human CD34+ cells. *Biochem. Biophys. Res. Commun.* **2007**, *353*, 978–984. [CrossRef]
60. Amigo, J.D.; Ackermann, G.E.; Cope, J.J.; Yu, M.; Cooney, J.D.; Ma, D.; Langer, N.B.; Shafizadeh, E.; Shaw, G.C.; Horsely, W.; et al. The role and regulation of friend of GATA-1 (FOG-1) during blood development in the zebrafish. *Blood* **2009**, *114*, 4654–4663. [CrossRef]
61. Gregory, G.D.; Miccio, A.; Bersenev, A.; Wang, Y.; Hong, W.; Zhang, Z.; Poncz, M.; Tong, W.; Blobel, G.A. FOG1 requires NuRD to promote hematopoiesis and maintain lineage fidelity within the megakaryocytic-erythroid compartment. *Blood* **2010**, *115*, 2156–2166. [CrossRef] [PubMed]
62. Mancini, E.; Sanjuan-Pla, A.; Luciani, L.; Moore, S.; Grover, A.; Zay, A.; Rasmussen, K.D.; Luc, S.; Bilbao, D.; O'Carroll, D.; et al. FOG-1 and GATA-1 act sequentially to specify definitive megakaryocytic and erythroid progenitors. *EMBO J.* **2012**, *31*, 351–365. [CrossRef] [PubMed]

63. Tripathy, N.K.; Rizvi, S.H.M.; Singh, S.P.; Garikpati, V.N.S.; Nityanand, S. Cardiomyogenic Heterogeneity of Clonal Subpopulations of Human Bone Marrow Mesenchymal Stem Cells. *J. Stem. Cells Regen. Med.* **2018**, *14*, 27–33. [PubMed]
64. Mzoughi, S.; Tan, Y.X.; Low, D.; Guccione, E. The role of PRDMs in cancer: One family, two sides. *Curr. Opin. Genet Dev.* **2016**, *36*, 83–91. [CrossRef] [PubMed]
65. Sorrentino, A.; Rienzo, M.; Ciccodicola, A.; Casamassimi, A.; Abbondanza, C. Human PRDM2: Structure, function and pathophysiology. *Biochim. Biophys. Acta Gene. Regul. Mech.* **2018**, *1861*, 657–671. [CrossRef]
66. Ren, B.; Chee, K.J.; Kim, T.H.; Maniatis, T. PRDI-BF1/Blimp-1 repression is mediated by corepressors of the Groucho family of proteins. *Genes Dev.* **1999**, *13*, 125–137. [CrossRef]
67. Di Zazzo, E.; De Rosa, C.; Abbondanza, C.; Moncharmont, B. PRDM Proteins: Molecular Mechanisms in Signal Transduction and Transcriptional Regulation. *Biology* **2013**, *2*, 107–141. [CrossRef]
68. Huang, S.; Shao, G.; Liu, L. The PR domain of the Rb-binding zinc finger protein RIZ1 is a protein binding interface and is related to the SET domain functioning in chromatin-mediated gene expression. *J. Biol. Chem.* **1998**, *273*, 15933–15939. [CrossRef]
69. Bartholomew, C.; Kilbey, A.; Clark, A.M.; Walker, M. The Evi-1 proto-oncogene encodes a transcriptional repressor activity associated with transformation. *Oncogene* **1997**, *14*, 569–577. [CrossRef]
70. Mochizuki, N.; Shimizu, S.; Nagasawa, T.; Tanaka, H.; Taniwaki, M.; Yokota, J.; Morishita, K. A novel gene, MEL1, mapped to 1p36.3 is highly homologous to the MDS1/EVI1 gene and is transcriptionally activated in t(1;3)(p36;q21)-positive leukemia cells. *Blood* **2000**, *96*, 3209–3214. [CrossRef]
71. Hanotel, J.; Bessodes, N.; Thelie, A.; Hedderich, M.; Parain, K.; Van Driessche, B.; Brandao Kde, O.; Kricha, S.; Jorgensen, M.C.; Grapin-Botton, A.; et al. The Prdm13 histone methyltransferase encoding gene is a Ptf1a-Rbpj downstream target that suppresses glutamatergic and promotes GABAergic neuronal fate in the dorsal neural tube. *Dev. Biol.* **2014**, *386*, 340–357. [CrossRef] [PubMed]
72. Zhou, B.; Wang, J.; Lee, S.Y.; Xiong, J.; Bhanu, N.; Guo, Q.; Ma, P.; Sun, Y.; Rao, R.C.; Garcia, B.A.; et al. PRDM16 Suppresses MLL1r Leukemia via Intrinsic Histone Methyltransferase Activity. *Mol. Cell* **2016**, *62*, 222–236. [CrossRef] [PubMed]
73. Ivanochko, D.; Halabelian, L.; Henderson, E.; Savitsky, P.; Jain, H.; Marcon, E.; Duan, S.; Hutchinson, A.; Seitova, A.; Barsyte-Lovejoy, D.; et al. Direct interaction between the PRDM3 and PRDM16 tumor suppressors and the NuRD chromatin remodeling complex. *Nucleic Acids Res.* **2019**, *47*, 1225–1238. [CrossRef]
74. Kajimura, S.; Seale, P.; Tomaru, T.; Erdjument-Bromage, H.; Cooper, M.P.; Ruas, J.L.; Chin, S.; Tempst, P.; Lazar, M.A.; Spiegelman, B.M. Regulation of the brown and white fat gene programs through a PRDM16/CtBP transcriptional complex. *Genes Dev.* **2008**, *22*, 1397–1409. [CrossRef] [PubMed]
75. Izutsu, K.; Kurokawa, M.; Imai, Y.; Maki, K.; Mitani, K.; Hirai, H. The corepressor CtBP interacts with Evi-1 to repress transforming growth factor beta signaling. *Blood* **2001**, *97*, 2815–2822. [CrossRef]
76. Garnatz, A.S.; Gao, Z.; Broman, M.; Martens, S.; Earley, J.U.; Svensson, E.C. FOG-2 mediated recruitment of the NuRD complex regulates cardiomyocyte proliferation during heart development. *Dev. Biol.* **2014**, *395*, 50–61. [CrossRef]
77. Snow, J.W.; Kim, J.; Currie, C.R.; Xu, J.; Orkin, S.H. Sumoylation regulates interaction of FOG1 with C-terminal-binding protein (CTBP). *J. Biol. Chem.* **2010**, *285*, 28064–28075. [CrossRef]
78. Wang, Y.; Meng, R.; Hayes, V.; Fuentes, R.; Yu, X.; Abrams, C.S.; Heijnen, H.F.; Blobel, G.A.; Marks, M.S.; Poncz, M. Pleiotropic platelet defects in mice with disrupted FOG1-NuRD interaction. *Blood* **2011**, *118*, 6183–6191. [CrossRef]
79. Nitta, E.; Izutsu, K.; Yamaguchi, Y.; Imai, Y.; Ogawa, S.; Chiba, S.; Kurokawa, M.; Hirai, H. Oligomerization of Evi-1 regulated by the PR domain contributes to recruitment of corepressor CtBP. *Oncogene* **2005**, *24*, 6165–6173. [CrossRef]
80. Lin, I.Y.; Chiu, F.L.; Yeang, C.H.; Chen, H.F.; Chuang, C.Y.; Yang, S.Y.; Hou, P.S.; Sintupisut, N.; Ho, H.N.; Kuo, H.C.; et al. Suppression of the SOX2 neural effector gene by PRDM1 promotes human germ cell fate in embryonic stem cells. *Stem. Cell Reports* **2014**, *2*, 189–204. [CrossRef]
81. Seki, Y. PRDM14 Is a Unique Epigenetic Regulator Stabilizing Transcriptional Networks for Pluripotency. *Front. Cell Dev. Biol.* **2018**, *6*, 12. [CrossRef] [PubMed]
82. Ficz, G.; Hore, T.A.; Santos, F.; Lee, H.J.; Dean, W.; Arand, J.; Krueger, F.; Oxley, D.; Paul, Y.L.; Walter, J.; et al. FGF signaling inhibition in ESCs drives rapid genome-wide demethylation to the epigenetic ground state of pluripotency. *Cell Stem. Cell* **2013**, *13*, 351–359. [CrossRef] [PubMed]

83. Habibi, E.; Brinkman, A.B.; Arand, J.; Kroeze, L.I.; Kerstens, H.H.; Matarese, F.; Lepikhov, K.; Gut, M.; Brun-Heath, I.; Hubner, N.C.; et al. Whole-genome bisulfite sequencing of two distinct interconvertible DNA methylomes of mouse embryonic stem cells. *Cell Stem. Cell* **2013**, *13*, 360–369. [CrossRef]
84. Burton, A.; Muller, J.; Tu, S.; Padilla-Longoria, P.; Guccione, E.; Torres-Padilla, M.E. Single-cell profiling of epigenetic modifiers identifies PRDM14 as an inducer of cell fate in the mammalian embryo. *Cell Rep.* **2013**, *5*, 687–701. [CrossRef] [PubMed]
85. Kunath, T.; Saba-El-Leil, M.K.; Almousailleakh, M.; Wray, J.; Meloche, S.; Smith, A. FGF stimulation of the Erk1/2 signalling cascade triggers transition of pluripotent embryonic stem cells from self-renewal to lineage commitment. *Development* **2007**, *134*, 2895–2902. [CrossRef]
86. Hao, J.; Li, T.G.; Qi, X.; Zhao, D.F.; Zhao, G.Q. WNT/beta-catenin pathway up-regulates Stat3 and converges on LIF to prevent differentiation of mouse embryonic stem cells. *Dev. Biol.* **2006**, *290*, 81–91. [CrossRef]
87. Hippenmeyer, S. Molecular pathways controlling the sequential steps of cortical projection neuron migration. *Adv. Exp. Med. Biol.* **2014**, *800*, 1–24.
88. Noctor, S.C.; Martinez-Cerdeno, V.; Ivic, L.; Kriegstein, A.R. Cortical neurons arise in symmetric and asymmetric division zones and migrate through specific phases. *Nat. Neurosci.* **2004**, *7*, 136–144. [CrossRef]
89. Inoue, M.; Kuroda, T.; Honda, A.; Komabayashi-Suzuki, M.; Komai, T.; Shinkai, Y.; Mizutani, K. Prdm8 regulates the morphological transition at multipolar phase during neocortical development. *PLoS ONE* **2014**, *9*, e86356. [CrossRef]
90. Ross, S.E.; McCord, A.E.; Jung, C.; Atan, D.; Mok, S.I.; Hemberg, M.; Kim, T.K.; Salogiannis, J.; Hu, L.; Cohen, S.; et al. Bhlhb5 and Prdm8 form a repressor complex involved in neuronal circuit assembly. *Neuron* **2012**, *73*, 292–303. [CrossRef]
91. Chen, Y.C.; Auer-Grumbach, M.; Matsukawa, S.; Zitzelsberger, M.; Themistocleous, A.C.; Strom, T.M.; Samara, C.; Moore, A.W.; Cho, L.T.; Young, G.T.; et al. Transcriptional regulator PRDM12 is essential for human pain perception. *Nat. Genet.* **2015**, *47*, 803–808. [CrossRef] [PubMed]
92. Desiderio, S.; Vermeiren, S.; Van Campenhout, C.; Kricha, S.; Malki, E.; Richts, S.; Fletcher, E.V.; Vanwelden, T.; Schmidt, B.Z.; Henningfeld, K.A.; et al. Prdm12 Directs Nociceptive Sensory Neuron Development by Regulating the Expression of the NGF Receptor TrkA. *Cell Rep.* **2019**, *26*, 3522–3536.e5. [CrossRef] [PubMed]
93. Galazo, M.J.; Emsley, J.G.; Macklis, J.D. Corticothalamic Projection Neuron Development beyond Subtype Specification: Fog2 and Intersectional Controls Regulate Intraclass Neuronal Diversity. *Neuron* **2016**, *91*, 90–106. [CrossRef] [PubMed]
94. Brzezinski, J.A.; Lamba, D.A.; Reh, T.A. Blimp1 controls photoreceptor versus bipolar cell fate choice during retinal development. *Development* **2010**, *137*, 619–629. [CrossRef] [PubMed]
95. Chang, D.H.; Cattoretti, G.; Calame, K.L. The dynamic expression pattern of B lymphocyte induced maturation protein-1 (Blimp-1) during mouse embryonic development. *Mech. Dev.* **2002**, *117*, 305–309. [CrossRef]
96. Katoh, K.; Omori, Y.; Onishi, A.; Sato, S.; Kondo, M.; Furukawa, T. Blimp1 suppresses Chx10 expression in differentiating retinal photoreceptor precursors to ensure proper photoreceptor development. *J. Neurosci.* **2010**, *30*, 6515–6526. [CrossRef]
97. Roy, S.; Ng, T. Blimp-1 specifies neural crest and sensory neuron progenitors in the zebrafish embryo. *Curr. Biol.* **2004**, *14*, 1772–1777. [CrossRef]
98. Barbier, E.; Johnstone, A.L.; Khomtchouk, B.B.; Tapocik, J.D.; Pitcairn, C.; Rehman, F.; Augier, E.; Borich, A.; Schank, J.R.; Rienas, C.A.; et al. Dependence-induced increase of alcohol self-administration and compulsive drinking mediated by the histone methyltransferase PRDM2. *Mol. Psychiatry* **2017**, *22*, 1746–1758. [CrossRef]
99. Garriga, G.; Guenther, C.; Horvitz, H.R. Migrations of the Caenorhabditis elegans HSNs are regulated by egl-43, a gene encoding two zinc finger proteins. *Genes Dev.* **1993**, *7*, 2097–2109. [CrossRef]
100. Hoyt, P.R.; Bartholomew, C.; Davis, A.J.; Yutzey, K.; Gamer, L.W.; Potter, S.S.; Ihle, J.N.; Mucenski, M.L. The Evi1 proto-oncogene is required at midgestation for neural, heart, and paraxial mesenchyme development. *Mech. Dev.* **1997**, *65*, 55–70. [CrossRef]
101. Kazama, H.; Kodera, T.; Shimizu, S.; Mizoguchi, H.; Morishita, K. Ecotropic viral integration site-1 is activated during, and is sufficient for, neuroectodermal P19 cell differentiation. *Cell Growth Differ.* **1999**, *10*, 565–573. [PubMed]

102. Leszczynski, P.; Smiech, M.; Salam Teeli, A.; Haque, E.; Viger, R.; Ogawa, H.; Pierzchala, M.; Taniguchi, H. Deletion of the Prdm3 Gene Causes a Neuronal Differentiation Deficiency in P19 Cells. *Int. J. Mol. Sci.* **2020**, *21*, 7192. [CrossRef] [PubMed]
103. Endo, K.; Karim, M.R.; Taniguchi, H.; Krejci, A.; Kinameri, E.; Siebert, M.; Ito, K.; Bray, S.J.; Moore, A.W. Chromatin modification of Notch targets in olfactory receptor neuron diversification. *Nat. Neurosci.* **2011**, *15*, 224–233. [CrossRef] [PubMed]
104. Hou, Q.; Ruan, H.; Gilbert, J.; Wang, G.; Ma, Q.; Yao, W.D.; Man, H.Y. MicroRNA miR124 is required for the expression of homeostatic synaptic plasticity. *Nat. Commun.* **2015**, *6*, 10045. [CrossRef]
105. Zhang, Y.; Liu, X.; Xue, H.; Liu, X.; Dai, A.; Song, Y.; Ke, K.; Cao, M. Upregulation of PRDM5 Is Associated with Astrocyte Proliferation and Neuronal Apoptosis Caused by Lipopolysaccharide. *J. Mol. Neurosci.* **2016**, *59*, 146–157. [CrossRef]
106. Ling, W.; Xu, X.; Liu, J. A causal relationship between the neurotherapeutic effects of miR182/7a and decreased expression of PRDM5. *Biochem. Biophys. Res. Commun.* **2017**, *490*, 1–7. [CrossRef]
107. Meani, N.; Pezzimenti, F.; Deflorian, G.; Mione, M.; Alcalay, M. The tumor suppressor PRDM5 regulates Wnt signaling at early stages of zebrafish development. *PLoS ONE* **2009**, *4*, e4273. [CrossRef]
108. Jung, C.C.; Atan, D.; Ng, D.; Ploder, L.; Ross, S.E.; Klein, M.; Birch, D.G.; Diez, E.; McInnes, R.R. Transcription factor PRDM8 is required for rod bipolar and type 2 OFF-cone bipolar cell survival and amacrine subtype identity. *Proc. Natl. Acad. Sci. USA* **2015**, *112*, E3010–E3019. [CrossRef]
109. Nagy, V.; Cole, T.; Van Campenhout, C.; Khoung, T.M.; Leung, C.; Vermeiren, S.; Novatchkova, M.; Wenzel, D.; Cikes, D.; Polyansky, A.A.; et al. The evolutionarily conserved transcription factor PRDM12 controls sensory neuron development and pain perception. *Cell Cycle* **2015**, *14*, 1799–1808. [CrossRef]
110. Mona, B.; Uruena, A.; Kollipara, R.K.; Ma, Z.; Borromeo, M.D.; Chang, J.C.; Johnson, J.E. Repression by PRDM13 is critical for generating precision in neuronal identity. *Elife* **2017**, *6*. [CrossRef]
111. Chang, J.C.; Meredith, D.M.; Mayer, P.R.; Borromeo, M.D.; Lai, H.C.; Ou, Y.H.; Johnson, J.E. Prdm13 mediates the balance of inhibitory and excitatory neurons in somatosensory circuits. *Dev. Cell* **2013**, *25*, 182–195. [CrossRef] [PubMed]
112. Liu, C.; Ma, W.; Su, W.; Zhang, J. Prdm14 acts upstream of islet2 transcription to regulate axon growth of primary motoneurons in zebrafish. *Development* **2012**, *139*, 4591–4600. [CrossRef] [PubMed]
113. Mzoughi, S.; Di Tullio, F.; Low, D.H.P.; Motofeanu, C.M.; Ong, S.L.M.; Wollmann, H.; Wun, C.M.; Kruszka, P.; Muenke, M.; Hildebrandt, F.; et al. PRDM15 loss of function links NOTCH and WNT/PCP signaling to patterning defects in holoprosencephaly. *Sci. Adv.* **2020**, *6*, eaax9852. [CrossRef] [PubMed]
114. Su, L.; Lei, X.; Ma, H.; Feng, C.; Jiang, J.; Jiao, J. PRDM16 orchestrates angiogenesis via neural differentiation in the developing brain. *Cell Death Differ.* **2020**, *27*, 2313–2329. [CrossRef] [PubMed]
115. Jia, Y.; Takimoto, K. GATA and FOG2 transcription factors differentially regulate the promoter for Kv4.2 K(+) channel gene in cardiac myocytes and PC12 cells. *Cardiovasc. Res.* **2003**, *60*, 278–287. [CrossRef]
116. Tsai, F.Y.; Keller, G.; Kuo, F.C.; Weiss, M.; Chen, J.; Rosenblatt, M.; Alt, F.W.; Orkin, S.H. An early haematopoietic defect in mice lacking the transcription factor GATA-2. *Nature* **1994**, *371*, 221–226. [CrossRef]
117. Shull, L.C.; Sen, R.; Menzel, J.; Goyama, S.; Kurokawa, M.; Artinger, K.B. The conserved and divergent roles of Prdm3 and Prdm16 in zebrafish and mouse craniofacial development. *Dev. Biol.* **2020**, *461*, 132–144. [CrossRef]
118. Seale, P.; Bjork, B.; Yang, W.; Kajimura, S.; Chin, S.; Kuang, S.; Scime, A.; Devarakonda, S.; Conroe, H.M.; Erdjument-Bromage, H.; et al. PRDM16 controls a brown fat/skeletal muscle switch. *Nature* **2008**, *454*, 961–967. [CrossRef]
119. Seale, P.; Kajimura, S.; Yang, W.; Chin, S.; Rohas, L.M.; Uldry, M.; Tavernier, G.; Langin, D.; Spiegelman, B.M. Transcriptional control of brown fat determination by PRDM16. *Cell Metab.* **2007**, *6*, 38–54. [CrossRef]
120. Arndt, A.K.; Schafer, S.; Drenckhahn, J.D.; Sabeh, M.K.; Plovie, E.R.; Caliebe, A.; Klopocki, E.; Musso, G.; Werdich, A.A.; Kalwa, H.; et al. Fine mapping of the 1p36 deletion syndrome identifies mutation of PRDM16 as a cause of cardiomyopathy. *Am. J. Hum. Genet.* **2013**, *93*, 67–77. [CrossRef]
121. Shaffer, J.R.; Orlova, E.; Lee, M.K.; Leslie, E.J.; Raffensperger, Z.D.; Heike, C.L.; Cunningham, M.L.; Hecht, J.T.; Kau, C.H.; Nidey, N.L.; et al. Genome-Wide Association Study Reveals Multiple Loci Influencing Normal Human Facial Morphology. *PLoS Genet* **2016**, *12*, e1006149. [CrossRef]
122. Ding, H.L.; Clouthier, D.E.; Artinger, K.B. Redundant roles of PRDM family members in zebrafish craniofacial development. *Dev. Dyn.* **2013**, *242*, 67–79. [CrossRef] [PubMed]

123. Bjork, B.C.; Turbe-Doan, A.; Prysak, M.; Herron, B.J.; Beier, D.R. Prdm16 is required for normal palatogenesis in mice. *Hum. Mol. Genet.* **2010**, *19*, 774–789. [CrossRef] [PubMed]
124. Li, X.; Wang, J.; Jiang, Z.; Guo, F.; Soloway, P.D.; Zhao, R. Role of PRDM16 and its PR domain in the epigenetic regulation of myogenic and adipogenic genes during transdifferentiation of C2C12 cells. *Gene* **2015**, *570*, 191–198. [CrossRef] [PubMed]
125. Clifton, M.K.; Westman, B.J.; Thong, S.Y.; O'Connell, M.R.; Webster, M.W.; Shepherd, N.E.; Quinlan, K.G.; Crossley, M.; Blobel, G.A.; Mackay, J.P. The identification and structure of an N-terminal PR domain show that FOG1 is a member of the PRDM family of proteins. *PLoS ONE* **2014**, *9*, e106011. [CrossRef] [PubMed]
126. Jack, B.H.; Crossley, M. GATA proteins work together with friend of GATA (FOG) and C-terminal binding protein (CTBP) co-regulators to control adipogenesis. *J. Biol. Chem.* **2010**, *285*, 32405–32414. [CrossRef]
127. Rodriguez, P.; Bonte, E.; Krijgsveld, J.; Kolodziej, K.E.; Guyot, B.; Heck, A.J.; Vyas, P.; De Boer, E.; Grosveld, F.; Strouboulis, J. GATA-1 forms distinct activating and repressive complexes in erythroid cells. *EMBO J.* **2005**, *24*, 2354–2366. [CrossRef]
128. Hong, W.; Nakazawa, M.; Chen, Y.Y.; Kori, R.; Vakoc, C.R.; Rakowski, C.; Blobel, G.A. FOG-1 recruits the NuRD repressor complex to mediate transcriptional repression by GATA-1. *EMBO J.* **2005**, *24*, 2367–2378. [CrossRef]
129. Tsang, A.P.; Visvader, J.E.; Turner, C.A.; Fujiwara, Y.; Yu, C.; Weiss, M.J.; Crossley, M.; Orkin, S.H. FOG, a multitype zinc finger protein, acts as a cofactor for transcription factor GATA-1 in erythroid and megakaryocytic differentiation. *Cell* **1997**, *90*, 109–119. [CrossRef]
130. Zhou, B.; Ma, Q.; Kong, S.W.; Hu, Y.; Campbell, P.H.; McGowan, F.X.; Ackerman, K.G.; Wu, B.; Zhou, B.; Tevosian, S.G.; et al. Fog2 is critical for cardiac function and maintenance of coronary vasculature in the adult mouse heart. *J. Clin. Investig.* **2009**, *119*, 1462–1476. [CrossRef]
131. Tan, Z.P.; Huang, C.; Xu, Z.B.; Yang, J.F.; Yang, Y.F. Novel ZFPM2/FOG2 variants in patients with double outlet right ventricle. *Clin. Genet.* **2012**, *82*, 466–471. [CrossRef] [PubMed]
132. Pizzuti, A.; Sarkozy, A.; Newton, A.L.; Conti, E.; Flex, E.; Digilio, M.C.; Amati, F.; Gianni, D.; Tandoi, C.; Marino, B.; et al. Mutations of ZFPM2/FOG2 gene in sporadic cases of tetralogy of Fallot. *Hum. Mutat.* **2003**, *22*, 372–377. [CrossRef] [PubMed]
133. Cuenco, G.M.; Nucifora, G.; Ren, R. Human AML1/MDS1/EVI1 fusion protein induces an acute myelogenous leukemia (AML) in mice: A model for human AML. *Proc. Natl. Acad. Sci. USA* **2000**, *97*, 1760–1765. [CrossRef] [PubMed]
134. Chan, E.M.; Comer, E.M.; Brown, F.C.; Richkind, K.E.; Holmes, M.L.; Chong, B.H.; Shiffman, R.; Zhang, D.E.; Slovak, M.L.; Willman, C.L.; et al. AML1-FOG2 fusion protein in myelodysplasia. *Blood* **2005**, *105*, 4523–4526. [CrossRef] [PubMed]
135. Tsang, A.P.; Fujiwara, Y.; Hom, D.B.; Orkin, S.H. Failure of megakaryopoiesis and arrested erythropoiesis in mice lacking the GATA-1 transcriptional cofactor FOG. *Genes Dev.* **1998**, *12*, 1176–1188. [CrossRef] [PubMed]
136. Querfurth, E.; Schuster, M.; Kulessa, H.; Crispino, J.D.; Doderlein, G.; Orkin, S.H.; Graf, T.; Nerlov, C. Antagonism between C/EBPbeta and FOG in eosinophil lineage commitment of multipotent hematopoietic progenitors. *Genes Dev.* **2000**, *14*, 2515–2525. [CrossRef]
137. Du Roure, C.; Versavel, A.; Doll, T.; Cao, C.; Pillonel, V.; Matthias, G.; Kaller, M.; Spetz, J.F.; Kopp, P.; Kohler, H.; et al. Hematopoietic overexpression of FOG1 does not affect B-cells but reduces the number of circulating eosinophils. *PLoS ONE* **2014**, *9*, e92836. [CrossRef]
138. Elkabetz, Y.; Panagiotakos, G.; Al Shamy, G.; Socci, N.D.; Tabar, V.; Studer, L. Human ES cell-derived neural rosettes reveal a functionally distinct early neural stem cell stage. *Genes Dev.* **2008**, *22*, 152–165. [CrossRef]
139. Hirabayashi, Y.; Gotoh, Y. Epigenetic control of neural precursor cell fate during development. *Nat. Rev. Neurosci.* **2010**, *11*, 377–388. [CrossRef]
140. Yamada, T.; Yang, Y.; Hemberg, M.; Yoshida, T.; Cho, H.Y.; Murphy, J.P.; Fioravante, D.; Regehr, W.G.; Gygi, S.P.; Georgopoulos, K.; et al. Promoter decommissioning by the NuRD chromatin remodeling complex triggers synaptic connectivity in the mammalian brain. *Neuron* **2014**, *83*, 122–134. [CrossRef]
141. Dickstein, J.; Senyuk, V.; Premanand, K.; Laricchia-Robbio, L.; Xu, P.; Cattaneo, F.; Fazzina, R.; Nucifora, G. Methylation and silencing of miRNA-124 by EVI1 and self-renewal exhaustion of hematopoietic stem cells in murine myelodysplastic syndrome. *Proc. Natl. Acad. Sci. USA* **2010**, *107*, 9783–9788. [CrossRef] [PubMed]
142. Walton, R.Z.; Bruce, A.E.; Olivey, H.E.; Najib, K.; Johnson, V.; Earley, J.U.; Ho, R.K.; Svensson, E.C. Fog1 is required for cardiac looping in zebrafish. *Dev. Biol.* **2006**, *289*, 482–493. [CrossRef] [PubMed]

143. Yang, Y.; Li, B.; Zhang, X.; Zhao, Q.; Lou, X. The zinc finger protein Zfpm1 modulates ventricular trabeculation through Neuregulin-ErbB signalling. *Dev. Biol.* **2019**, *446*, 142–150. [CrossRef] [PubMed]
144. Meier, S.; Strohmaier, J.; Breuer, R.; Mattheisen, M.; Degenhardt, F.; Muhleisen, T.W.; Schulze, T.G.; Nothen, M.M.; Cichon, S.; Rietschel, M.; et al. Neuregulin 3 is associated with attention deficits in schizophrenia and bipolar disorder. *Int. J. Neuropsychopharmacol.* **2013**, *16*, 549–556. [CrossRef] [PubMed]
145. Benzel, I.; Bansal, A.; Browning, B.L.; Galwey, N.W.; Maycox, P.R.; McGinnis, R.; Smart, D.; St Clair, D.; Yates, P.; Purvis, I. Interactions among genes in the ErbB-Neuregulin signalling network are associated with increased susceptibility to schizophrenia. *Behav. Brain Funct.* **2007**, *3*, 1–11. [CrossRef] [PubMed]
146. Mei, L.; Nave, K.A. Neuregulin-ERBB signaling in the nervous system and neuropsychiatric diseases. *Neuron* **2014**, *83*, 27–49. [CrossRef] [PubMed]
147. Lu, J.R.; McKinsey, T.A.; Xu, H.; Wang, D.Z.; Richardson, J.A.; Olson, E.N. FOG-2, a heart- and brain-enriched cofactor for GATA transcription factors. *Mol. Cell Biol.* **1999**, *19*, 4495–4502. [CrossRef]
148. Agnihotri, S.; Wolf, A.; Picard, D.; Hawkins, C.; Guha, A. GATA4 is a regulator of astrocyte cell proliferation and apoptosis in the human and murine central nervous system. *Oncogene* **2009**, *28*, 3033–3046. [CrossRef]
149. Kamnasaran, D.; Guha, A. Expression of GATA6 in the human and mouse central nervous system. *Brain Res. Dev. Brain Res.* **2005**, *160*, 90–95. [CrossRef]
150. Bortone, D.S.; Olsen, S.R.; Scanziani, M. Translaminar inhibitory cells recruited by layer 6 corticothalamic neurons suppress visual cortex. *Neuron* **2014**, *82*, 474–485. [CrossRef]
151. Olsen, S.R.; Bortone, D.S.; Adesnik, H.; Scanziani, M. Gain control by layer six in cortical circuits of vision. *Nature* **2012**, *483*, 47–52. [CrossRef] [PubMed]
152. Simon, R.; Brylka, H.; Schwegler, H.; Venkataramanappa, S.; Andratschke, J.; Wiegreffe, C.; Liu, P.; Fuchs, E.; Jenkins, N.A.; Copeland, N.G.; et al. A dual function of Bcl11b/Ctip2 in hippocampal neurogenesis. *EMBO J.* **2012**, *31*, 2922–2936. [CrossRef] [PubMed]
153. Thierry, G.; Pichon, O.; Briand, A.; Poulain, D.; Sznajer, Y.; David, A.; Le Caignec, C. Autosomal insertional translocation mimicking an X-linked mode of inheritance. *Eur. J. Med. Genet.* **2013**, *56*, 46–49. [CrossRef] [PubMed]
154. Wat, M.J.; Veenma, D.; Hogue, J.; Holder, A.M.; Yu, Z.; Wat, J.J.; Hanchard, N.; Shchelochkov, O.A.; Fernandes, C.J.; Johnson, A.; et al. Genomic alterations that contribute to the development of isolated and non-isolated congenital diaphragmatic hernia. *J. Med. Genet.* **2011**, *48*, 299–307. [CrossRef]
155. Ee, L.S.; McCannell, K.N.; Tang, Y.; Fernandes, N.; Hardy, W.R.; Green, M.R.; Chu, F.; Fazzio, T.G. An Embryonic Stem Cell-Specific NuRD Complex Functions through Interaction with WDR5. *Stem. Cell Rep.* **2017**, *8*, 1488–1496. [CrossRef]
156. Xue, Y.; Wong, J.; Moreno, G.T.; Young, M.K.; Cote, J.; Wang, W. NURD, a novel complex with both ATP-dependent chromatin-remodeling and histone deacetylase activities. *Mol. Cell* **1998**, *2*, 851–861. [CrossRef]
157. Allen, H.F.; Wade, P.A.; Kutateladze, T.G. The NuRD architecture. *Cell Mol. Life Sci.* **2013**, *70*, 3513–3524. [CrossRef]
158. Zhang, Y.; LeRoy, G.; Seelig, H.P.; Lane, W.S.; Reinberg, D. The dermatomyositis-specific autoantigen Mi2 is a component of a complex containing histone deacetylase and nucleosome remodeling activities. *Cell* **1998**, *95*, 279–289. [CrossRef]
159. Zhang, Y.; Ng, H.H.; Erdjument-Bromage, H.; Tempst, P.; Bird, A.; Reinberg, D. Analysis of the NuRD subunits reveals a histone deacetylase core complex and a connection with DNA methylation. *Genes Dev.* **1999**, *13*, 1924–1935. [CrossRef]
160. Bornelov, S.; Reynolds, N.; Xenophontos, M.; Gharbi, S.; Johnstone, E.; Floyd, R.; Ralser, M.; Signolet, J.; Loos, R.; Dietmann, S.; et al. The Nucleosome Remodeling and Deacetylation Complex Modulates Chromatin Structure at Sites of Active Transcription to Fine-Tune Gene Expression. *Mol. Cell* **2018**, *71*, 56–72.e4. [CrossRef]
161. Reynolds, N.; Latos, P.; Hynes-Allen, A.; Loos, R.; Leaford, D.; O'Shaughnessy, A.; Mosaku, O.; Signolet, J.; Brennecke, P.; Kalkan, T.; et al. NuRD suppresses pluripotency gene expression to promote transcriptional heterogeneity and lineage commitment. *Cell Stem. Cell* **2012**, *10*, 583–594. [CrossRef] [PubMed]
162. Jung, B.P.; Zhang, G.; Nitsch, R.; Trogadis, J.; Nag, S.; Eubanks, J.H. Differential expression of methyl CpG-binding domain containing factor MBD3 in the developing and adult rat brain. *J. Neurobiol.* **2003**, *55*, 220–232. [CrossRef] [PubMed]

163. Knock, E.; Pereira, J.; Lombard, P.D.; Dimond, A.; Leaford, D.; Livesey, F.J.; Hendrich, B. The methyl binding domain 3/nucleosome remodelling and deacetylase complex regulates neural cell fate determination and terminal differentiation in the cerebral cortex. *Neural Dev.* **2015**, *10*, 13. [CrossRef] [PubMed]
164. Muralidharan, B.; Khatri, Z.; Maheshwari, U.; Gupta, R.; Roy, B.; Pradhan, S.J.; Karmodiya, K.; Padmanabhan, H.; Shetty, A.S.; Balaji, C.; et al. LHX2 Interacts with the NuRD Complex and Regulates Cortical Neuron Subtype Determinants Fezf2 and Sox11. *J. Neurosci.* **2017**, *37*, 194–203. [CrossRef] [PubMed]
165. Harb, K.; Magrinelli, E.; Nicolas, C.S.; Lukianets, N.; Frangeul, L.; Pietri, M.; Sun, T.; Sandoz, G.; Grammont, F.; Jabaudon, D.; et al. Area-specific development of distinct projection neuron subclasses is regulated by postnatal epigenetic modifications. *Elife* **2016**, *5*, e09531. [CrossRef] [PubMed]
166. Schmitges, F.W.; Prusty, A.B.; Faty, M.; Stutzer, A.; Lingaraju, G.M.; Aiwazian, J.; Sack, R.; Hess, D.; Li, L.; Zhou, S.; et al. Histone methylation by PRC2 is inhibited by active chromatin marks. *Mol. Cell* **2011**, *42*, 330–341. [CrossRef] [PubMed]
167. Roche, A.E.; Bassett, B.J.; Samant, S.A.; Hong, W.; Blobel, G.A.; Svensson, E.C. The zinc finger and C-terminal domains of MTA proteins are required for FOG-2-mediated transcriptional repression via the NuRD complex. *J. Mol. Cell Cardiol.* **2008**, *44*, 352–360. [CrossRef]
168. Shimahara, A.; Yamakawa, N.; Nishikata, I.; Morishita, K. Acetylation of lysine 564 adjacent to the C-terminal binding protein-binding motif in EVI1 is crucial for transcriptional activation of GATA2. *J. Biol. Chem.* **2010**, *285*, 16967–16977. [CrossRef]
169. Senyuk, V.; Sinha, K.K.; Chakraborty, S.; Buonamici, S.; Nucifora, G. P/CAF and GCN5 acetylate the AML1/MDS1/EVI1 fusion oncoprotein. *Biochem. Biophys. Res. Commun.* **2003**, *307*, 980–986. [CrossRef]
170. Chakraborty, S.; Senyuk, V.; Sitailo, S.; Chi, Y.; Nucifora, G. Interaction of EVI1 with cAMP-responsive element-binding protein-binding protein (CBP) and p300/CBP-associated factor (P/CAF) results in reversible acetylation of EVI1 and in co-localization in nuclear speckles. *J. Biol. Chem.* **2001**, *276*, 44936–44943. [CrossRef]
171. Miccio, A.; Wang, Y.; Hong, W.; Gregory, G.D.; Wang, H.; Yu, X.; Choi, J.K.; Shelat, S.; Tong, W.; Poncz, M.; et al. NuRD mediates activating and repressive functions of GATA-1 and FOG-1 during blood development. *EMBO J.* **2010**, *29*, 442–456. [CrossRef] [PubMed]
172. Svensson, E.C.; Tufts, R.L.; Polk, C.E.; Leiden, J.M. Molecular cloning of FOG-2: A modulator of transcription factor GATA-4 in cardiomyocytes. *Proc. Natl. Acad. Sci. USA* **1999**, *96*, 956–961. [CrossRef] [PubMed]
173. Fears, S.; Mathieu, C.; Zeleznik-Le, N.; Huang, S.; Rowley, J.D.; Nucifora, G. Intergenic splicing of MDS1 and EVI1 occurs in normal tissues as well as in myeloid leukemia and produces a new member of the PR domain family. *Proc. Natl. Acad. Sci. USA* **1996**, *93*, 1642–1647. [CrossRef] [PubMed]
174. Groschel, S.; Lugthart, S.; Schlenk, R.F.; Valk, P.J.; Eiwen, K.; Goudswaard, C.; Van Putten, W.J.; Kayser, S.; Verdonck, L.F.; Lubbert, M.; et al. High EVI1 expression predicts outcome in younger adult patients with acute myeloid leukemia and is associated with distinct cytogenetic abnormalities. *J. Clin. Oncol.* **2010**, *28*, 2101–2107. [CrossRef] [PubMed]
175. Lugthart, S.; Van Drunen, E.; Van Norden, Y.; Van Hoven, A.; Erpelinck, C.A.; Valk, P.J.; Beverloo, H.B.; Lowenberg, B.; Delwel, R. High EVI1 levels predict adverse outcome in acute myeloid leukemia: Prevalence of EVI1 overexpression and chromosome 3q26 abnormalities underestimated. *Blood* **2008**, *111*, 4329–4337. [CrossRef] [PubMed]
176. Suzukawa, K.; Parganas, E.; Gajjar, A.; Abe, T.; Takahashi, S.; Tani, K.; Asano, S.; Asou, H.; Kamada, N.; Yokota, J. Identification of a breakpoint cluster region 3′ of the ribophorin I gene at 3q21 associated with the transcriptional activation of the EVI1 gene in acute myelogenous leukemias with inv(3)(q21q26). *Blood* **1994**, *84*, 2681–2688. [CrossRef] [PubMed]
177. Brooks, D.J.; Woodward, S.; Thompson, F.H.; Dos Santos, B.; Russell, M.; Yang, J.M.; Guan, X.Y.; Trent, J.; Alberts, D.S.; Taetle, R. Expression of the zinc finger gene EVI-1 in ovarian and other cancers. *Br. J. Cancer* **1996**, *74*, 1518–1525. [CrossRef]
178. Sattler, H.P.; Lensch, R.; Rohde, V.; Zimmer, E.; Meese, E.; Bonkhoff, H.; Retz, M.; Zwergel, T.; Bex, A.; Stoeckle, M.; et al. Novel amplification unit at chromosome 3q25-q27 in human prostate cancer. *Prostate* **2000**, *45*, 207–215. [CrossRef]
179. Yasui, K.; Konishi, C.; Gen, Y.; Endo, M.; Dohi, O.; Tomie, A.; Kitaichi, T.; Yamada, N.; Iwai, N.; Nishikawa, T.; et al. EVI1, a target gene for amplification at 3q26, antagonizes transforming growth factor-beta-mediated growth inhibition in hepatocellular carcinoma. *Cancer Sci.* **2015**, *106*, 929–937. [CrossRef]

180. Sorrentino, A.; Federico, A.; Rienzo, M.; Gazzerro, P.; Bifulco, M.; Ciccodicola, A.; Casamassimi, A.; Abbondanza, C. PR/SET Domain Family and Cancer: Novel Insights from the Cancer Genome Atlas. *Int. J. Mol. Sci.* **2018**, *19*, 3250. [CrossRef]
181. Shing, D.C.; Trubia, M.; Marchesi, F.; Radaelli, E.; Belloni, E.; Tapinassi, C.; Scanziani, E.; Mecucci, C.; Crescenzi, B.; Lahortiga, I.; et al. Overexpression of sPRDM16 coupled with loss of p53 induces myeloid leukemias in mice. *J. Clin. Investig.* **2007**, *117*, 3696–3707. [CrossRef] [PubMed]
182. Ramirez, J.; Hagman, J. The Mi-2/NuRD complex: A critical epigenetic regulator of hematopoietic development, differentiation and cancer. *Epigenetics* **2009**, *4*, 532–536. [CrossRef] [PubMed]
183. Hoffmann, A.; Spengler, D. Chromatin Remodeling Complex NuRD in Neurodevelopment and Neurodevelopmental Disorders. *Front. Genet.* **2019**, *10*, 682. [CrossRef]
184. Chinnadurai, G. CtBP family proteins: More than transcriptional corepressors. *Bioessays* **2003**, *25*, 9–12. [CrossRef] [PubMed]
185. Ivanova, D.; Dirks, A.; Montenegro-Venegas, C.; Schone, C.; Altrock, W.D.; Marini, C.; Frischknecht, R.; Schanze, D.; Zenker, M.; Gundelfinger, E.D.; et al. Synaptic activity controls localization and function of CtBP1 via binding to Bassoon and Piccolo. *EMBO J.* **2015**, *34*, 1056–1077. [CrossRef]
186. Nishikata, I.; Nakahata, S.; Saito, Y.; Kaneda, K.; Ichihara, E.; Yamakawa, N.; Morishita, K. Sumoylation of MEL1S at lysine 568 and its interaction with CtBP facilitates its repressor activity and the blockade of G-CSF-induced myeloid differentiation. *Oncogene* **2011**, *30*, 4194–4207. [CrossRef]
187. Lee, L.; Dale, E.; Staniszewski, A.; Zhang, H.; Saeed, F.; Sakurai, M.; Fa', M.; Orozco, I.; Michelassi, F.; Akpan, N.; et al. Regulation of synaptic plasticity and cognition by SUMO in normal physiology and Alzheimer's disease. *Sci. Rep.* **2014**, *4*, 7190. [CrossRef]
188. Henley, J.M.; Craig, T.J.; Wilkinson, K.A. Neuronal SUMOylation: Mechanisms, physiology, and roles in neuronal dysfunction. *Physiol. Rev.* **2014**, *94*, 1249–1285. [CrossRef]
189. Hasegawa, Y.; Yoshida, D.; Nakamura, Y.; Sakakibara, S. Spatiotemporal distribution of SUMOylation components during mouse brain development. *J. Comp. Neurol.* **2014**, *522*, 3020–3036. [CrossRef]
190. Maruyama, T.; Wada, H.; Abe, Y.; Niikura, T. Alteration of global protein SUMOylation in neurons and astrocytes in response to Alzheimer's disease-associated insults. *Biochem. Biophys. Res. Commun.* **2018**, *500*, 470–475. [CrossRef]
191. Henley, J.M.; Carmichael, R.E.; Wilkinson, K.A. Extranuclear SUMOylation in Neurons. *Trends Neurosci.* **2018**, *41*, 198–210. [CrossRef] [PubMed]
192. Thiruvalluvan, M.; Barghouth, P.G.; Tsur, A.; Broday, L.; Oviedo, N.J. SUMOylation controls stem cell proliferation and regional cell death through Hedgehog signaling in planarians. *Cell Mol. Life Sci.* **2018**, *75*, 1285–1301. [CrossRef] [PubMed]
193. Singh, S.; Pradhan, A.K.; Chakraborty, S. SUMO1 negatively regulates the transcriptional activity of EVI1 and significantly increases its co-localization with EVI1 after treatment with arsenic trioxide. *Biochim. Biophys. Acta* **2013**, *1833*, 2357–2368. [CrossRef] [PubMed]
194. Chen, Q.; Huang, L.; Pan, D.; Zhu, L.J.; Wang, Y.X. Cbx4 Sumoylates Prdm16 to Regulate Adipose Tissue Thermogenesis. *Cell Rep.* **2018**, *22*, 2860–2872. [CrossRef] [PubMed]
195. Dong, S.; Chen, J. SUMOylation of sPRDM16 promotes the progression of acute myeloid leukemia. *BMC Cancer* **2015**, *15*, 1–13. [CrossRef] [PubMed]
196. Yang, X.J.; Gregoire, S. A recurrent phospho-sumoyl switch in transcriptional repression and beyond. *Mol. Cell* **2006**, *23*, 779–786. [CrossRef]
197. Chi, Y.; Senyuk, V.; Chakraborty, S.; Nucifora, G. EVI1 promotes cell proliferation by interacting with BRG1 and blocking the repression of BRG1 on E2F1 activity. *J. Biol. Chem.* **2003**, *278*, 49806–49811. [CrossRef]
198. Trotter, K.W.; Archer, T.K. The BRG1 transcriptional coregulator. *Nucl. Recept. Signal.* **2008**, *6*, e004. [CrossRef]
199. Kadam, S.; Emerson, B.M. Transcriptional specificity of human SWI/SNF BRG1 and BRM chromatin remodeling complexes. *Mol. Cell* **2003**, *11*, 377–389. [CrossRef]
200. Hoffmeister, H.; Fuchs, A.; Erdel, F.; Pinz, S.; Grobner-Ferreira, R.; Bruckmann, A.; Deutzmann, R.; Schwartz, U.; Maldonado, R.; Huber, C.; et al. CHD3 and CHD4 form distinct NuRD complexes with different yet overlapping functionality. *Nucleic Acids Res.* **2017**, *45*, 10534–10554. [CrossRef]
201. Kajimura, S.; Seale, P.; Kubota, K.; Lunsford, E.; Frangioni, J.V.; Gygi, S.P.; Spiegelman, B.M. Initiation of myoblast to brown fat switch by a PRDM16-C/EBP-beta transcriptional complex. *Nature* **2009**, *460*, 1154–1158. [CrossRef] [PubMed]

202. Menard, C.; Hein, P.; Paquin, A.; Savelson, A.; Yang, X.M.; Lederfein, D.; Barnabe-Heider, F.; Mir, A.A.; Sterneck, E.; Peterson, A.C.; et al. An essential role for a MEK-C/EBP pathway during growth factor-regulated cortical neurogenesis. *Neuron* **2002**, *36*, 597–610. [CrossRef]
203. Cortes-Canteli, M.; Aguilar-Morante, D.; Sanz-Sancristobal, M.; Megias, D.; Santos, A.; Perez-Castillo, A. Role of C/EBPbeta transcription factor in adult hippocampal neurogenesis. *PLoS ONE* **2011**, *6*, e24842. [CrossRef] [PubMed]
204. Bard-Chapeau, E.A.; Gunaratne, J.; Kumar, P.; Chua, B.Q.; Muller, J.; Bard, F.A.; Blackstock, W.; Copeland, N.G.; Jenkins, N.A. EVI1 oncoprotein interacts with a large and complex network of proteins and integrates signals through protein phosphorylation. *Proc. Natl. Acad. Sci. USA* **2013**, *110*, E2885–E2894. [CrossRef] [PubMed]
205. Tokita, K.; Maki, K.; Mitani, K. RUNX1/EVI1, which blocks myeloid differentiation, inhibits CCAAT-enhancer binding protein alpha function. *Cancer Sci.* **2007**, *98*, 1752–1757. [CrossRef] [PubMed]
206. Senyuk, V.; Chakraborty, S.; Mikhail, F.M.; Zhao, R.; Chi, Y.; Nucifora, G. The leukemia-associated transcription repressor AML1/MDS1/EVI1 requires CtBP to induce abnormal growth and differentiation of murine hematopoietic cells. *Oncogene* **2002**, *21*, 3232–3240. [CrossRef] [PubMed]
207. Turner, J.; Crossley, M. Cloning and characterization of mCtBP2, a co-repressor that associates with basic Kruppel-like factor and other mammalian transcriptional regulators. *EMBO J.* **1998**, *17*, 5129–5140. [CrossRef] [PubMed]
208. Senyuk, V.; Sinha, K.K.; Li, D.; Rinaldi, C.R.; Yanamandra, S.; Nucifora, G. Repression of RUNX1 activity by EVI1: A new role of EVI1 in leukemogenesis. *Cancer Res.* **2007**, *67*, 5658–5666. [CrossRef]
209. Laricchia-Robbio, L.; Fazzina, R.; Li, D.; Rinaldi, C.R.; Sinha, K.K.; Chakraborty, S.; Nucifora, G. Point mutations in two EVI1 Zn fingers abolish EVI1-GATA1 interaction and allow erythroid differentiation of murine bone marrow cells. *Mol. Cell Biol.* **2006**, *26*, 7658–7666. [CrossRef]
210. Laricchia-Robbio, L.; Premanand, K.; Rinaldi, C.R.; Nucifora, G. EVI1 Impairs myelopoiesis by deregulation of PU.1 function. *Cancer Res.* **2009**, *69*, 1633–1642. [CrossRef]
211. Kurokawa, M.; Mitani, K.; Imai, Y.; Ogawa, S.; Yazaki, Y.; Hirai, H. The t(3;21) fusion product, AML1/Evi-1, interacts with Smad3 and blocks transforming growth factor-beta-mediated growth inhibition of myeloid cells. *Blood* **1998**, *92*, 4003–4012. [CrossRef] [PubMed]
212. Kurokawa, M.; Mitani, K.; Yamagata, T.; Takahashi, T.; Izutsu, K.; Ogawa, S.; Moriguchi, T.; Nishida, E.; Yazaki, Y.; Hirai, H. The evi-1 oncoprotein inhibits c-Jun N-terminal kinase and prevents stress-induced cell death. *EMBO J.* **2000**, *19*, 2958–2968. [CrossRef] [PubMed]
213. Lu, Y.; Liang, Y.; Zheng, X.; Deng, X.; Huang, W.; Zhang, G. EVI1 promotes epithelial-to-mesenchymal transition, cancer stem cell features and chemo-/radioresistance in nasopharyngeal carcinoma. *J. Exp. Clin. Cancer Res.* **2019**, *38*, 1–17. [CrossRef] [PubMed]
214. Senyuk, V.; Premanand, K.; Xu, P.; Qian, Z.; Nucifora, G. The oncoprotein EVI1 and the DNA methyltransferase Dnmt3 co-operate in binding and de novo methylation of target DNA. *PLoS ONE* **2011**, *6*, e20793. [CrossRef] [PubMed]
215. Goyama, S.; Nitta, E.; Yoshino, T.; Kako, S.; Watanabe-Okochi, N.; Shimabe, M.; Imai, Y.; Takahashi, K.; Kurokawa, M. EVI-1 interacts with histone methyltransferases SUV39H1 and G9a for transcriptional repression and bone marrow immortalization. *Leukemia* **2010**, *24*, 81–88. [CrossRef] [PubMed]
216. Spensberger, D.; Delwel, R. A novel interaction between the proto-oncogene Evi1 and histone methyltransferases, SUV39H1 and G9a. *FEBS Lett.* **2008**, *582*, 2761–2767. [CrossRef]
217. Pradhan, A.K.; Halder, A.; Chakraborty, S. Physical and functional interaction of the proto-oncogene EVI1 and tumor suppressor gene HIC1 deregulates Bcl-xL mediated block in apoptosis. *Int. J. Biochem. Cell Biol.* **2014**, *53*, 320–328. [CrossRef]
218. Xu, X.; Woo, C.H.; Steere, R.R.; Lee, B.C.; Huang, Y.; Wu, J.; Pang, J.; Lim, J.H.; Xu, H.; Zhang, W.; et al. EVI1 acts as an inducible negative-feedback regulator of NF-kappaB by inhibiting p65 acetylation. *J. Immunol.* **2012**, *188*, 6371–6380. [CrossRef]
219. Spensberger, D.; Vermeulen, M.; Le Guezennec, X.; Beekman, R.; Van Hoven, A.; Bindels, E.; Stunnenberg, H.; Delwel, R. Myeloid transforming protein Evi1 interacts with methyl-CpG binding domain protein 3 and inhibits in vitro histone deacetylation by Mbd3/Mi-2/NuRD. *Biochemistry* **2008**, *47*, 6418–6426. [CrossRef]
220. Ohno, H.; Shinoda, K.; Ohyama, K.; Sharp, L.Z.; Kajimura, S. EHMT1 controls brown adipose cell fate and thermogenesis through the PRDM16 complex. *Nature* **2013**, *504*, 163–167. [CrossRef]

221. Takahata, M.; Inoue, Y.; Tsuda, H.; Imoto, I.; Koinuma, D.; Hayashi, M.; Ichikura, T.; Yamori, T.; Nagasaki, K.; Yoshida, M.; et al. SKI and MEL1 cooperate to inhibit transforming growth factor-beta signal in gastric cancer cells. *J. Biol. Chem.* **2009**, *284*, 3334–3344. [CrossRef] [PubMed]
222. Zeng, X.; Jedrychowski, M.P.; Chen, Y.; Serag, S.; Lavery, G.G.; Gygi, S.P.; Spiegelman, B.M. Lysine-specific demethylase 1 promotes brown adipose tissue thermogenesis via repressing glucocorticoid activation. *Genes Dev.* **2016**, *30*, 1822–1836. [CrossRef] [PubMed]
223. Harms, M.J.; Lim, H.W.; Ho, Y.; Shapira, S.N.; Ishibashi, J.; Rajakumari, S.; Steger, D.J.; Lazar, M.A.; Won, K.J.; Seale, P. PRDM16 binds MED1 and controls chromatin architecture to determine a brown fat transcriptional program. *Genes Dev.* **2015**, *29*, 298–307. [CrossRef] [PubMed]
224. Dempersmier, J.; Sambeat, A.; Gulyaeva, O.; Paul, S.M.; Hudak, C.S.; Raposo, H.F.; Kwan, H.Y.; Kang, C.; Wong, R.H.; Sul, H.S. Cold-inducible Zfp516 activates UCP1 transcription to promote browning of white fat and development of brown fat. *Mol. Cell* **2015**, *57*, 235–246. [CrossRef]
225. Fox, A.H.; Liew, C.; Holmes, M.; Kowalski, K.; Mackay, J.; Crossley, M. Transcriptional cofactors of the FOG family interact with GATA proteins by means of multiple zinc fingers. *EMBO J.* **1999**, *18*, 2812–2822. [CrossRef]
226. Liew, C.K.; Simpson, R.J.; Kwan, A.H.; Crofts, L.A.; Loughlin, F.E.; Matthews, J.M.; Crossley, M.; Mackay, J.P. Zinc fingers as protein recognition motifs: Structural basis for the GATA-1/friend of GATA interaction. *Proc. Natl. Acad. Sci. USA* **2005**, *102*, 583–588. [CrossRef]
227. Deconinck, A.E.; Mead, P.E.; Tevosian, S.G.; Crispino, J.D.; Katz, S.G.; Zon, L.I.; Orkin, S.H. FOG acts as a repressor of red blood cell development in Xenopus. *Development* **2000**, *127*, 2031–2040.
228. Snow, J.W.; Orkin, S.H. Translational isoforms of FOG1 regulate GATA1-interacting complexes. *J. Biol. Chem.* **2009**, *284*, 29310–29319. [CrossRef]
229. Huggins, G.S.; Bacani, C.J.; Boltax, J.; Aikawa, R.; Leiden, J.M. Friend of GATA 2 physically interacts with chicken ovalbumin upstream promoter-TF2 (COUP-TF2) and COUP-TF3 and represses COUP-TF2-dependent activation of the atrial natriuretic factor promoter. *J. Biol. Chem.* **2001**, *276*, 28029–28036. [CrossRef]
230. Carter, D.R.; Buckle, A.D.; Tanaka, K.; Perdomo, J.; Chong, B.H. Art27 interacts with GATA4, FOG2 and NKX2.5 and is a novel co-repressor of cardiac genes. *PLoS ONE* **2014**, *9*, e95253. [CrossRef]
231. Clabby, M.L.; Robison, T.A.; Quigley, H.F.; Wilson, D.B.; Kelly, D.P. Retinoid X receptor alpha represses GATA-4-mediated transcription via a retinoid-dependent interaction with the cardiac-enriched repressor FOG-2. *J. Biol. Chem.* **2003**, *278*, 5760–5767. [CrossRef] [PubMed]
232. Boi, M.; Zucca, E.; Inghirami, G.; Bertoni, F. PRDM1/BLIMP1: A tumor suppressor gene in B and T cell lymphomas. *Leuk. Lymphoma* **2015**, *56*, 1223–1228. [CrossRef] [PubMed]
233. Kucuk, C.; Iqbal, J.; Hu, X.; Gaulard, P.; De Leval, L.; Srivastava, G.; Au, W.Y.; McKeithan, T.W.; Chan, W.C. PRDM1 is a tumor suppressor gene in natural killer cell malignancies. *Proc. Natl. Acad. Sci. USA* **2011**, *108*, 20119–20124. [CrossRef] [PubMed]
234. Nie, K.; Gomez, M.; Landgraf, P.; Garcia, J.F.; Liu, Y.; Tan, L.H.; Chadburn, A.; Tuschl, T.; Knowles, D.M.; Tam, W. MicroRNA-mediated down-regulation of PRDM1/Blimp-1 in Hodgkin/Reed-Sternberg cells: A potential pathogenetic lesion in Hodgkin lymphomas. *Am. J. Pathol.* **2008**, *173*, 242–252. [CrossRef] [PubMed]
235. Zhu, Z.; Wang, H.; Wei, Y.; Meng, F.; Liu, Z.; Zhang, Z. Downregulation of PRDM1 promotes cellular invasion and lung cancer metastasis. *Tumour. Biol.* **2017**, *39*, 1010428317695929. [CrossRef]
236. Nie, K.; Zhang, T.; Allawi, H.; Gomez, M.; Liu, Y.; Chadburn, A.; Wang, Y.L.; Knowles, D.M.; Tam, W. Epigenetic down-regulation of the tumor suppressor gene PRDM1/Blimp-1 in diffuse large B cell lymphomas: A potential role of the microRNA let-7. *Am. J. Pathol.* **2010**, *177*, 1470–1479. [CrossRef]
237. Tam, W.; Gomez, M.; Chadburn, A.; Lee, J.W.; Chan, W.C.; Knowles, D.M. Mutational analysis of PRDM1 indicates a tumor-suppressor role in diffuse large B-cell lymphomas. *Blood* **2006**, *107*, 4090–4100. [CrossRef]
238. Wang, X.; Wang, K.; Han, L.; Zhang, A.; Shi, Z.; Zhang, K.; Zhang, H.; Yang, S.; Pu, P.; Shen, C.; et al. PRDM1 is directly targeted by miR-30a-5p and modulates the Wnt/beta-catenin pathway in a Dkk1-dependent manner during glioma growth. *Cancer Lett.* **2013**, *331*, 211–219. [CrossRef]
239. Morishita, K.; Parker, D.S.; Mucenski, M.L.; Jenkins, N.A.; Copeland, N.G.; Ihle, J.N. Retroviral activation of a novel gene encoding a zinc finger protein in IL-3-dependent myeloid leukemia cell lines. *Cell* **1988**, *54*, 831–840. [CrossRef]

240. Nucifora, G.; Laricchia-Robbio, L.; Senyuk, V. EVI1 and hematopoietic disorders: History and perspectives. *Gene* **2006**, *368*, 1–11. [CrossRef]
241. Dettman, E.J.; Justice, M.J. The zinc finger SET domain gene Prdm14 is overexpressed in lymphoblastic lymphomas with retroviral insertions at Evi32. *PLoS ONE* **2008**, *3*, e3823. [CrossRef] [PubMed]
242. Dettman, E.J.; Simko, S.J.; Ayanga, B.; Carofino, B.L.; Margolin, J.F.; Morse, H.C., 3rd; Justice, M.J. Prdm14 initiates lymphoblastic leukemia after expanding a population of cells resembling common lymphoid progenitors. *Oncogene* **2011**, *30*, 2859–2873. [CrossRef] [PubMed]
243. Steenbergen, R.D.; Ongenaert, M.; Snellenberg, S.; Trooskens, G.; Van der Meide, W.F.; Pandey, D.; Bloushtain-Qimron, N.; Polyak, K.; Meijer, C.J.; Snijders, P.J.; et al. Methylation-specific digital karyotyping of HPV16E6E7-expressing human keratinocytes identifies novel methylation events in cervical carcinogenesis. *J. Pathol.* **2013**, *231*, 53–62. [CrossRef] [PubMed]
244. Tan, S.X.; Hu, R.C.; Liu, J.J.; Tan, Y.L.; Liu, W.E. Methylation of PRDM2, PRDM5 and PRDM16 genes in lung cancer cells. *Int. J. Clin. Exp. Pathol.* **2014**, *7*, 2305–2311.
245. Tan, S.X.; Hu, R.C.; Xia, Q.; Tan, Y.L.; Liu, J.J.; Gan, G.X.; Wang, L.L. The methylation profiles of PRDM promoters in non-small cell lung cancer. *Onco Targets Ther.* **2018**, *11*, 2991–3002. [CrossRef]
246. Fei, L.R.; Huang, W.J.; Wang, Y.; Lei, L.; Li, Z.H.; Zheng, Y.W.; Wang, Z.; Yang, M.Q.; Liu, C.C.; Xu, H.T. PRDM16 functions as a suppressor of lung adenocarcinoma metastasis. *J. Exp. Clin. Cancer Res.* **2019**, *38*, 35. [CrossRef]
247. Lv, W.; Yu, X.; Li, W.; Feng, N.; Feng, T.; Wang, Y.; Lin, H.; Qian, B. Low expression of LINC00982 and PRDM16 is associated with altered gene expression, damaged pathways and poor survival in lung adenocarcinoma. *Oncol. Rep.* **2018**, *40*, 2698–2709. [CrossRef]
248. Zhang, D.L.; Qu, L.W.; Ma, L.; Zhou, Y.C.; Wang, G.Z.; Zhao, X.C.; Zhang, C.; Zhang, Y.F.; Wang, M.; Zhang, M.Y.; et al. Genome-wide identification of transcription factors that are critical to non-small cell lung cancer. *Cancer Lett.* **2018**, *434*, 132–143. [CrossRef]
249. Laitinen, M.P.; Anttonen, M.; Ketola, I.; Wilson, D.B.; Ritvos, O.; Butzow, R.; Heikinheimo, M. Transcription factors GATA-4 and GATA-6 and a GATA family cofactor, FOG-2, are expressed in human ovary and sex cord-derived ovarian tumors. *J. Clin. Endocrinol. Metab.* **2000**, *85*, 3476–3483.
250. Anttonen, M.; Unkila-Kallio, L.; Leminen, A.; Butzow, R.; Heikinheimo, M. High GATA-4 expression associates with aggressive behavior, whereas low anti-Mullerian hormone expression associates with growth potential of ovarian granulosa cell tumors. *J. Clin. Endocrinol. Metab.* **2005**, *90*, 6529–6535. [CrossRef]
251. Efimenko, E.; Padua, M.B.; Manuylov, N.L.; Fox, S.C.; Morse, D.A.; Tevosian, S.G. The transcription factor GATA4 is required for follicular development and normal ovarian function. *Dev. Biol.* **2013**, *381*, 144–158. [CrossRef] [PubMed]
252. Bashamboo, A.; Brauner, R.; Bignon-Topalovic, J.; Lortat-Jacob, S.; Karageorgou, V.; Lourenco, D.; Guffanti, A.; McElreavey, K. Mutations in the FOG2/ZFPM2 gene are associated with anomalies of human testis determination. *Hum. Mol. Genet.* **2014**, *23*, 3657–3665. [CrossRef] [PubMed]
253. Turnbull, J.; Girard, J.M.; Lohi, H.; Chan, E.M.; Wang, P.; Tiberia, E.; Omer, S.; Ahmed, M.; Bennett, C.; Chakrabarty, A.; et al. Early-onset Lafora body disease. *Brain* **2012**, *135*, 2684–2698. [CrossRef] [PubMed]
254. Bowne, S.J.; Sullivan, L.S.; Wheaton, D.K.; Locke, K.G.; Jones, K.D.; Koboldt, D.C.; Fulton, R.S.; Wilson, R.K.; Blanton, S.H.; Birch, D.G.; et al. North Carolina macular dystrophy (MCDR1) caused by a novel tandem duplication of the PRDM13 gene. *Mol. Vis.* **2016**, *22*, 1239–1247.
255. Shapira, S.K.; McCaskill, C.; Northrup, H.; Spikes, A.S.; Elder, F.F.; Sutton, V.R.; Korenberg, J.R.; Greenberg, F.; Shaffer, L.G. Chromosome 1p36 deletions: The clinical phenotype and molecular characterization of a common newly delineated syndrome. *Am. J. Hum. Genet.* **1997**, *61*, 642–650. [CrossRef]

Publisher's Note: MDPI stays neutral with regard to jurisdictional claims in published maps and institutional affiliations.

© 2020 by the authors. Licensee MDPI, Basel, Switzerland. This article is an open access article distributed under the terms and conditions of the Creative Commons Attribution (CC BY) license (http://creativecommons.org/licenses/by/4.0/).